THE EVALUATION OF A FINE GRINDER AND AIR CLASSIFIER IN THE PERFORMANCE OF PROTEIN SHIFTING OF WHEAT FLOUR

by

FRED ALBERT FRANZ 265

B. S., Kansas State University, 1962

A MASTER'S THESIS

submitted in partial fulfillment of the

requirements for the degree

MASTER OF SCIENCE

Department of Grain Science and Industry

KANSAS STATE UNIVERSITY
Manhattan, Kansas

1968

Approved by:

Major Professor

TABLE OF CONTENTS

INTRODUCTION AND REVIEW OF LITERATURE

Fine grinding and air classification of wheat flour became a popular topic of conversation to millers in the late 1950's (1). It became widely known that air classifiers could be used to separate flour into several fine and coarse fractions according to particle size. Separation according to sub-sieve particle size results in various fractions with greatly different properties and analyses. Flour with 10% protein can be separated so as to obtain a small fraction with 20 - 25% protein and another fraction with 5 - 7% protein. Fine grinders can be used to increase the amount of smaller particles available to be separated by air classification.

A high degree of interest in these subjects was maintained until about 1964. During this period research was performed in an attempt to learn more about the principles involved. Since that period work and interest have been on a less intense scale.

Today there are numerous commercial installations in operation. Air classification and fine grinding can be used to control flour uniformity even though the wheat mix changes in age or composition (32,40). The removal of various fractions of a flour by air classification helps extend shelf life of flour products (32,40). Several flours of different uses can be produced by size fractionating and then blending the resulting fractions from one flour. The concept of producing many flours from one parent flour can be used to reduce transportation expenditures on wheat mix components by using local wheats. This savings applies especially well to the Pacific Northwest because approximately 90% of its wheat production is in the soft, low protein classes, and they must ship in the strong bread flour wheats from areas to the east (34).

Protein concentrates are currently getting much attention. Air classification and fine grinding can be used to produce these concentrates, such as aluerone concentrate (21). It therefore appears that fine grinding and air classification will play a growing role in the milling industry.

The purpose of this study was to evaluate a fine grinder and air classifier in the performance of protein shifting of wheat flour.

Structure and Properties of Wheat Endosperm and Its Components

When wheat endosperm is ground the resulting flour is composed of particles of variable composition. Wheat endosperm is made up of three basic types of endosperm cells: the peripheral, the prismatic, and the central cells (22). The names are derived from the cells' general locations within the kernel in the cases of the peripheral and central cells, and as to overall cell shape in the case of the prismatic cells. Endosperm cells contain many starch granules embedded in a proteinaceous matrix.

During milling the endosperm and its cells are broken. The forces applied during milling cleave the protein network and leave the starch granules intact (41). Most workers who have described the particles in flour generally agree that there are at least three basic components. These include agglomerates (portions and combinations of endosperm cells), starch cells (both relatively free of adhering protein and with adhering protein), and protein fragments. Sandstedt (33) described two basic size groups of starch granules: large lenticular granules and smaller spherical granules. The smaller spherical granules are embedded in the protein material that surrounds the larger granules. The large lenticular granules have an oval to circular outline. Kaiser (20) reported the diameter of starch granules to be from 1 to 50 microns. The larger lenticular granules generally are over 20 microns and the smaller ones in the 2 to 8 micron range. He reported approximately 3% by weight to be below 17 microns and 20% by weight to be above 40 microns.

Wolf et al (43) found that starch granules which are relatively free of adhering protein are in the below 10 micron size range. These smaller granules are formed in the later stages of kernel development after the larger lenticular granules have been deposited (33). Wolf et al (43) suggested that because of their later development these granules are not bonded as tightly by the surrounding protein. Many particle size distributions of wheat flour show a bimodal characteristic that is possibly due to the two size groups of starch granules.

Hess et al (15) (1955) concluded that wheat endosperm protein could be classified as either wedge or adhesive protein. Wedge protein refers to the wedge-shaped deposits which lie between starch granules. Adhesive protein refers to fibrillar deposits adhering to starch granule surfaces. Hess (1960) further proposed a structural relationship of protein, lipid, and starch in wheat flour, in which wedge protein deposits are surrounded by a lipoid and lipoprotein layer, beyond which lies the adhesive protein and the starch granules. This proposal was confirmed by Jennings et al (19). Buttrose (2) suggested that the wedge protein corresponds to the discrete protein deposits and that the surrounding lipoprotein membranes enable the wedge deposits to be more easily separated. In mature cells, adjacent large starch grains appear to distort the shape of protein bodies. He further suggested that the fibrillar structure of adhesive protein as observed by Hess and Mahl (1954) is due to desiccation of non-fibrillar soluble proteins and lipoprotein membranes.

From the specifications of patents assigned to the Pillsbury Company (32), it is shown that by using air classification and making separations at approximately 18 microns and 40 microns (determined by sedimentation), the fractions have different compositional properties: the fine fraction is substantially higher in protein content than the parent flour; the middle fraction is lower in protein content than the parent; and the coarse fraction is substantially the same protein content as the parent. The particles in the fine fraction are mostly protein fragments and small starch granules. The intermediate fraction contains starch granules and small endosperm chunks, while the coarsest fraction contains mostly large chunks of endosperm and very large starch granules.

The protein particles in flour have lower densities than the starch granules. The density of the protein has been reported at approximately 1.32 g/cm^3 and the density of starch at approximately 1.50 g/cm^3 (15). The smaller granules are generally higher in density than the larger ones. Gracza (9) reported the specific gravity of the highest protein fraction (obtained by air classification) to be 1.43 g/cm^3. From microscopic examinations of air classified fractions of both hard and soft wheat flours, Gracza noted these differences: the protein particles were smaller, thinner, and less irregular in hard wheat flour; the starch granules were flatter and more lenticular in hard wheat flour; the surfaces of more starch granules were free of protein in the soft wheat flour; soft wheat flour contained more large elementary starch granules; and the endosperm chunks of hard wheat flour have polygonal shapes with distinct edges while soft wheat flour endosperm chunks have more rounded edges and occasional protruding starch granules.

Sullivan et al (36) reported studies that were made to investigate the relationship of particle size and endosperm structure to ash, protein, maltose value, and gassing power as determined from air classified fractions. They found higher ash contents in the high protein fine fraction as reported by others (32). The ash content of the fine fractions obtained from hard wheat flour were noted to be higher in ash content than fine fractions of soft wheat flour. This is due to the greater amount of small broken pieces of cell wall material in the hard wheat flour (36).

Fine Particle Sizing Methods and Distribution Curves

Sub-sieve particle size measurement is needed for research and control of processes such as air classification and fine grinding. The main separating process involved in air classification is separation by size (42). The lower size limit for practical sieve separation is 50 microns (50 microns is the average measured lineal dimension of the mesh openings of the sieve). The size range below 50 microns is known as the sub-sieve size range. Protein shifting of wheat flour involves the separation of particles below 50 microns. For this reason air classifiers, not sifters, are used.

Particle size measurement methods generally are used to obtain size distribution curves. These curves are often plots of cumulative percent smaller than a given particle size. From such curves it is possible to obtain the percent finer than any given particle size of the distribution. Working with these curves is much simpler than working with numbers of particles at a given size. In a pound of wheat flour there are approximately three hundred billion 10 micron particles (24).

Most of the particle sizing methods do not measure a linear dimension directly, but instead measure some property dependent on size from which a "size" is calculated (42). Fluid drag and settling velocity as related to particle size by Stokes Law is the principle used in sedimentation methods. Some sedimentation methods measure the height of accumulated, settled particles in a column. Thus the relative percent finer, by volume or weight, can be calculated without counting the actual number of particles.

There are many problems involved in fine particle measurement. Many particles are not spherical and therefore cannot be defined by one dimension (17). Workers have shown that size data are meaningful as long as the ratio of maximum to minimum dimension does not exceed about four. The particles in flour are mostly within this limit.

Fine particle size distributions are obtained from analysis of a sample of the desired material. This sample must be representative of the entire lot. Not only must sampling be representative but the distribution must remain representative after it is dispersed and prepared for measurement (17). As particle size decreases, the surface electric charge on particles increases, causing particles to adhere to each other and making dispersion difficult. These and other problems make it difficult to prepare microscope slides that are truly representative. Flocculation, the re-grouping of fine particles, becomes a problem in sedimentation methods. It is therefore imperative to achieve and maintain complete dispersion and unbiased sampling in particle size measurement.

Another problem may arise when a distribution curve obtained by one method is compared to a curve plotted from results of a second method. Before comparing two curves it should be determined exactly what is plotted on both the vertical and horizontal axes of each curve. Whitby (42) discussed this problem and showed the nine different curves that can be used to represent the same particle distribution.

The various methods of particle size measurement measure different moments and weightings of the size distribution. The distribution weighting is the variable that is summed. For instance, when using the microscope one counts or sums by number, and thus the data is number weighted. In sedimentation methods, volume or weight is summed. Summing by area is the third weighting that can be used. The distribution moment is the power of the distribution variable. There are also three moments: these are the first moment or lineal size such as diameter, second moment or area such as cross-sectional area, and third moment or volume.

Data can be converted from one moment and weighting to another but precautions are required when shifting from one weighting to another (42). For example, converting weighting by number to weighting by volume often involves a serious loss of accuracy at the coarse end of the distribution, due to the proportionately large contributions of volume of a few large particles. Converting from weighting by volume to weighting by number can result in a loss of accuracy at the fine end of the distribution. This is because there are more small particles than large particles in a given volume, and an error in volume measurement will be increased for finer particles in converting to number weighting.

Moment conversion is quite common and does not involve the high risk of loss of accuracy involved with weighting conversions. Accuracy may be either increased or decreased: conversion from second moment to first moment is quite common in making sedimentation calculations and increases accuracy.

The statistical handling of fine particle data is broadly covered by Herdan (14). Irani (18) offers many methods of representing data by use of histograms and frequency distributions, as well as covering the reconstruction of a parent curve from the distribution curves of the fine and coarse fractions.

Various graph papers are used for plotting particle size distribution curves. Two common types are semi-log and log-probability. Most flour fractions have S-shaped curves on the semi-log paper. Many size distributions are approximately linear on log-probability plots (14,42). The value of the geometric mean corresponds to the size at 50% or the median on the ordinate scale of the log-probability plot. The geometric deviation can be obtained either by dividing the size at 84.13% by the size at 50% or by dividing the size at 50% by the size at 15.87%. If the plot is not linear, the average of the geometric deviations can be used. Thus, the log-probability plot is very handy because both a measure of central tendency and a measure of deviation can be obtained easily from the curve.

The Fisher Sub-Sieve-Sizer gives only one index of the particle size of flour; it does not give information that can be plotted to obtain the particle size distribution. However, this apparatus is quite simple, gives fast results, and is used quite often for control work. It measures the permeability of a bed of particles. Permeability is related to specific surface among other things as described by Kozeny (5). The Fisher number or surface mean diameter is generally smaller than sedimentation mean diameters. As size range decreases and particles become more spherical, the means are more alike (5). They do not represent the same moment and weighting.

Discrepancies exist between the results of different particle sizing methods and as Gracza (11) stated, "A skilled investigator approaches with caution a critical comparison of size data of two different methods unless a correlation between the two methods has been established for the materials."

Indices of Classification Efficiency

The many methods of expressing the efficiency of a classifier generally rely on information obtained from particle size distributions.

Catlin (3) reported, "The efficiency of any selective apparatus, such as an air separator, is naturally the ratio existing between the amount of finished material recovered and the amount introduced into the machine in a given interval of time." Newton and Newton (27) suggested that classifier efficiencies should penalize a classifier for the oversize which occurs in the undersize product and vice versa. They further suggested that the efficiency should be the same regardless of whether based on the oversize or the undersize product. If a classifier were judged only on its ability to produce a fine fraction, then a sifter would always have an efficiency of near 100%. However, according to the Newtons, efficiency is decreased if fines remain on top of the sieve.

In most of the efficiency tests, the size distributions of the parent flour, fine fraction, and coarse fraction are needed along with the relative weights or percents of each fraction. Quite often when the fine and coarse fractions are used to reconstruct the parent, the resulting curve is different from the true curve of the parent. This is due to errors in determining the percent of each fraction, inaccuracies of particle size determination, sampling and other errors and difficulties (11).

Cracza (11) compared four selected efficiency concepts by using a hypothetical sample pair of fractions and their reconstructed parent. He compared Catlin's, the Newtons', and average efficiency, plus sharpness.

Average efficiency was suggested by the Tyler Sieve Co. (38). At an arbitrary particle size it is defined as the ratio of the weight of properly classified material in both products to the weight of classifiable material, expressed in percent of the feed material. Sharpness does not involve the percentage of each fraction but is merely the difference between the ordinates of the percent finer curves of the fine and coarse fractions at a given particle size.

Whitby (42) defined classifier efficiency as the ratio of the amount of coarse fraction within a given size range to the original amount within the same size range. He plotted the size frequency plots of the coarse and fine fractions so that the area under the coarse curve was proportional to the weight of particles in that fraction, and the area between the coarse and total curves was proportional to the weight of the fine fraction. The efficiencies of the various size ranges were plotted on a log-probability plot. The plot is generally linear and the geometric deviation can be easily obtained and used as a measure of sharpness. The closer the geometric deviation is to unity, the sharper the classification.

Hall (13) stated, "In any statement of efficiency, the exact formula and particle size cut-point must be clearly defined."

Cut Point and Critical Particle Size

As air classification became more widely used, a need arose for a term to express the size at which a single classification step was made (11). Air classifiers unlike screening operations do not have the benefit of absolute physical limitations. Air classification cut-points are taken from the information available on the particle size distribution curves of the fine and coarse fractions. The cut size is dependent on the definition of particle size and the method used for particle size measurement (23).

Many of the definitions of cut-point are based on the various definitions of classifier performance. If a graph of efficiency plotted against particle size is made, a maximum efficiency usually is obtained at the cut size, which is defined as the size of feed particle having equal probability of entering either the fine or coarse fraction (11).

In a second part of his Studies of Size Classification Indices (11), Gracza explained and showed the use of seven different methods for determining critical particle size. These seven methods involve the classification efficiency concepts covered in Part I. Most of these seven methods require a reconstructed parent distribution. One method involves determining the particle size at which maximum sharpness occurs. This critical particle size is easy to determine from the particle size distribution curves of the fine and coarse fractions.

Gracza compared the seven methods on sixteen pairs of air classified flours and offered their advantages and disadvantages. Many methods require very accurate particle size information and accurate percentages of the fractions. In protein shift work, especially the first separation where the highest protein fraction is produced, the percent of fines is quite small (often below 5%) and errors in its determination may be large, percentage-wise.

Air Classifier Principles

At a symposium on Air Classification in 1957, Hall stated to a group of mining engineers, "The purpose of this symposium is to challenge industry to better classification" (13). At the time of this symposium there were increasing demands for equipment capable of separating 99.9% finer than 20 microns. This requirement was generally not within the capabilities of classifiers at that time.

At the 1957 symposium many papers were presented which dealt with the optimal or free vortex classifier. Designers had attempted to create a constant cut-point classification zone (28). Inside this zone the forces acting upon the particles would be stabilized and the particles would go one way or the other, depending on whether they were smaller or larger than the cut size. Turbulence inside the zone had to be minimized. The great turbulence needed in fine grinding fluid energy mills is not desired at all in classifiers. Rumpf and Kaiser (23) reduced the wall turbulence by rotating the walls. Rumpf also suggested that particles travel in an Archimedian spiral. This type of spiral vortex is used in some classifiers because it could be maintained independent of feed rate and particle size distribution.

Other workers developed other classifiers utilizing different designs. As a result of the great deal of effort by many workers, some basic principles of air classification have been set forth.

Lykken in 1957 (24) stressed the need for adequate dilution of the particles with air. He called for at least one pound (13 cubic feet) of air for each pound of solids. He also stressed complete and uniform distribution of the particles and complete aeration such that each particle is coated with an air film. Small particles must be kept separated or they will agglomerate due to static electricity and other causes.

Lykken (24) suggested that the principle of classification can be based on (1) the drag of an air flow on particles suspended in the flow, which varies with the first power of their diameter, and (2) centrifugal force, which varies as the cube of their diameter, in the opposite direction.

Treasure in 1965 (39) suggested four principles of classification around which classifiers should be designed. These principles are:

1. There must be a definite system of forces acting on each particle. These forces in air classifiers are primarily fluid drag and centrifugal force.

2. There must be a defined zone which all particles must enter and in which the separation occurs. At worst this will be a surface; at best, it will possess depth.

3. The particles should be introduced into the classification zone uniformly and discretely, so that no mutual interference occurs and only the calculated forces act.

4. Once classification has occurred, the fractions should be removed from the scene of action as soon as possible to prevent interference and avoid remixing.

Grinding Principles

Tanaka (37) reviewed the conventional laws of Rittenger, Kick, and Bond. He introduced probabilities and correlated these with the conventional laws. One probability involved in crushing in an impact mill is whether or not a particle hits an objective. Particles are given a velocity and then strike either another particle or the mill liner. A second probability is that even if there is a collision, crushing cannot take place unless the energy of collision produces a stress larger than the breaking stress of the material. These two probabilities are mutually independent and crushing therefore cannot occur if the product of the probabilities is not greater than zero. The nearer the probability is to unity, the better the performance. Tanaka also showed the particle sizes at which the conventional laws best apply. Rittenger's law best describes the grinding of particles in the size range of flour. This law relates surface area to work expended. For a given mechanism, crushing cannot be expected below a certain particle size.

Rumpf (7) pointed out some of the factors involved in grinding. He mentioned that the stress the particles can withstand varies with the presence of impurities, cracks, and grooves. The path of particles before impact, the impact angle, and rotation before and after impact are also factors. The general shape, size, and elastic properties of the material must also be considered.

In a paper dealing with impact grinding of cereals and cereal products, Hibbs _et_ _al_ (16) suggested that less force is required to break materials by breaking than by compression. As the area of particles approaches the size of the impact area there is less breaking action due to the decreasing moment arm. For small particles the reduction has to be accomplished by compression alone, and consequently more power is required.

The specifications of a patent assigned to the Pillsbury Company (31) report that roller mills are not good for fine grinding flour for most uses. Roller mills produce too much heat and pressure which cause changes in the properties of the protein and damage the starch. The patent specifications suggest the use of impact milling to disintegrate the chunks of endosperm and fluid activated rubbing and multiple oblique impact steps to surface dress the starch granules.

Lykken (24) reported the open rotor, fluid energy mill as being the most effective grinding principle known. Intense intra blade vortex action causes particle on particle attrition and helps surface dress the starch granules.

Graham (12) reported that pin mill speeds of 350 to 400 ft/sec caused remarkably small amounts of starch damage in relation to the degree of reduction. These speeds did not break up the protein adequately. At 750 ft/sec the protein was broken up, but too much starch damage resulted.

Kaiser (20) described the various particle paths in pin mills (Alpine types) and reported that starch granules can withstand 440-660 ft/sec with some injury resulting at 820 ft/sec. He mentioned the importance of maintaining baking quality by not damaging starch and keeping temperature rises low.

MATERIALS AND METHODS

General Method

Two air classifiers and two fine grinders were used in this study. Results obtained from a Pillsbury Laboratory Turbo Separator were used as criteria to judge the ability of a MS-1 Hosokawa Micron Separator to shift the protein content of wheat flour. Similarly, results obtained from an Alpine 160Z Kolloplex were used as criteria to judge the ability of a Mikro 'ACM-10' to fine grind flour used for protein shifting.

The Turbo separator and Alpine mill are known to have the capability of reasonable performance in protein shifting wheat flour. The objective of the tests run in this study was to ascertain if the Micron separator and Mikro grinder could match the performance of the Turbo and Alpine, respectively.

A commercially milled 11.2% protein (14% M.B.) flour was used for the comparative tests. This flour (unground, Alpine ground, and Mikro ground) was separated on both of the separators giving six sets of fractions as shown below.

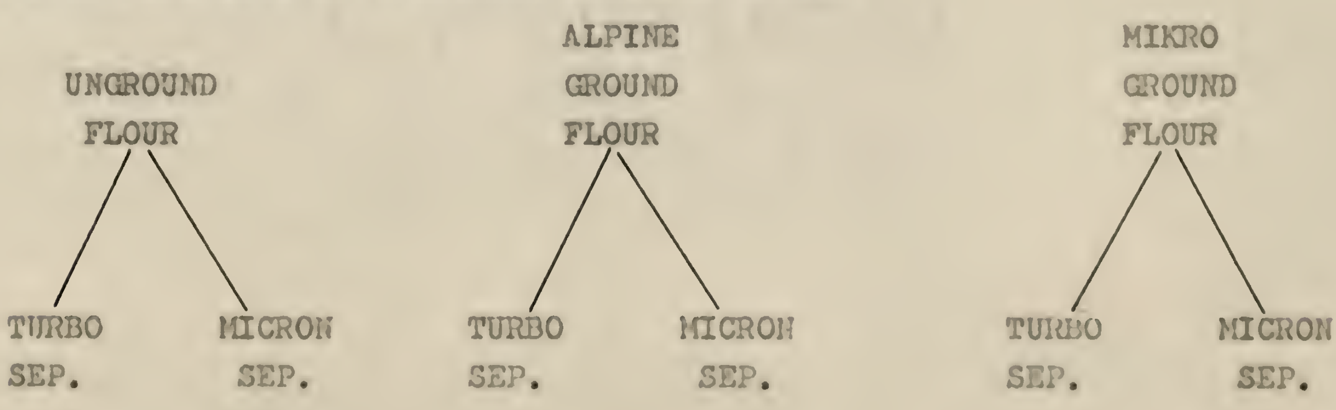

Turbo Separator

The unground flour was first fractionated by the Turbo using adjustment settings known to provide good protein shifts. Four fine fractions were obtained by making four separations using the settings shown in Fig. 1. These four separations or "cuts" were designated, in the order accomplished, as B, C, D, and E. The parent flour is called A; the fine fractions are designated by single letters B, C, D, and E; and the coarse fractions are designated by double letters BB, CC, DD, and EE.

Figure 2 shows a simplified cross-section of the Turbo. Flour was introduced at the top of the machine and dispersed by a dispersing rotor. The dispersed particles were then subjected to fluid drag and centrifugal forces in the classifying zone. Drag forces were greater than centrifugal forces on the finer particles and the fine fraction was separated from the coarse fraction. The fine and coarse fractions were collected with cyclone collectors. The air exiting from the cyclone used for the coarse fraction was recirculated back into the classifier. The air exiting the fines cyclone was filtered by a fabric filter bag and released to the atmosphere.

Particle Size Analysis

Samples of the parent flour and eight fractions were analyzed for particle size by the Fisher Sub-Sieve Sizer and MSA (Mine Safety Appliance) Particle Size Analyzer. The Fisher number was obtained by using the methods outlined in the user's

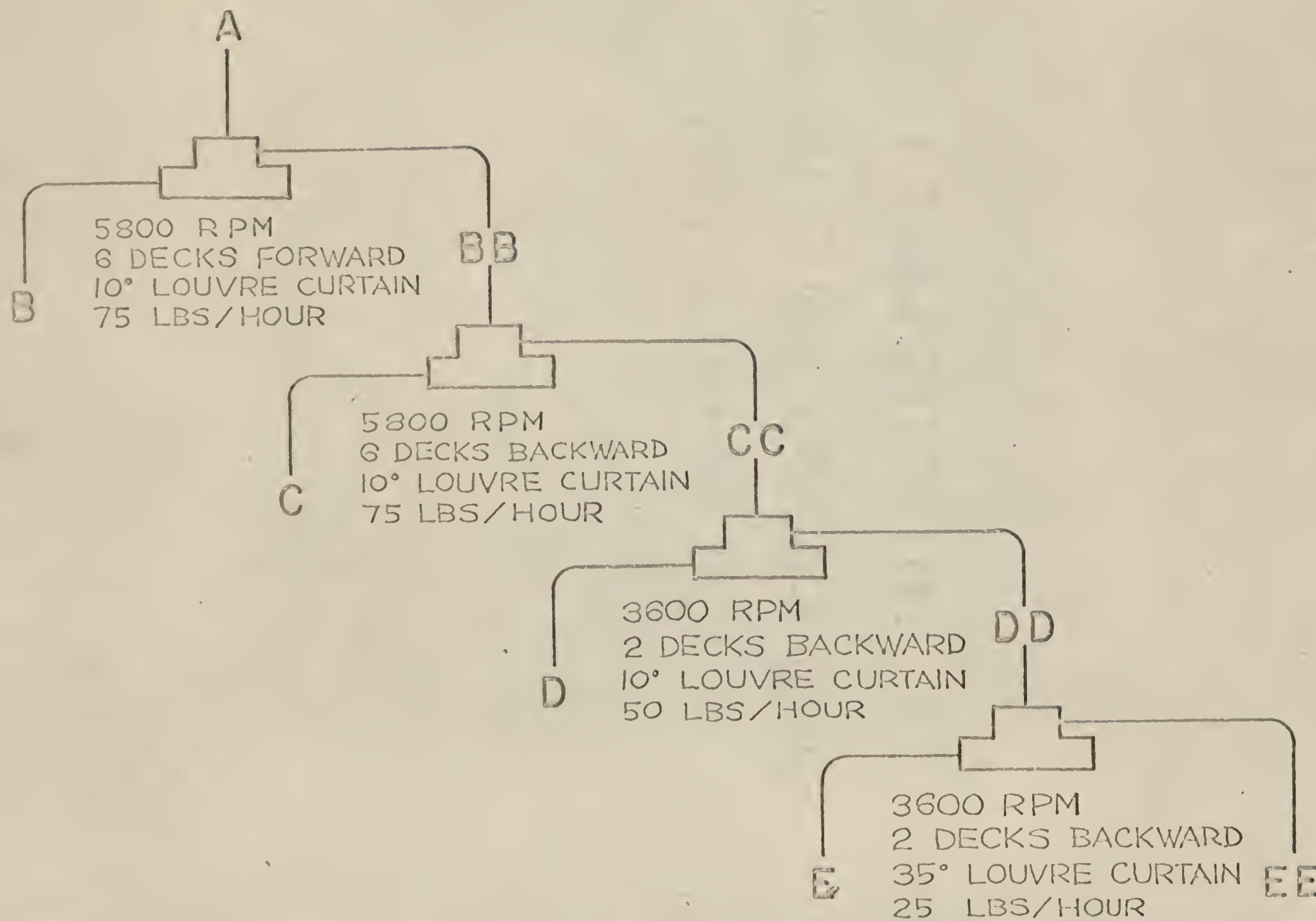

Fig. 1. Turbo Separator Settings

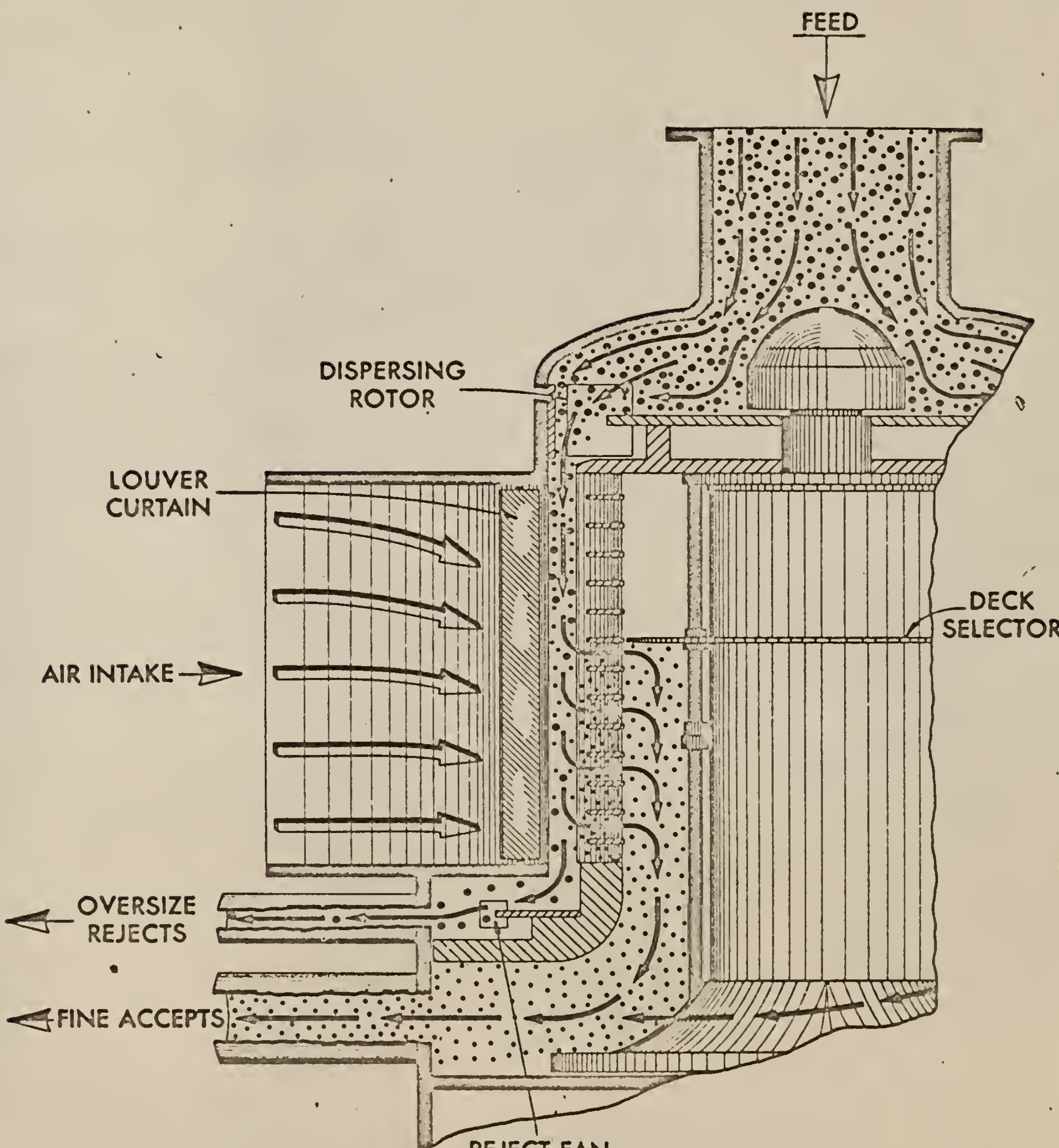

Fig. 2. Cross-sectional schematic drawing of Turbo separator.

manual (8). A sample weight of 1.44 grams was used along with a porosity setting of 0.465. A spacer was used to control the height of the compressed flour in the chamber to keep it exactly at the line marked on the apparatus. Calibration for the first set of samples (Turbo on unground flour) was accomplished by using a calibrated cylinder furnished with the apparatus. On subsequent sample sets a two-step calibration was used. First the calibrated cylinder was used and then the parent (A) and the fine fraction (B) from the first set of samples were used to calibrate the upper and lower end of the scale respectively. During the second step of the calibration the apparatus was adjusted to give the same readings on (A) and (B) as were obtained when they were first tested.

Size distribution data were obtained by use of the MSA equipment. Reading schedules and general procedures were followed as outlined in the operating manual (25). Benzene with 4 drops of Twitchell Base per 100 ml was used as the sedimentation liquid. A feeding liquid of 50% by volume Skellysolve S and 50% of the sedimentation liquid was used. A specific gravity of 1.44 was used for the feeding schedule calculations giving a Kg = 19.8 x 10^4. Two different reading schedules were used: one for fine fractions B, C, and D; and the second for all the coarse fractions and parents. The coarse fractions, unground parents, and E fraction were dispersed in the feeding chamber. The ground parents and fine fractions B, C, and D were dispersed by mixing a small sample in approximately 5 ml of feeding liquid in a test tube with an air stirrer. The mixture was stirred for 15 seconds, let stand for 30 seconds, stirred again for 15 seconds, then let stand for 10 minutes, and then stirred briefly before using. This procedure was developed in order to avoid flocculation of the fine particles. Portions of this well-dispersed sample were put into the feeding chamber by use of an eyedropper. The tapered glass tube of the eyedropper was replaced by a section of straight-walled common glass tubing. The tapered section was found to be a source of variation in preliminary operator training runs. If a sample was taken too rapidly by the tapered eyedropper, the sample contained too many small particles.

The samples dispersed by the air stirrer method were run using 0.5 ml tubes and the samples dispersed in the feeding chamber were run in 0.75 ml tubes. In both cases the final column height was kept below 40 units on the optical projector. Regardless of the dispersion method, the feeding chamber was filled 2/3 full. Duplicate runs were made and averages reported. If either flocculation or column packing during centrifuging occurred during any run, the results were not used and a rerun was made.

The 'cumulative percent finer than particle size' data obtained by the MSA method was plotted on semi-log graph paper. The plots or 'curves' were compared by holding two or three curves, one on top of the other with the ordinates aligned, up to a source of light. The curves could then be observed simultaneously and any differences could be noted.

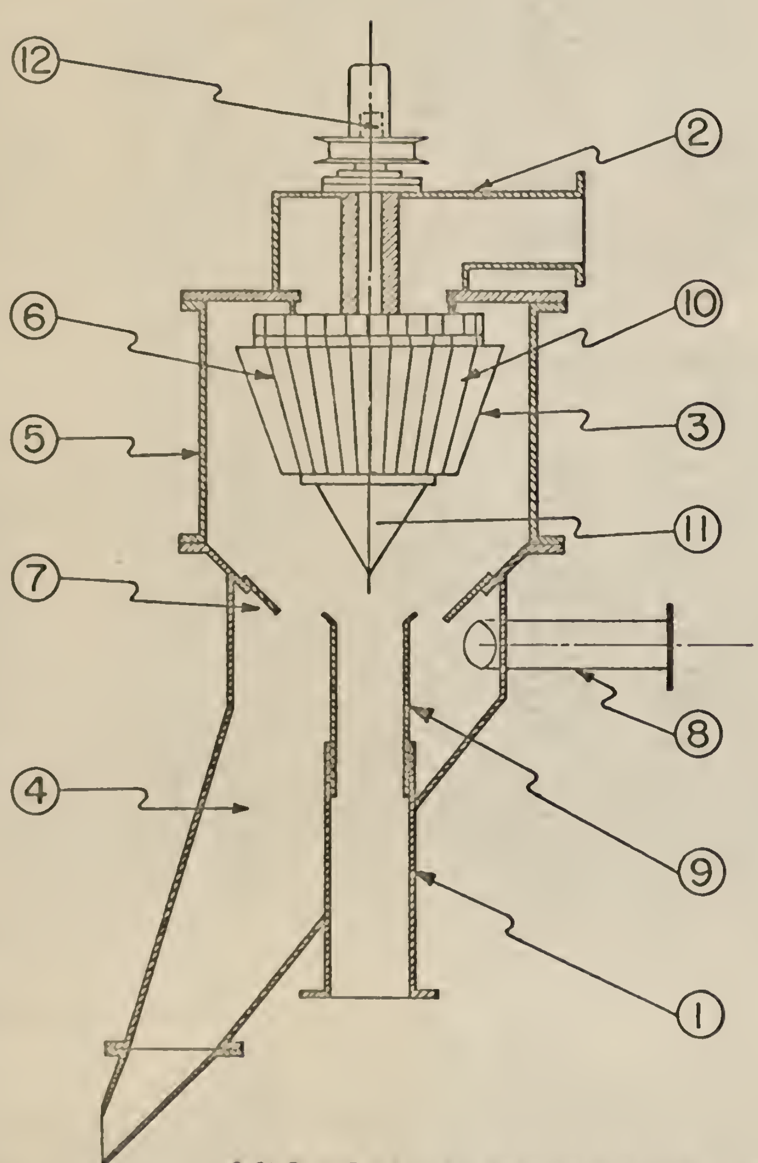

KEY:

1. CONVEYOR PIPE FOR MATERIAL
2. OUTLET DUCT FOR FINE MATERIAL
3. ROTOR
4. TAILINGS DUCT
5. BODY CHAMBER
6. AIRWAY BETWEEN ROTOR BLADES
7. ELUTRIATION RING
8. SECONDARY AIR
9. ADJUSTABLE INNER FEED PIPE
10. ROTOR BLADES
11. ROTOR CONE
12. ROTOR SHAFT

Fig. 3. MICRON SEPARATOR CROSS SECTION

Micron Separator

Particle size distribution curves of the fractions produced by the Turbo were used as guidelines for establishing the proper adjustment settings for the Micron. Figure 3 shows a cross-section of the entire machine, and Fig. 4 shows a cross-section of the separator rotor. The flour to be separated was fed into the conveyor pipe and carried upward by a flow of air through the adjustable inner feed pipe. The material was then distributed over the rotating classifying rotor by the rotor cone. As shown in Fig. 4, the particles were subjected to fluid resistance of the conveying air stream and opposing centrifugal forces imparted by the rapidly moving rotor blades. The finer particles were separated from the coarse particles by the fluid drag force and conveyed by the air stream away from the separator. With coarse particles the centrifugal force was greater than the fluid resistance, so they were rejected by the separator rotor. The rejected coarse particles then move downward in a spiral path along the

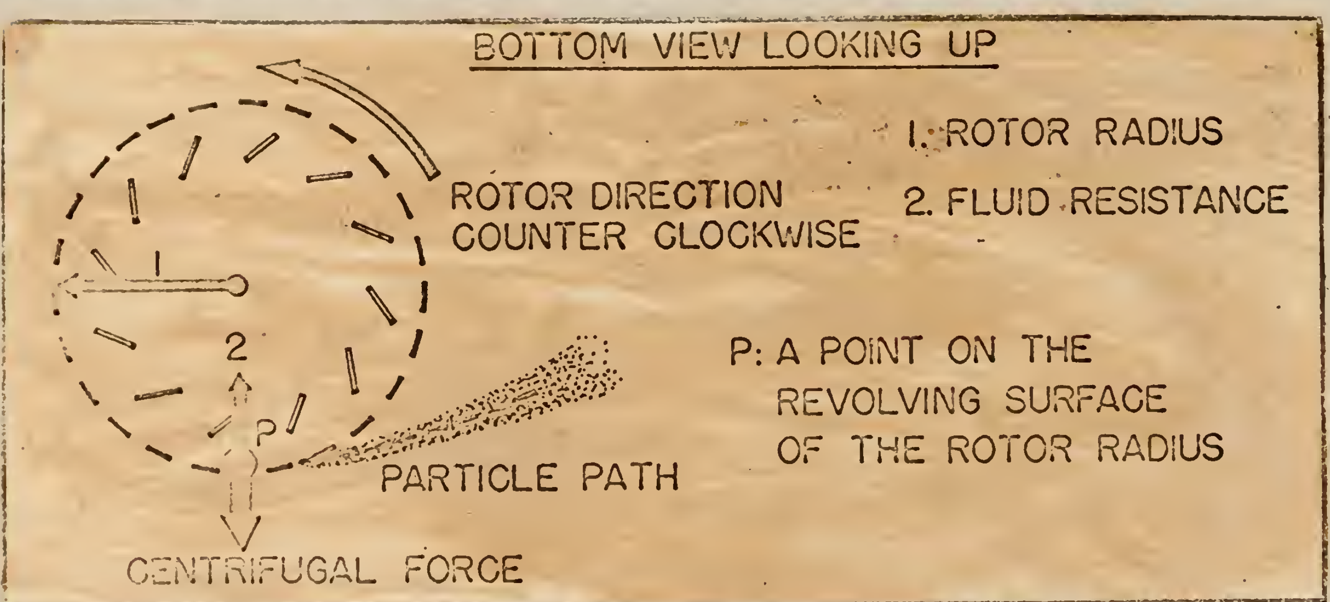

Fig. 4. Cross-section of Micron Separator rotor.

body chamber wall into an area of high turbulence caused by the elutriation ring (30). The elutriation removed or 'washed' acceptable fines from the coarse material and the washed-out particles were carried upward into the classifying zone. The air for the elutriation was provided by the secondary air inlet. Coarse particles descended by gravity into the tailings duct and were collected below the outlet.

The fine fraction was collected by a cyclone collector and the exit air from the cyclone was filtered by a traveling ring, sock type dust collector. There were extremely small amounts of material collected in the fabric bag of the Turbo and the dust collector of the Micron; these small amounts were not considered in this study.

A venturi was installed in the conveyor pipe above the point of feed-in so as to provide an area of high turbulence to break up agglomerates and aid in the dispersion of the feed. An air vibrator was mounted near the middle of the tailings duct to help keep the coarse fraction flowing and aid in cleaning out the machine between runs.

Many runs were attempted on the Micron in efforts to learn the effects of the various adjustments and to obtain settings that provided fractions similar to those from the Turbo. The main adjustments on the Micron are: rotor rpm, total air volume, secondary air volume, inner tube height, elutriation ring size, and feed rate. The effects of the adjustments were determined by using the Fisher number and the MSA size distribution curves. The Fisher number was used to detect the larger effects of the adjustments; once the optimum area of adjustment was located, bracketed tests were run in this area and the results analyzed by the curves to determine the best setting. Some of the adjustments had very little effect when adjusted from one extreme to another; these effects were studied by using only the curves. The settings for the Micron which gave separations most similar to the Turbo's performance were determined and used to fractionate the unground flour.

Alpine Grinder

The grinding was accomplished next. First the Alpine was tested to obtain a feed rate and pin velocity to use for the comparative tests. Figure 5 shows a photograph of the Alpine and Fig. 6 shows a diagram that illustrates the typical particle paths in the mill. The Alpine mill has two pinned discs with four circular rows of pins on each disc. One disc is stationary in the Kolloplex 160Z and the other rotates at high speed. The flour to be ground is fed into the grinder at the center of the discs via a hole in the stationary disc. The inner rows of pins have lower lineal velocities than the outer rows of pins and the easy-to-grind material is ground by the slower pins. Harder-to-grind material requires higher velocities and is ground by the outer rows of faster pins. It is possible some particles are too small and/or too difficult to grind and are not ground at all as shown in Fig. 6 (20).

Fig. 5. Photograph of the Alpine grinder.

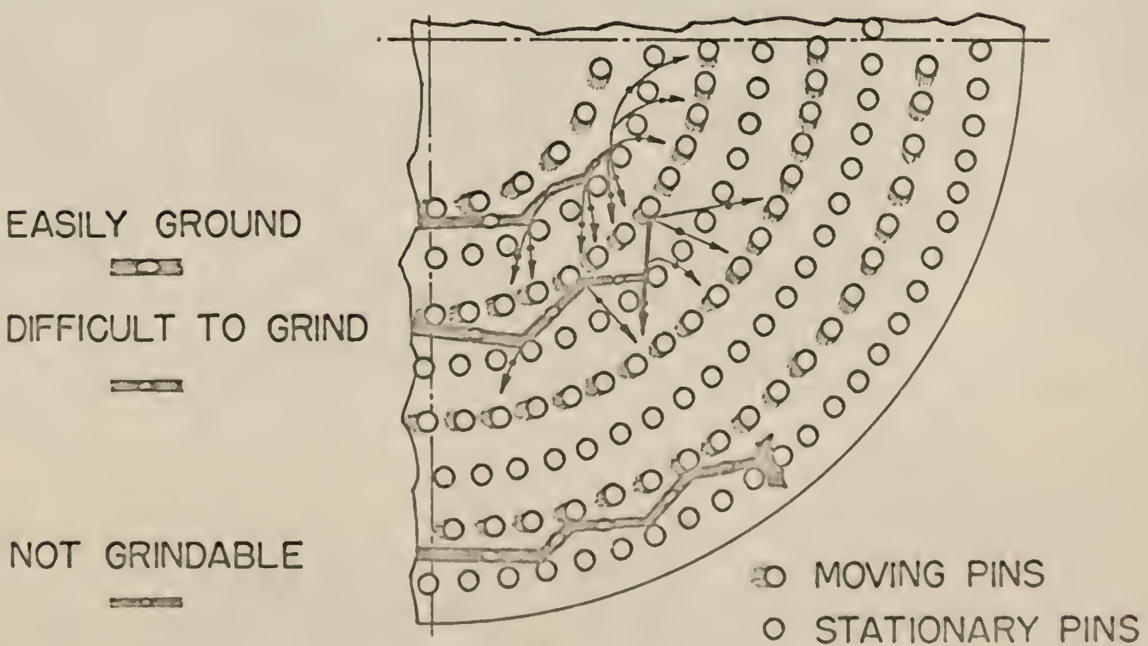

Fig. 6. Illustration of typical particle paths in the Alpine grinder.

Mikro Grinder

Information obtained from the Alpine preliminary tests was used as a guideline for setting the Mikro. Figure 7 shows a cross-section and Fig. 8 shows a cutaway of the Mikro. The Mikro is an impact mill with an air classifier built on top. The feed is by a screw feeder that feeds the material into the grinding chamber. The feed is impacted briefly by the grinding rotor and then transported upward by an air flow that enters the grinder from below the grinding rotor. Much of the rotation of the material and air is removed by the baffles. This reduction of centrifugal force allows the material to be carried to the classifier for separation (6). The fine acceptable material is removed through the separator ports by the main air flow; the rejected material is pulled down and under the shroud by the fanning action of the rotor and directed into the grinding zone again. This process continues until all particles are accepted by the separator. Wattmeters were installed midway through the study to measure the power consumption of the classifier and grinding rotor drive motors. Power readings were taken on all tests after the wattmeters were installed.

The first tests on the Mikro were performed to ascertain the effects of the various adjustments. Main adjustments on the Mikro are: separator rpm, cfm of air, grinding rotor design (bar (1) and pin (2) as seen in Fig. 9), grinding rotor rpm, and feed rate. Effects of the various adjustments were determined by use of Fisher numbers and particle size distribution curves. Once the effects of the adjustments were learned, tests were run

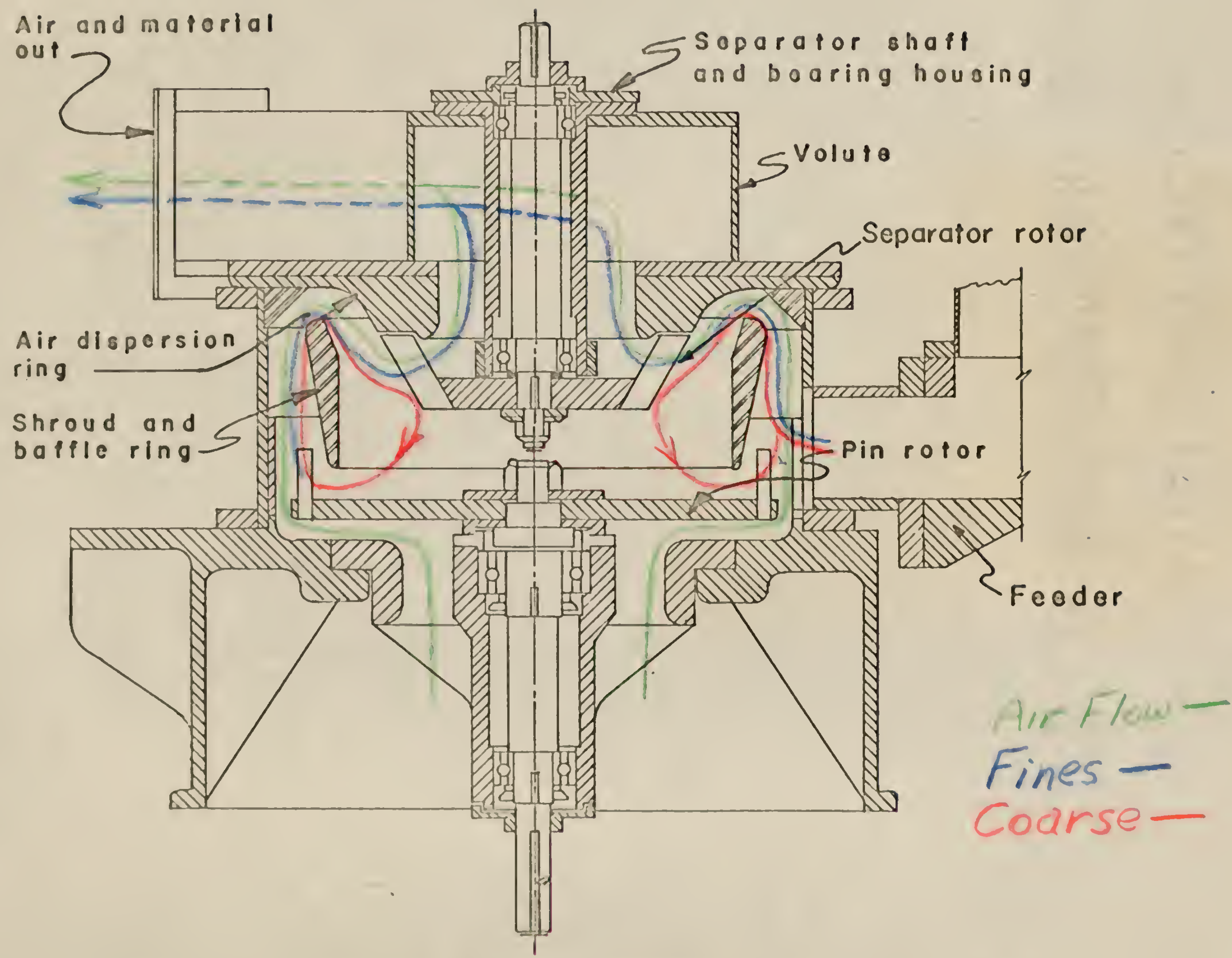

Fig. 7. Cross-section of the Mikro grinder.

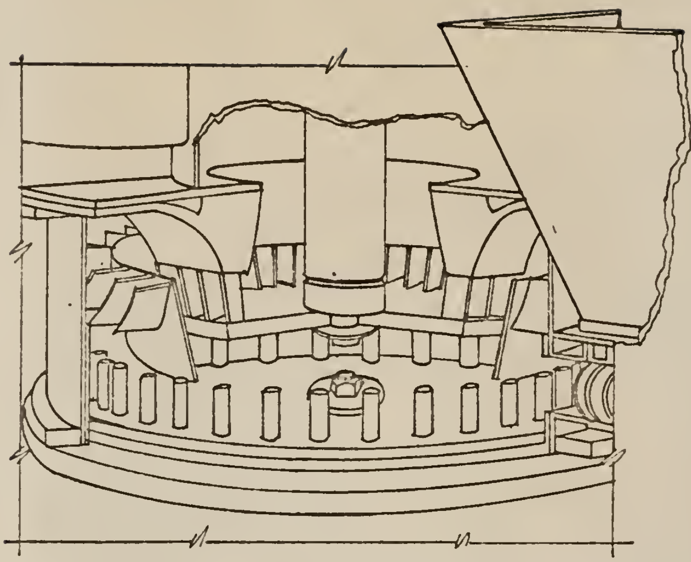

Fig. 8. Cut-away drawing of Mikro grinder.

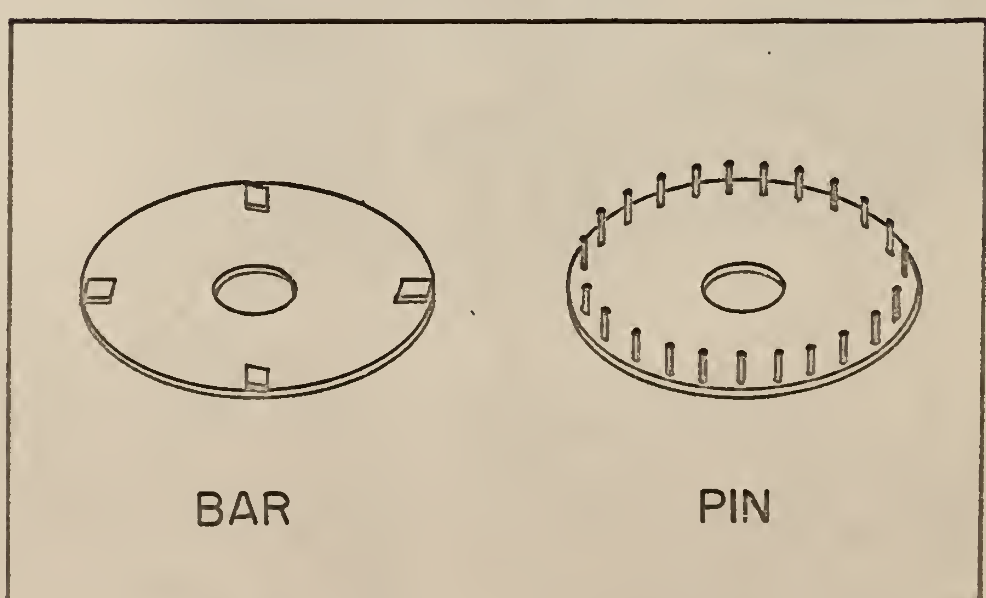

Fig. 9. Bar and pin grinding rotors of the Mikro grinder.

to determine the settings required to give grinding results similar to those of the Alpine at approximately the same pin velocity and temperature rise of the product.

Analysis of the Six Sets of Fractions

Batches of the special flour were ground on the two grinders and then fractionated on both of the separators giving the final four sets of fractions. Fisher numbers and particle size distributions were determined for all parents and fractions. Moisture, ash, protein, farinograph, and amylograph determinations were also run on all of the parents and fractions. Methods as outlined by the AACC (4) were used for the laboratory analysis.

The percents of the various fractions were obtained by first determining the percent of coarse fraction obtained from the feed flour (A,BB,CC,DD) for each of the four cuts. The percent of fine fraction was obtained by subtracting the percent of coarse fraction of the same cut from 100. This procedure gave percentages of fines and coarse that totaled to 100 for each cut. These percents were converted to percent of parent so that 100% of the parent was obtained when B, C, D, E, and EE fractions were totaled.

Protein shift index as outlined by Gracza (10) was calculated for the 6 sets of fractions. The average of the positive and negative indices was used. The formula used for the positive index is:

$$\text{Protein shift index} = \frac{1}{P} \sum_{x=1}^{n} (P_x - P)Y$$

where: P = percent protein content of parent

P_x = percent protein content of fractions having higher protein contents than the parent

Y = yield of individual fractions expressed as percent of parent

n = number of fractions produced

The same formula was used for the negative shift index except that P_y was substituted for P_x where:

P_y = percent protein content of fractions having lower protein content than the parent

Blending

The three parent flours (Alpine ground, unground, and Mikro ground) were blended in a large ribbon type blender before being divided into two lots, one for each separator. The individual fractions were blended in a tumbler type blender before sampling.

The bake blends were first blended in a tumbler type blender and then passed through an entoleter to break up the small lumps of the sticky high protein fractions.

RPM Determination

A built-in, mechanically-driven tachometer was used to measure the rpm of the Mikro separator rotor. Other rpm determinations below 3600 rpm were made by a speed indicator and those above 3600 rpm by a Strobotac.

Air Rate of Flow Measurement

Air velocity measurements on the Turbo, Hosokawa, and Mikro were made by measuring velocity pressure with a pitot tube and inclined manometer. Volume flow rate calculations (cfm) were made assuming standard conditions.

RESULTS AND DISCUSSION

Turbo Separator on Unground Flour

The results of the fractionation of the unground flour using the Turbo separator are shown in Fig. 10. The particle size distribution curves of this fractionation are shown on pages 69-72 of the appendix. Good protein shifts and the expected accompanying ash shifts were obtained.

Micron Separator Preliminary Tests

The finest cut (B) was attempted first on the Micron. The following settings were used: separator rotor 2300 rpm, 150 cfm total air flow, 80 cfm primary air flow, medium elutriation ring, adjustable inner pipe ½ inch above the lower lip of the elutriation ring (hereafter referred to as low position), and a feed rate of 150 pounds per hour. According to the basic operating principles this combination of settings should produce a very fine B fraction. The B fraction was less than 2% of the feed; the mass median diameter at '50% finer than' was 6.5 sedimentation equivalent diameter (S.E.D.) microns. The Turbo's B fraction had a median diameter of 5.3 microns and the fraction was 4% of the parent. At this point it was clear that further tests on the Micron were necessary in order to (1) obtain a finer B fraction, and (2) to obtain a larger percentage of the fraction with improved fineness.

Feed rates were varied from 90 to 240 pounds per hour and it was found that at the higher feed rates a smaller amount of

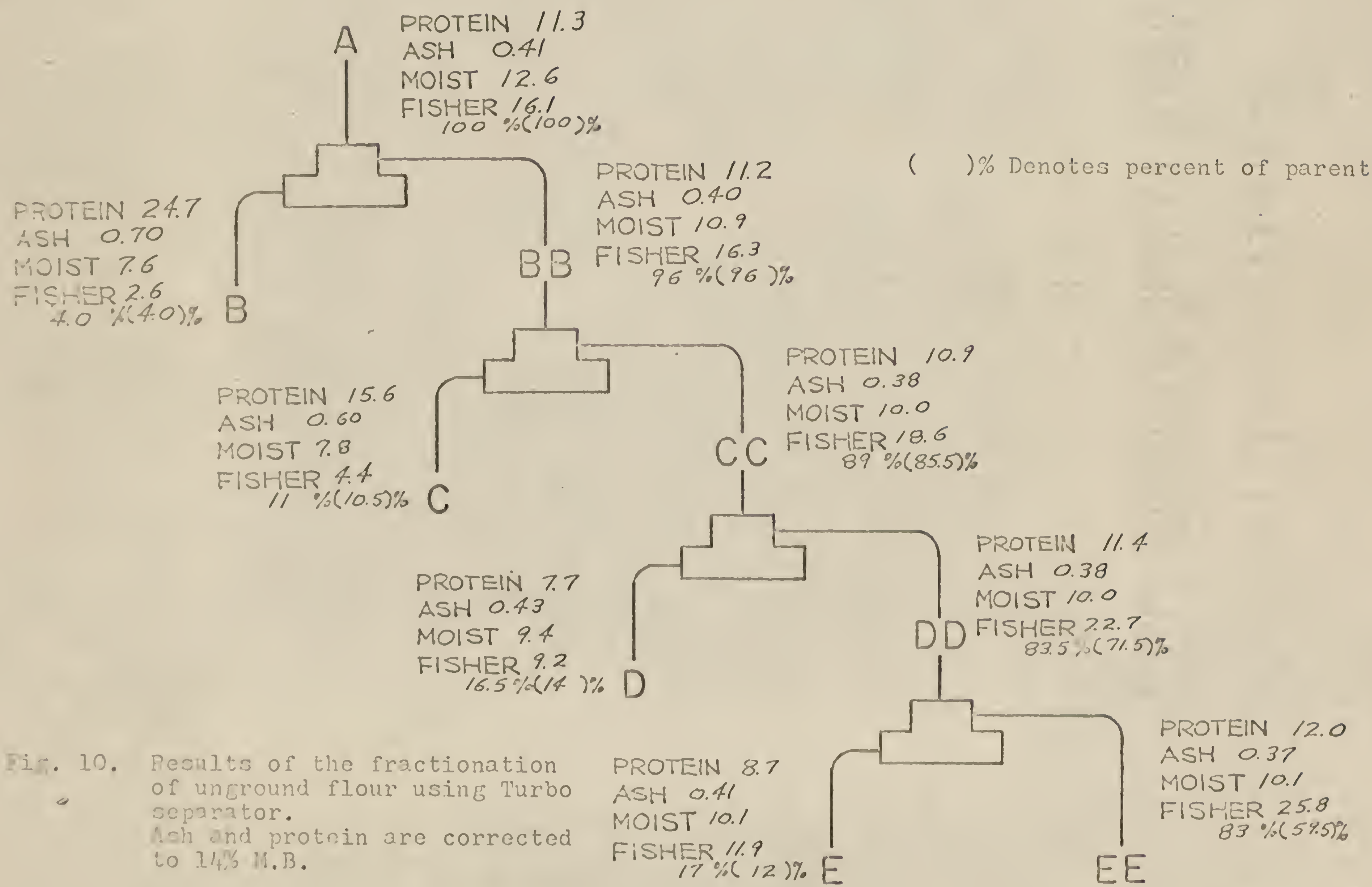

Fig. 10. Results of the fractionation of unground flour using Turbo separator.
Ash and protein are corrected to 14% M.B.

finer product was obtained. Since the pullout (percentage of feed) was already low and since feed rates below 125 pounds per hour seemed unreasonable for the Micron, feedrates of 125 to 150 pounds per hour were used.

Elutriation rings were changed and tests were run to determine their effect. The rings were extremely difficult to interchange due to the crude method of hooking the rings in place. Results of the tests indicated that none of the three different rings caused very much change in the fractions. The ring with the smallest inside diameter caused more large particles to be accepted into the fines with no measurable increase in pullout. For the reasons above, the medium ring was used for all subsequent tests.

The tests showed that moving the adjustable inner pipe up and down from one extreme to the other caused very little difference in both the pullout and particle size distribution of the B fractions obtained, as seen on page 73 of the appendix. According to the manufacturer (30), dispersion is better when the tube is in the low position. For these reasons the tube was used in the low position. Page 74 of the appendix shows that a finer fraction was obtained with no measurable loss of pullout when 2700 rpm (max recommended) was used. The only adjustment that remained to be tested was total air flow and the primary-secondary air ratio. Tests showed (see page 75 of the appendix) that the total air flow could be increased from 150 to 300 cfm with only a small loss of fineness and a major increase in pullout. It was found that 300 cfm total air was the best setting.

A primary-secondary air ratio of 2:1 was best, and thus 200 cfm of primary air and 100 cfm of secondary air were used on B cut. The settings for the other three cuts were determined in the same manner and the final settings used in the comparative tests are shown in Fig. 11.

Micron Separator on Unground Flour

Figure 12 shows the results of the fractionation of the unground flour using the Micron. The particle size distribution curves are on pages 76-79 of the appendix. When the results of the first two fractionations are compared, the major differences are: B and C fractions produced by the Turbo were higher in protein than those produced by the Micron, and a larger amount of each of the four fine fractions was produced by the Turbo. The B fraction produced by the Turbo had a median size 0.8 microns finer than the Micron's B fraction; this 0.8 microns of additional fineness resulted in a 4% higher protein content. The two separators produced C fractions with very similar particle size distributions; the Turbo's C fraction had more fine particles and this probably was the source of the higher protein content of the Turbo's C fraction. Both D and E fractions produced by the Micron compared very favorably, except that the pullout was lower.

Alpine Grinder Results

Preliminary tests showed that the rpm of the rotor decreased considerably when loading the Alpine. For this reason, the Strobotac was used to determine the rpm under load and to monitor

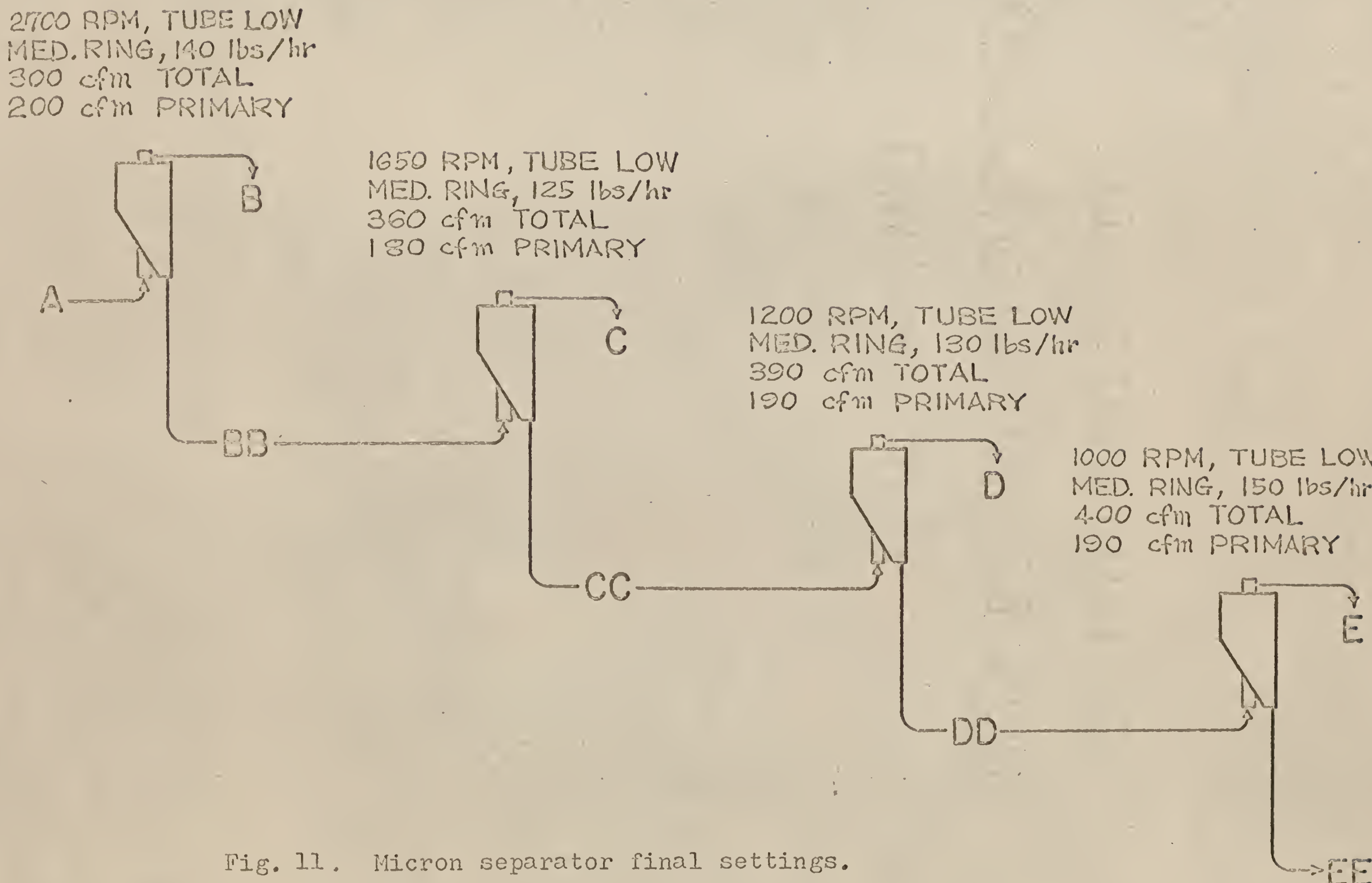

Fig. 11. Micron separator final settings.

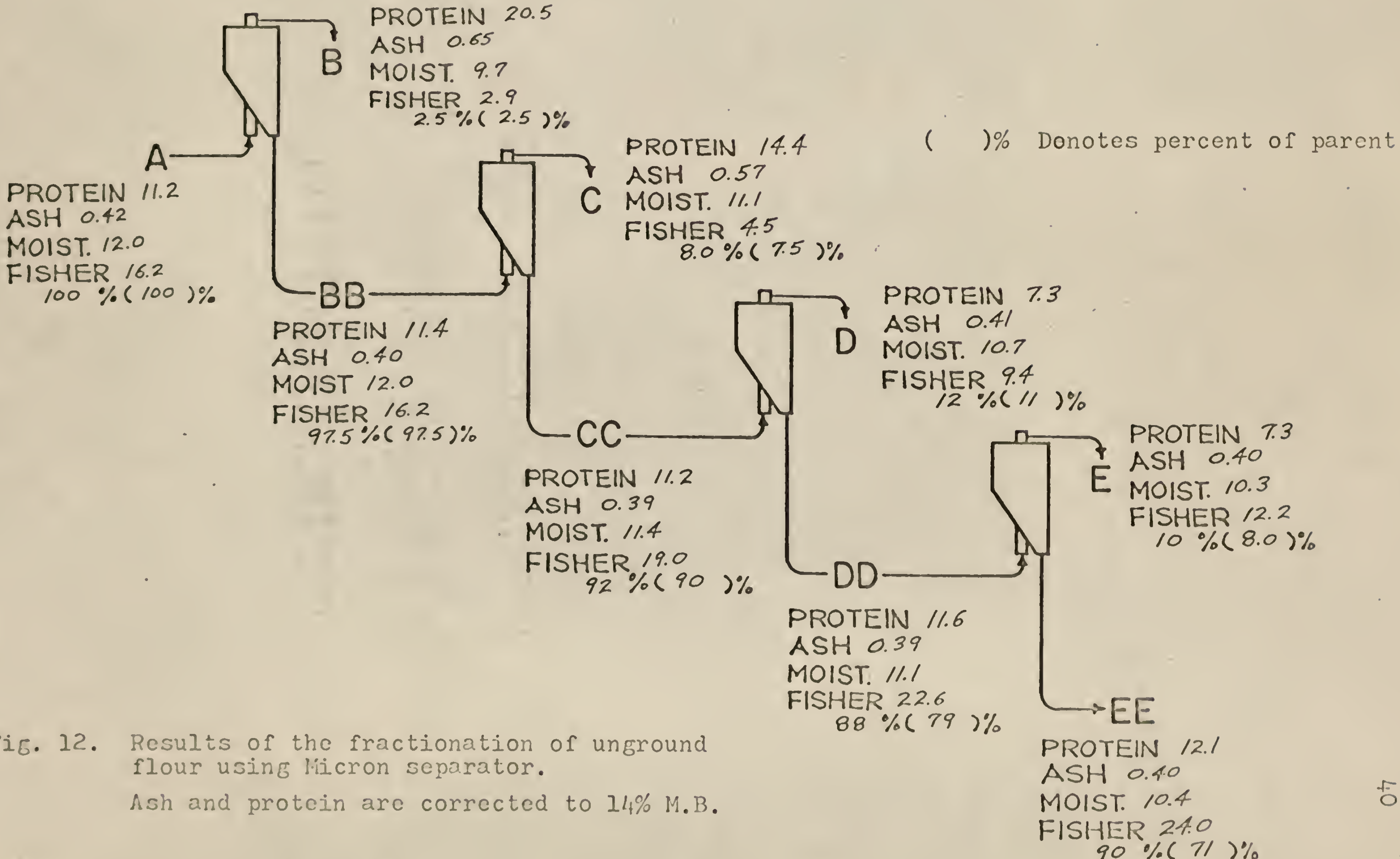

Fig. 12. Results of the fractionation of unground flour using Micron separator.

Ash and protein are corrected to 14% M.B.

the speed during the grinding. The rpm of the driven belt pulley was measured with the Strobotac. The gear ratio of the Alpine was determined to be 4:1 and the diameter of the outside row of pins measured from pin centers was a measured 5.40 inch. These two measurements were used to calculate a conversion factor of 5.68 to be applied to the pulley speed to obtain pin velocity in feet per minute (fpm). A feed rate of 30 pounds per hour caused a pull down from 23,500 fpm at no load to 21,300 fpm under load. These settings provided good grinding and were used to grind the flour for the comparative tests. The percentage finer than 20 microns was increased more (16.6% to 51.0%) than that finer than 10 microns (4.3% to 19.0%). The particle size distribution curve and product temperature before and after grinding are shown in Fig. 13.

Preliminary Tests on Mikro Grinder

The effect of varying only the separator rpm is shown on page 80 of the appendix. Increasing the rpm narrows the size range of the ground product. The percentage finer than 20 microns was increased more than that finer than 10 microns when using higher rpm. At the same grinding rotor rpm, separator rpm, and feed rate, higher air flow rates cause the ground product to be coarser as seen on page 81 of the appendix. These first two tests were run on a flour made from Gaines wheat; all other tests were made using the special flour. Page 82 of the appendix shows the results of changing only the grinding rotor rpm when using the pin rotor. This test and subsequent tests were run using a feed

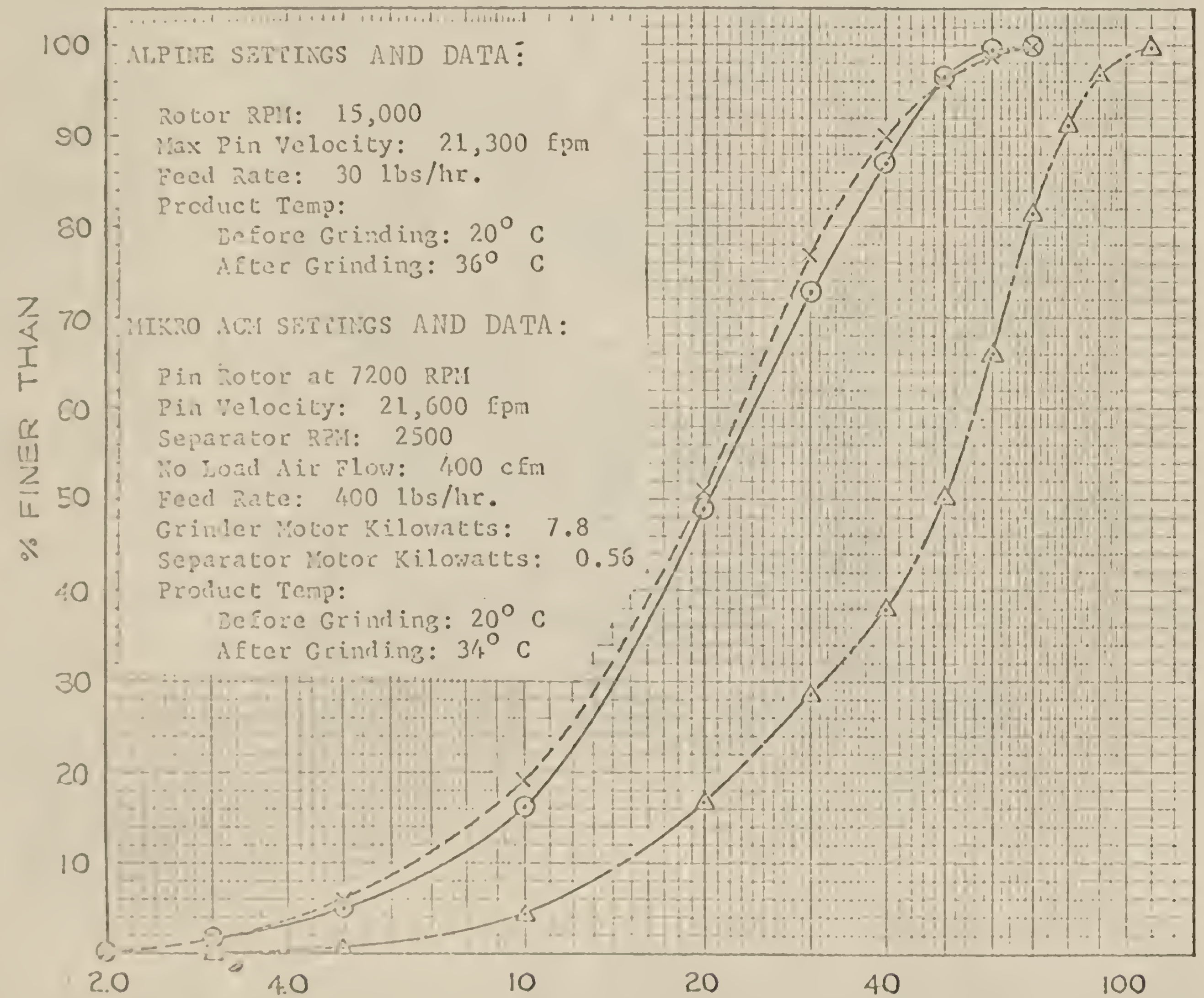

Fig. 13. Particle size distribution of Alpine ground, Mikro ground, and unground flour, plus grinder settings and data.

	Alpine Ground	Mikro Ground	Un-Ground
Graph Symbols	×	⊙	△
Sample Number	F072	F073	F023
Fraction	A	A	A
S.E.D. (Micron) Size	% Finer		
160			
140			
120			
110			99.9
100			
90			96.7
80			91.2
70	99.9	99.9	81.5
60	98.8	99.6	66.0
50	96.1	96.6	50.0
40	90.0	87.0	37.8
30	77.0	73.0	28.8
20	51.0	49.0	16.6
19			
12			
10	19.0	16.0	4.3
9			
7			
5	6.0	5.0	0.6
3	1.5	1.5	0.1
2	0.1	0.1	
1			
Fisher	9.3	9.7	16.4
Prot.	11.0	11.0	11.3

S.E.D. (Micron) Size ⟶

rate of 400 pounds per hour since this feed rate produced the best results without overloading the grinding motor and/or plugging the grinder. Higher grinding rotor speeds considerably increased the 'percent finer than' in the 20-40 micron range, but did not increase the percent finer than 10 microns and below. The power requirements were higher at the higher rotor speeds, but these increases seemed to be due mostly to the increased "no load" power requirements. The temperature rise of the product was greater at higher grinding rotor speeds. Due to the greater power requirement, higher temperature rise, and possibility of increased starch damage at the higher speeds, the low speed (7300 rpm) was used with the pin rotor on all subsequent tests.

The pin and bar rotors were compared and the results are recorded on page 83 of the appendix. Attempts were made to operate the bar rotor at higher speeds, but the grinding motor was overloaded unless the feed rate was kept below 400 pounds per hour. When using the bar rotor at higher speeds, higher temperature rises resulted with no major improvement in fineness; therefore, the bar and pin rotors were compared only at 7300 rpm. The bar rotor required more power but gave a finer product. It was suspected that the increased fineness produced by the bar rotor was at least partly due to a decreased air flow, since the separator motor was using more power which indicated a more congested condition inside the mill. An assistant, who recorded the static pressure at the grinder's outlet, found that the pressure was greater (more negative) when the bar rotor was used. By increasing the separator rpm the pin rotor gave the same degree of fineness as the bar rotor and required less power; therefore, the pin rotor was chosen for the comparative tests. Settings were used which gave a particle size distribution curve and temperature rise similar to those produced by the Alpine. The pin velocities were very similar: see Fig. 13 for the grinding results. The Mikro ground flour was somewhat coarser than the Alpine ground flour but it should be emphasized that the Mikro was capable of producing a finer grind.

Turbo Separator on Mikro and Alpine Ground Flour

Analysis of the fractions produced by the Turbo on the Mikro and Alpine ground flours are shown respectively in Figs. 14 and 15. The particle size distribution curves are on pages 84-87 and 88-91 of the appendix, respectively. Two major differences were noted when these fractions were compared to those obtained from the unground flour: (1) the E fractions obtained from the two ground flours were lower in protein than the E fraction from the unground flour; and (2) greater amounts of the fine fractions B, C, D, and E were produced from the ground flours.

Micron Separator on Mikro and Alpine Ground Flour

Figures 16 and 17 respectively show the results of the Micron separated Mikro and Alpine ground flours. The particle size distribution curves of the Mikro ground flour are on pages 92-95, and those of the Alpine ground flour are on pages 96-99 of the appendix. When these two fractionations were compared to the fractionation of the unground flour, the major difference noted was

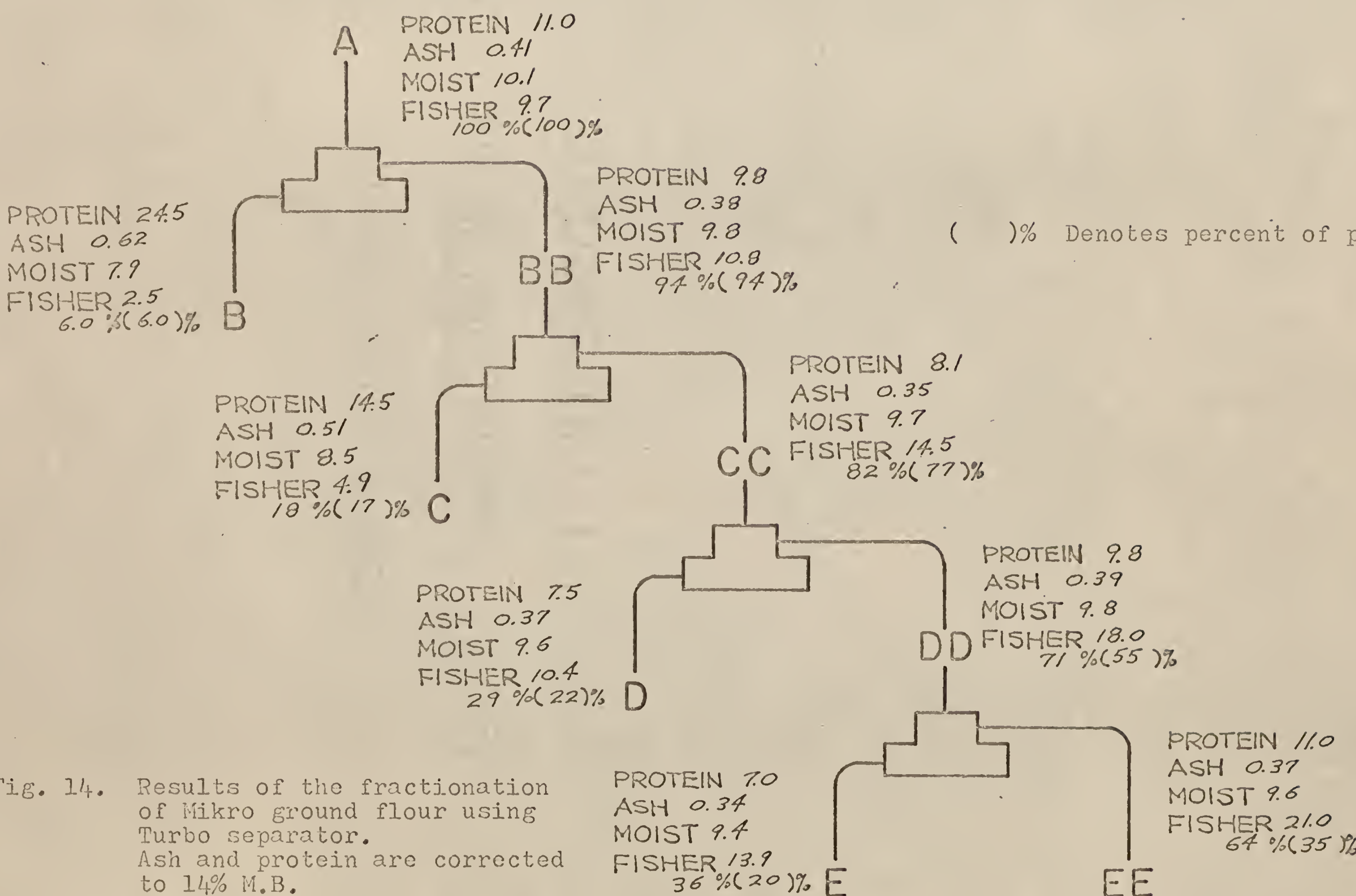

Fig. 14. Results of the fractionation of Mikro ground flour using Turbo separator.
Ash and protein are corrected to 14% M.B.

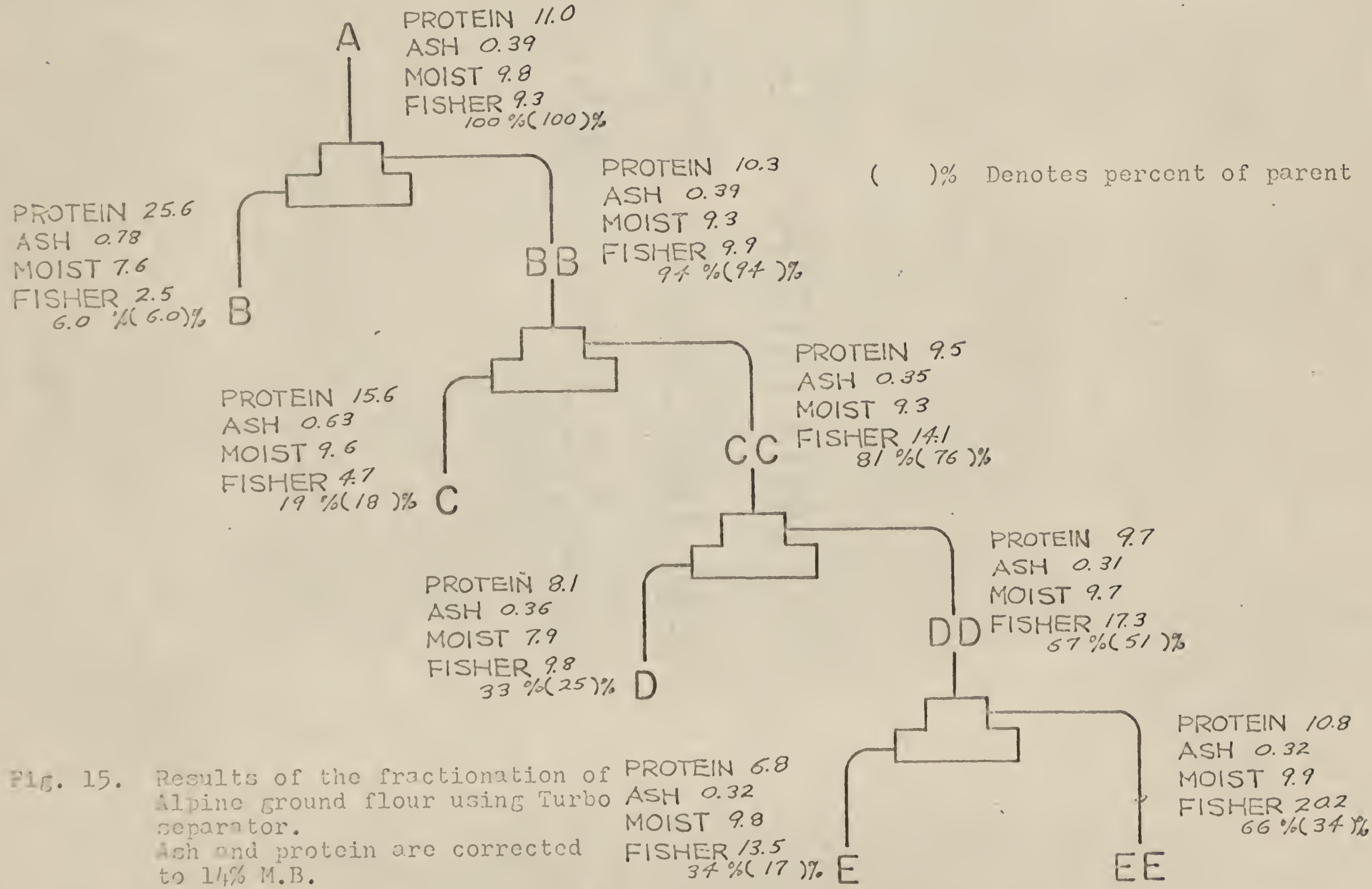

Fig. 15. Results of the fractionation of Alpine ground flour using Turbo separator.
Ash and protein are corrected to 14% M.B.

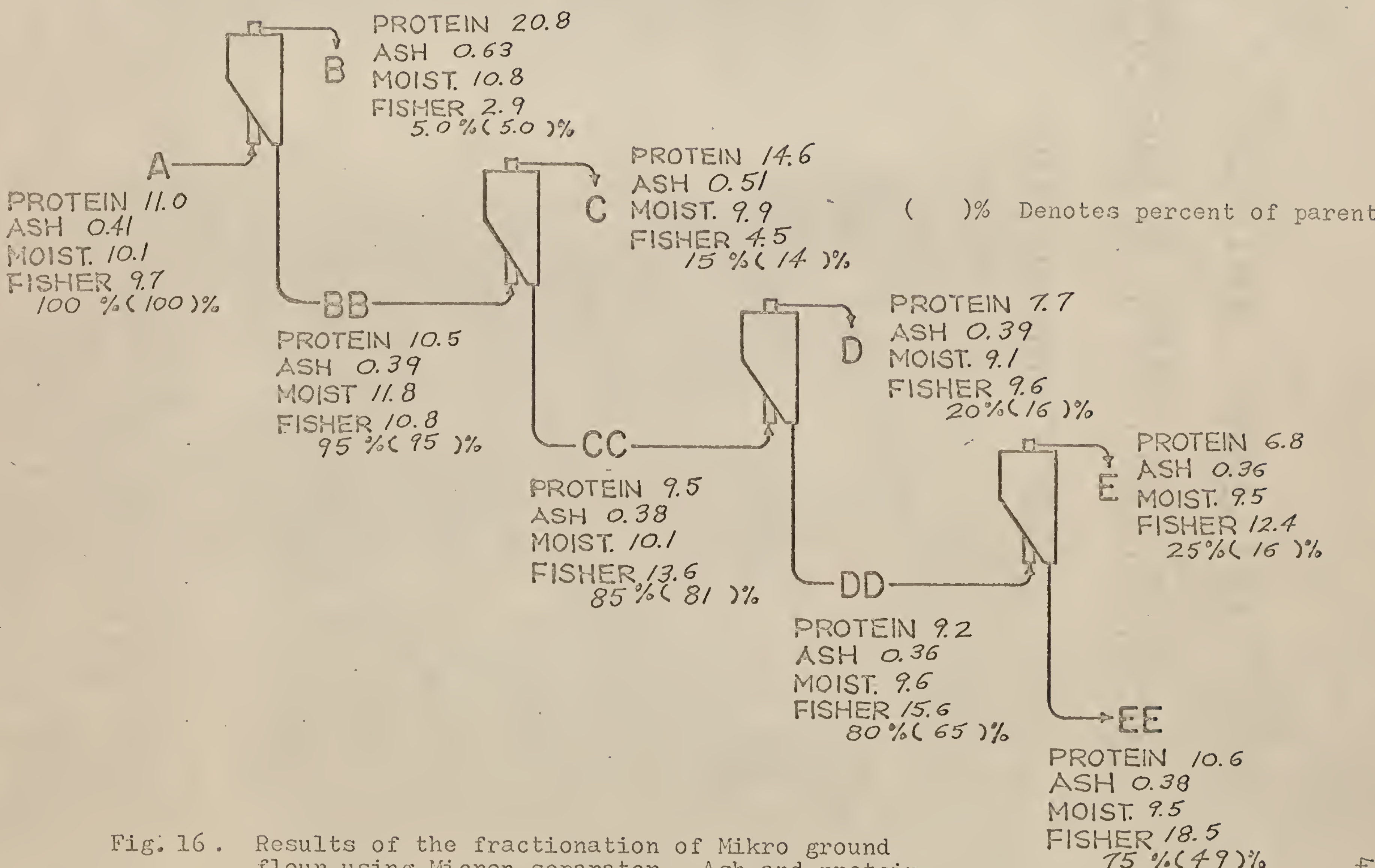

Fig. 16. Results of the fractionation of Mikro ground flour using Micron separator. Ash and protein are corrected to 14% M.B.

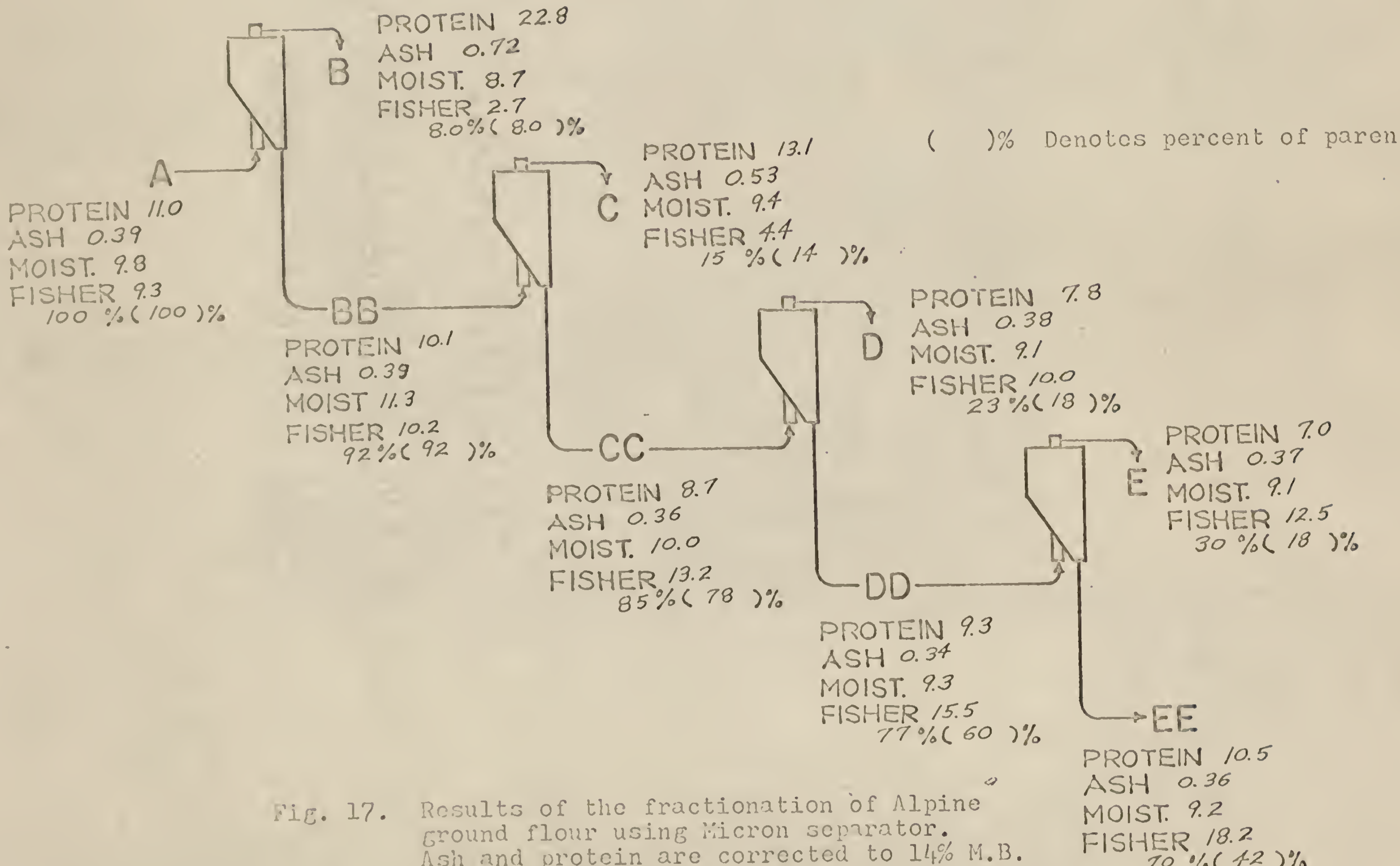

Fig. 17. Results of the fractionation of Alpine ground flour using Micron separator. Ash and protein are corrected to 14% M.B.

that greater amounts of the fine fractions were produced from the ground flours.

Comparison and Summary of the Six Fractionations

The Fisher number of the four fine fractions (A, B, C, D) and fraction EE are presented in the histogram form in Fig. 18. The dashed line denotes the Fisher number of the parent flour used for each of the six fractionations. The Fisher number was greatest for the EE fraction; in all six instances it was greater than the Fisher number of the parent. Both separators when used to fractionate the unground flour produced four fine fractions (B, C, D, E) with Fisher numbers lower than the parent's Fisher number. The four fractionations which involved using ground flour had D and E fractions with Fisher numbers nearly equal to or greater than the parent's. In all six instances, fractions B and C had Fisher numbers considerably lower than the parent's.

Figure 19 shows protein histograms and protein shift indices for the six fractionations. The protein shift indices of the fractionations produced by the Micron were lower than those of the Turbo, mainly because (1) the Micron produced B and C fractions of lower protein content, and (2) the Micron produced smaller percentages of all four fine fractions. The Alpine ground flour was finer than the Mikro ground flour: therefore, the separators produced greater amounts of the fine fractions from the Alpine ground flour. The histograms and protein shift indices verify this. Fractions B and C from each of the six fractionations had higher protein contents than their respective parent. Fractions

Fig. 18. Histograms of the Fisher numbers of the six fractionations. The dashed line indicates the Fisher number of the parent flour.

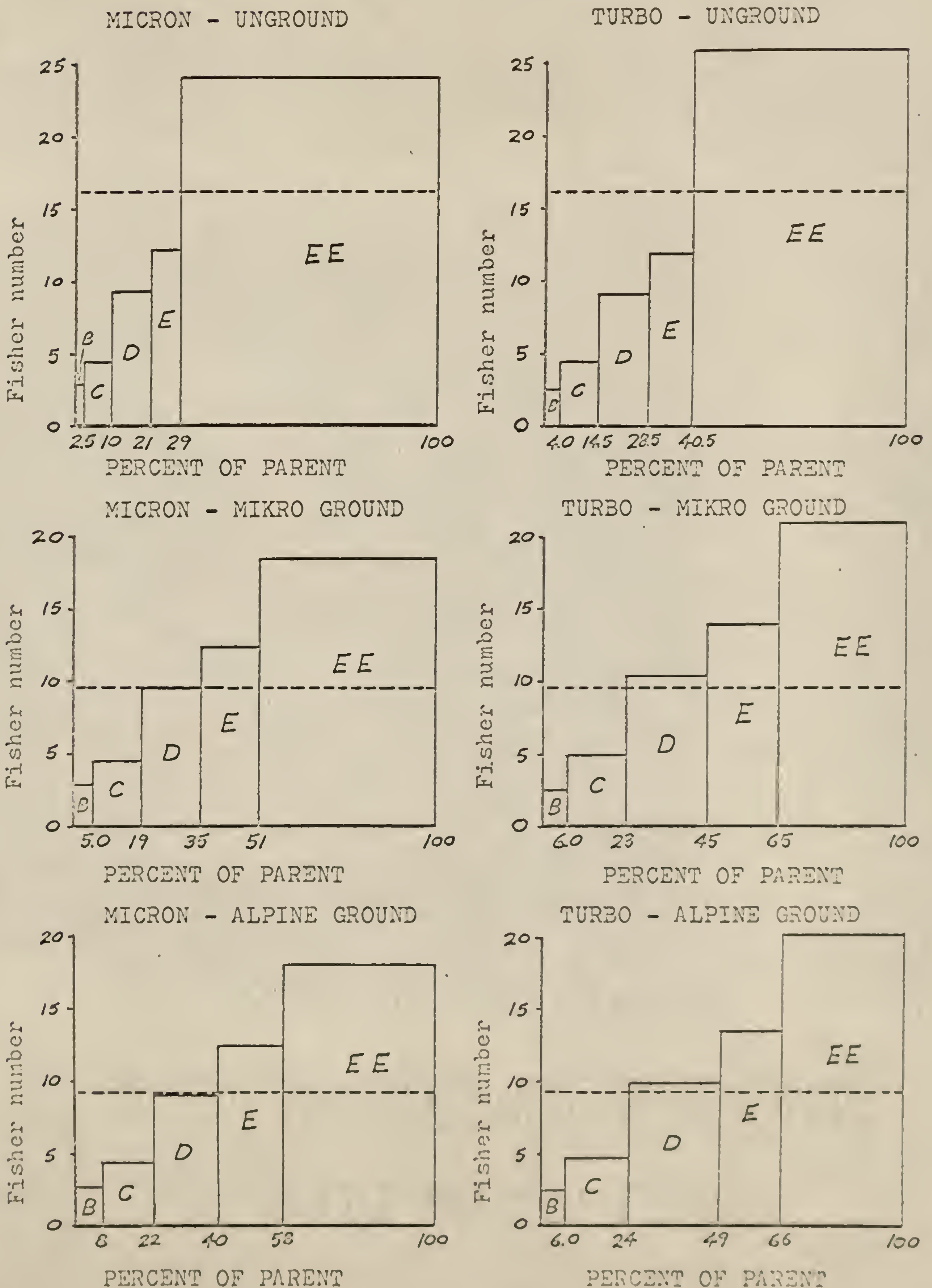

Fig. 19. Protein histograms and Protein Shift Indices of the six fractionations. The dashed line indicates the protein content of the parent flour.

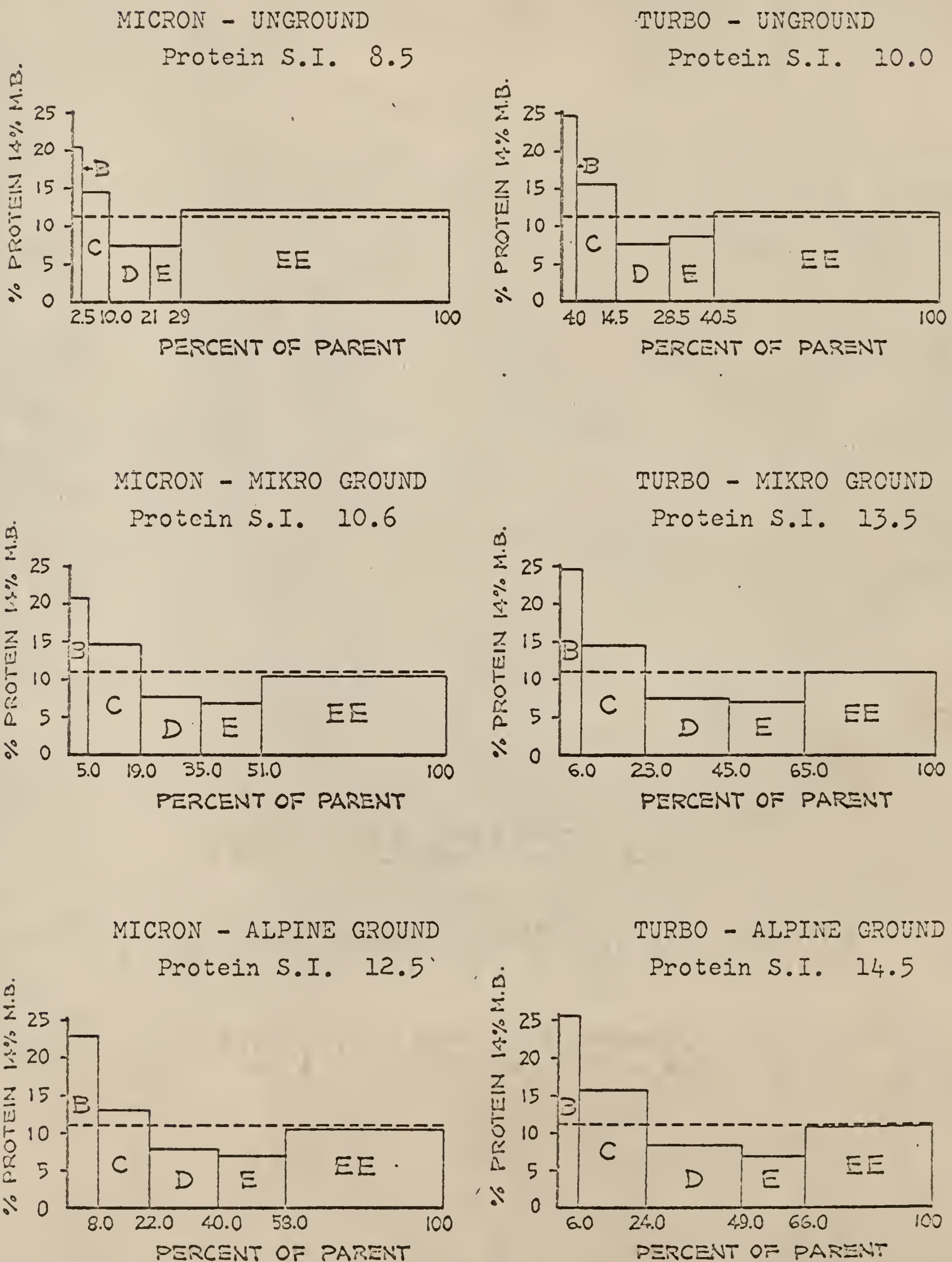

D and E had lower protein contents than their respective parent. Each of the six EE fractions had a protein content nearly equal to or greater than that of its parent.

Ash histograms of the six fractionations are shown in Fig. 20. As the fractions became coarser, the ash content decreased except for the EE fractions produced from the Mikro ground flour. The EE fractions produced by the Turbo from each of the three parent flours all had lower ash contents than those produced by the Micron separator. The EE fraction produced by the Turbo from the Alpine ground flour was especially low in ash.

Histograms of the Amylograph Brabender Units are shown in Fig. 21. The two finest fractions B and C had readings lower than the parent and the other fractions. The six E fractions had the highest readings from their respective fractionation; the four E fractions produced from ground flour all had readings that were greater than 960 B.U. In all six instances the EE fractions had lower readings than their respective E fractions.

The farinographs of fractions A, B, C, D, E, and EE from each of the six fractionations are shown in Figs. 22-27. These farinographs were run at the moisture contents that existed after the fractionations were accomplished. The low moisture contents of many of the fractions may have influenced the determined absorptions even though they were corrected to 14% M.B. All the high protein B and C fractions had longer peak times and higher valorimeter scores than their parents. The higher protein B and C fractions produced by the Turbo separator had longer peak times than those of the B and C fractions produced by the Micron

Fig. 20. Ash histograms of the six fractionations. The dashed line indicates the ash content of parent flour.

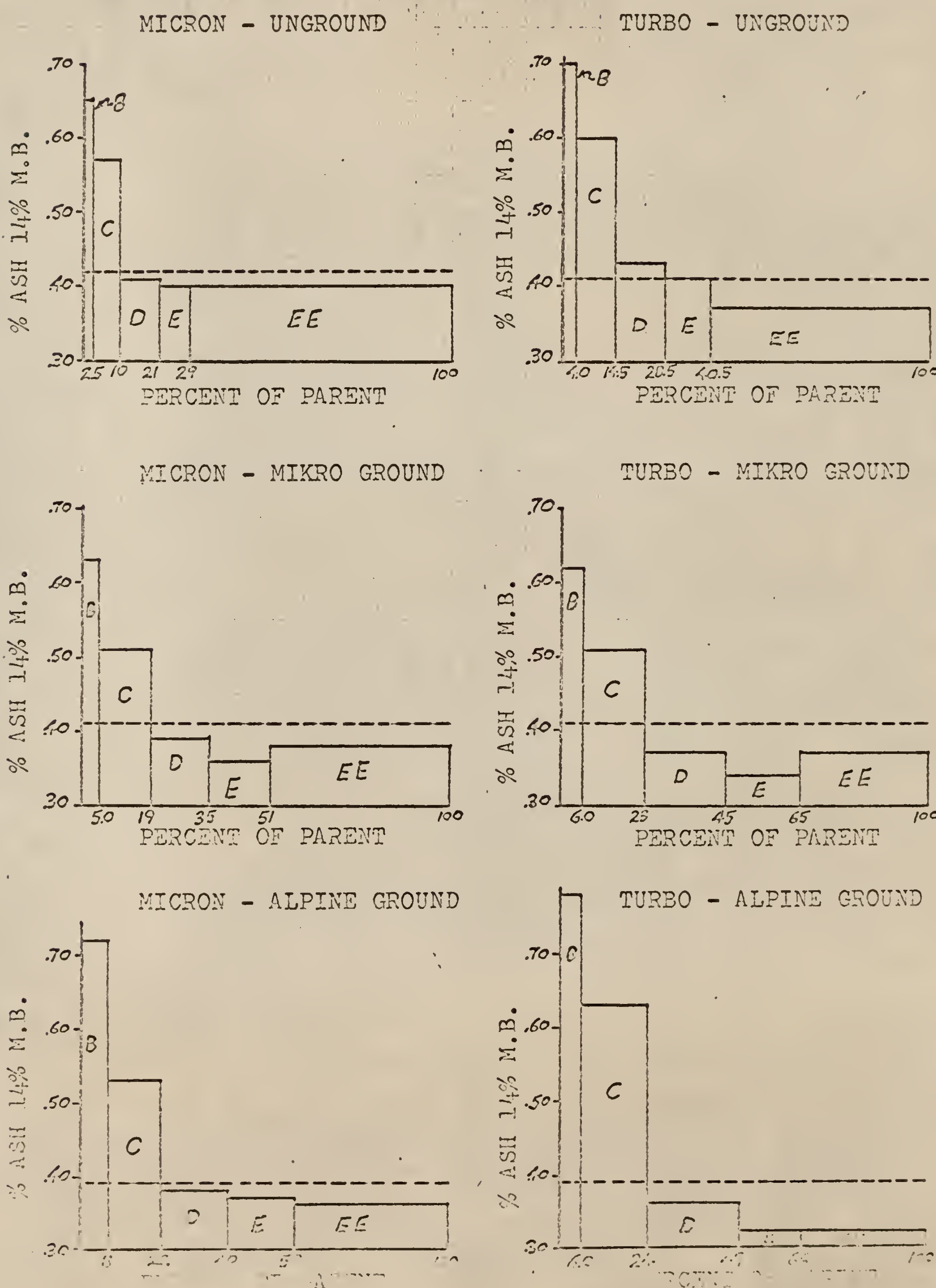

Fig. 21. Histograms of the Amylograph Brabender Units (B.U.) of the six fractionations. The dashed line indicates the B.U. of the parent flour.

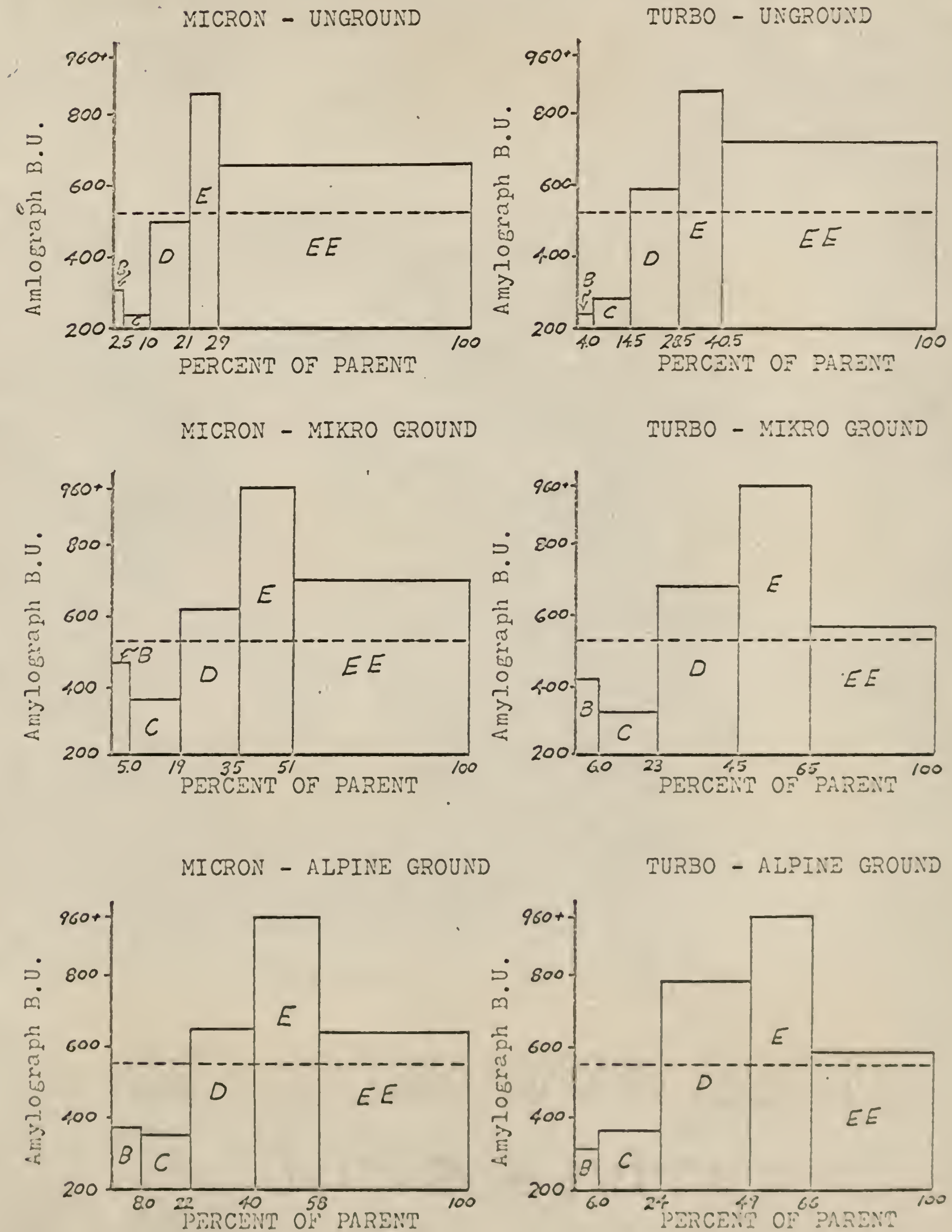

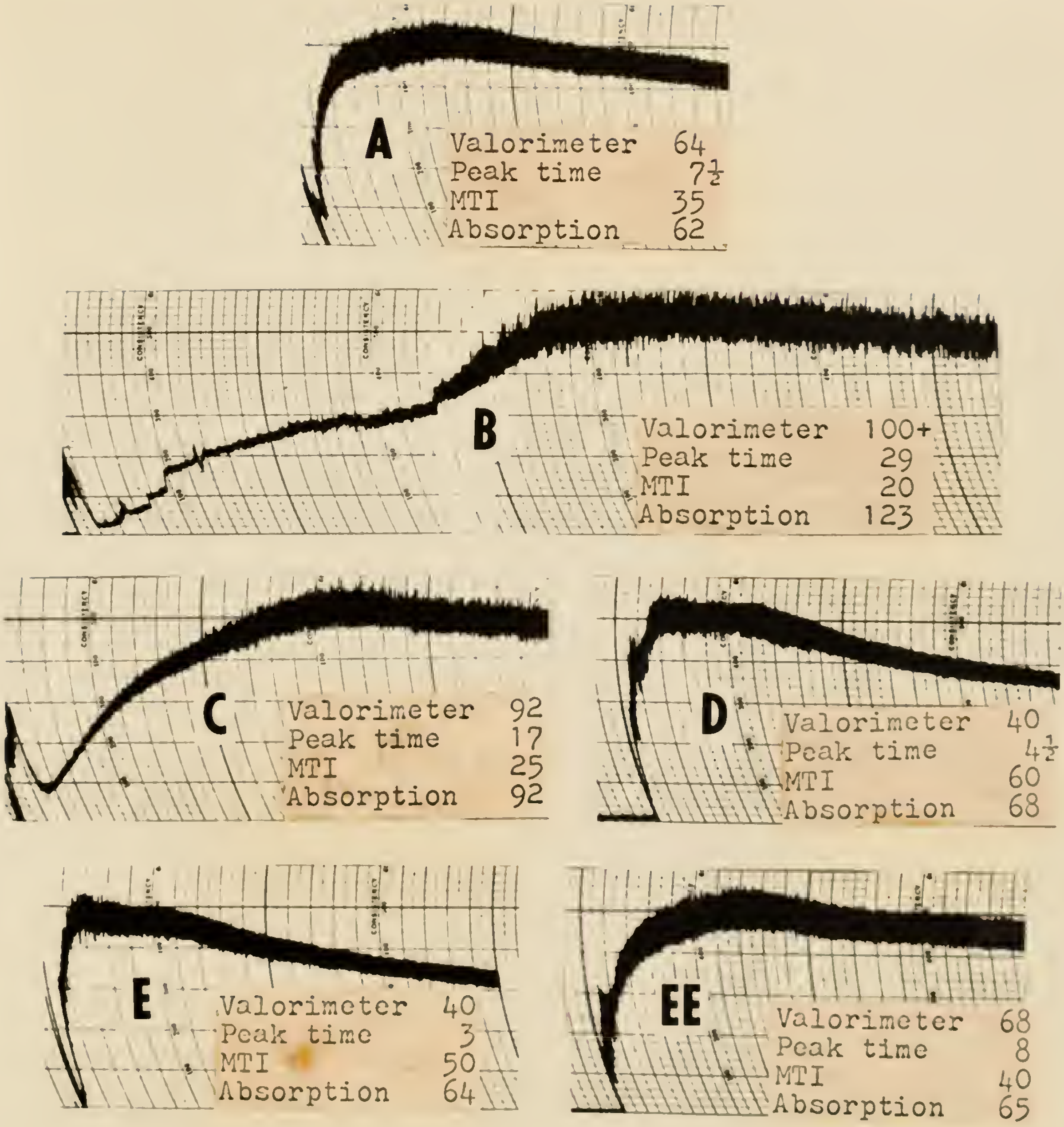

Fig. 22. Farinographs of the unground parent, four sub-seive-size fractions, and EE fraction produced by the Turbo separator.

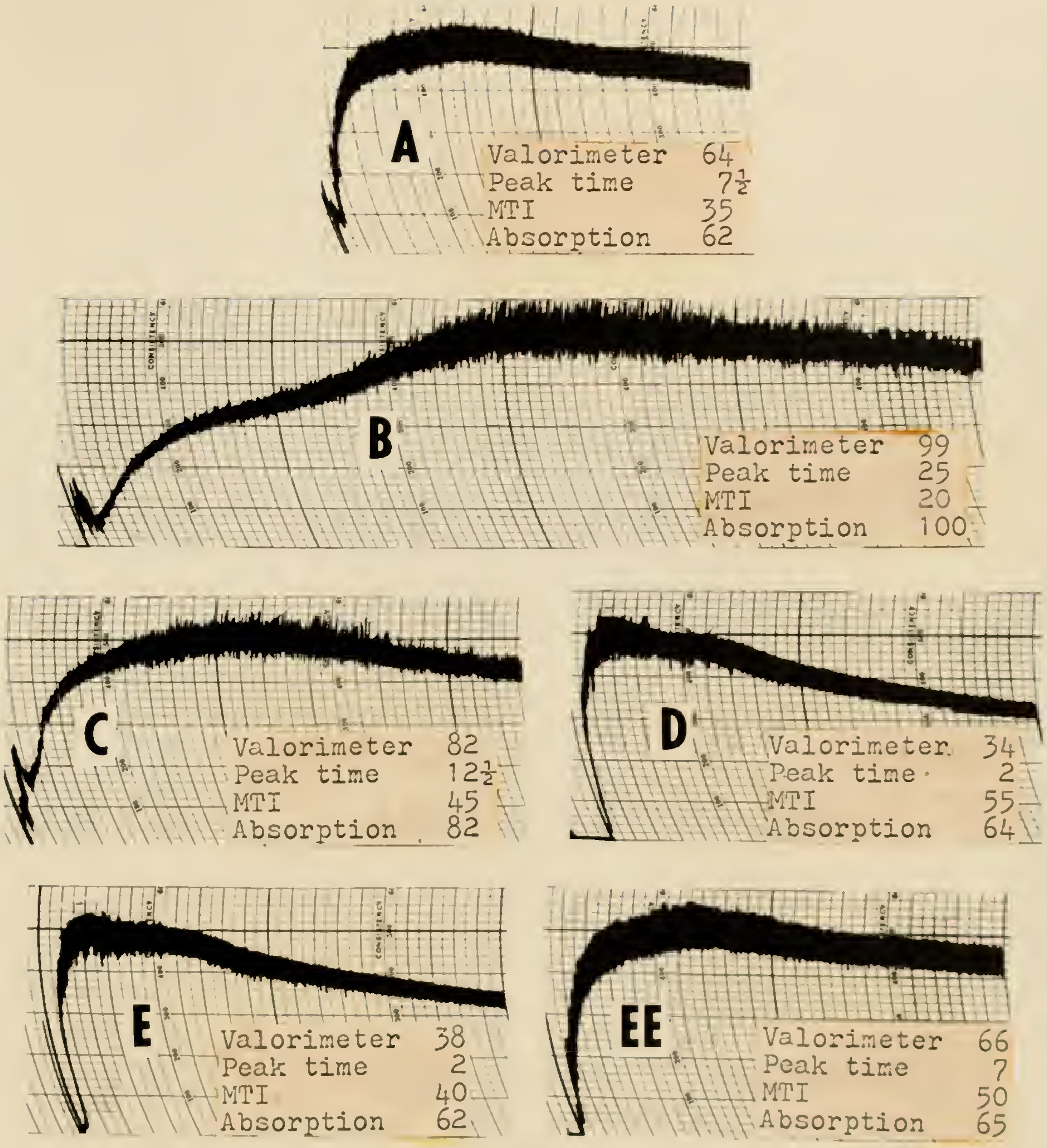

Fig. 23. Farinographs of the unground parent, four sub-seive-size fractions, and EE fraction produced by the Micron separator.

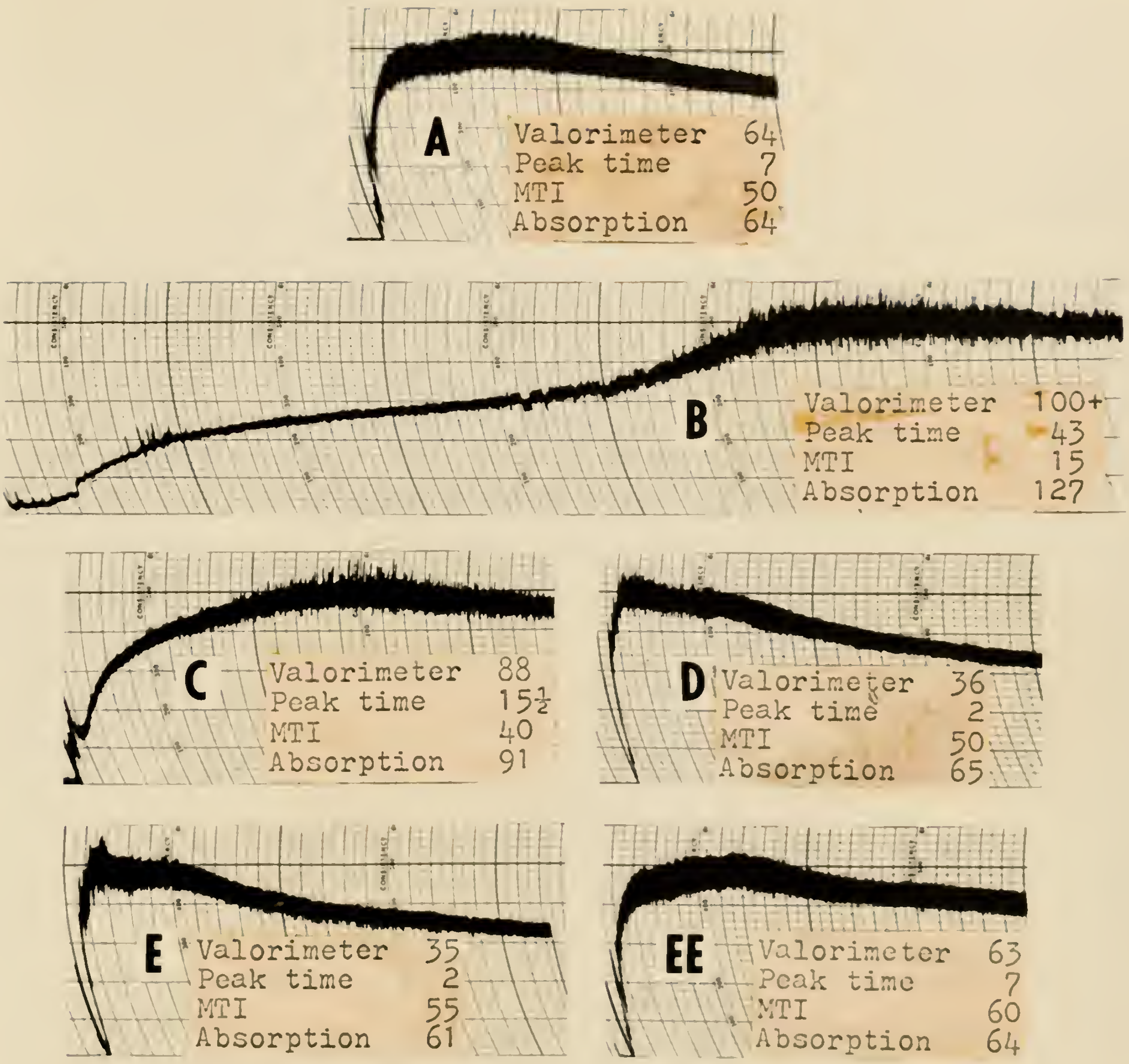

Fig. 24. Farinographs of the Mikro ground parent, four sub-seive-size fractions, and EE fraction produced by the Turbo separator.

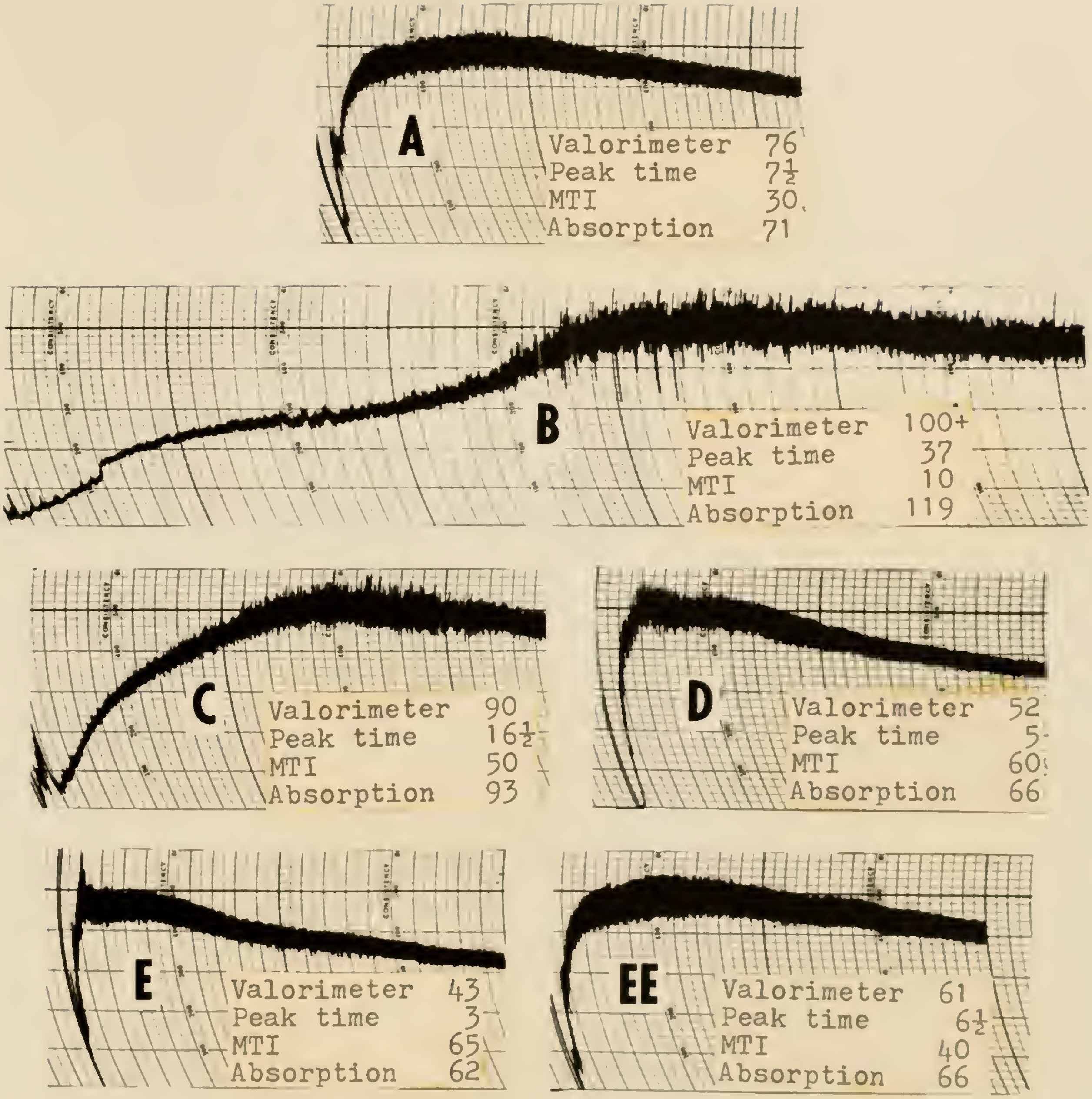

Fig. 25. Farinographs of the Alpine ground parent, four sub-seive-size fractions, and EE fraction produced by the Turbo separator.

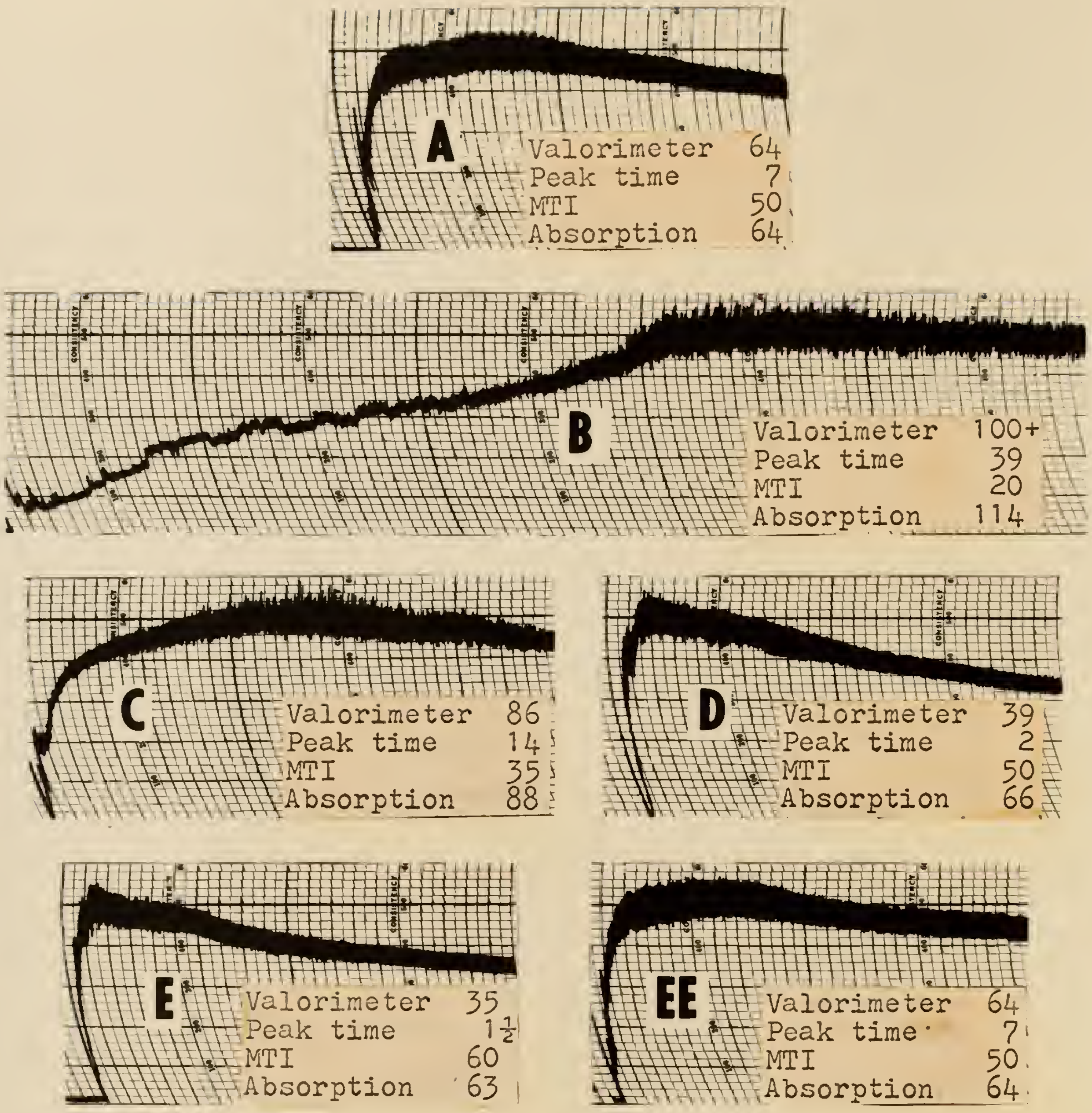

Fig. 26. Farinographs of the Mikro ground parent, four sub-seive-size fractions, and EE fraction produced by the Micron separator.

separator. Peak times of the B fractions produced by both separators from the Mikro ground flour were longer than those of the other B fractions even though the protein contents were not higher. All the low protein D and E fractions had shorter peak times and lower valorimeter scores than their parents. For all six of the fractionations, the farinograph measurements of EE fraction were most similar to the measurements of the parent.

The Micron separator produced B fractions which were lower in protein content and smaller in quantity than the B fractions produced by the Turbo separator. Analyses of variance were performed on the geometric means of the B fractions from the six fractionations. The particle size distributions of the B fractions produced by the two separators from the unground flour plotted as two substantially straight and parallel lines on log-probability graph paper. The two B fractions produced from each of the Alpine and Mikro ground flours plotted in the same manner. Duplicate M-S-A sedimentation particle size determinations were made on each of the six B fractions. The twelve resulting particle size distributions were plotted on log-probability paper and the twelve geometric mean diameters (in S.E.D. microns) were determined at the '50% finer than' point. Figure 28 shows an analysis of variance of the geometric means using a triply nested fixed effects model. The separator effects were very significant and the grinder effects were not significant.

A one-way analysis of variance seen in Fig. 29 shows that the three geometric means (average of two determinations in each instance) produced by the Micron separator were not significantly

Fig. 28. Analysis of variance using a triply nested fixed effects model on the geometric means of the six (B) fractions.

Source	DF	MS	F calc.	$F_{\alpha=0.005}$	$F_{\alpha=0.100}$
Separators	1	2.260	226***	18.64	3.78
Grinders	4	0.015	1.5	12.03	3.18
Error	6	0.010	------	-----	---

Fig. 29. One-way analysis of variance on the geometric means of the six (B) fractions.

Source	DF	MS	F calc.	$F_{\alpha=0.005}$	$F_{\alpha=0.100}$
Treatments	5	.464	46.4**	11.46	3.11
Error	6	.01	----	-----	----

Solid line indicates not signif. different using $LSD_{\alpha=0.005}$ =.43

Dotted line indicates not signif. different using $LSD_{\alpha=0.100}$ =.19

MICRON-ALPINE	MICRON-UNGROUND	MICRON-MIKRO	TURBO-UNGROUND	TURBO-MIKRO	TURBO-ALPINE
6.00	5.95	5.90	5.15	5.15	4.95

different. Also, the three geometric means of the B fractions produced by the Turbo separator were not significantly different. The geometric means of the Micron separator's three B fractions were all very significantly different from each and all of the three geometric means of the B fractions produced by the Turbo separator.

CONCLUSIONS

The results of the grinding tests and six fractionations indicated that the Mikro grinder was substantially capable of meeting the standards set by using the Alpine grinder. The Mikro is capable of grinding flour very fine in one pass through the grinder. However, due to its design, the Mikro removes the fine product from the grinding zone soon after it is produced. This action helps the Mikro produce a ground product of narrow particle size distribution. This study found that this type of grinding controls the top size and minimizes the grinding of the fines.

The grinding tests showed that the particle size distribution could be narrowed and the median particle size reduced by using singly or in combination the following adjustments: higher grinding rotor rpm, higher separator rpm, and/or lower air flow rates. However, these finer grinds did not normally produce substantially more product finer than 10 S.E.D. microns. The settings required to substantially increase the amount of product finer than 10 S.E.D. microns resulted in ground product temperature rises much higher than those produced with the settings used for the comparative tests.

The results of the six fractionations performed in this study showed that the Micron separator was not capable of meeting the overall standards established by using the Turbo separator. Specifically, the Micron separator did not produce B and C fractions with protein contents as high as those produced by the Turbo. The Micron separator produced lower percentages of the four fine fractions (B,C,D,E). The Micron did appear capable of producing D and E fractions with protein contents as low as those produced by the Turbo.

LITERATURE CITED

1. Anonymous. Seal of secrecy on air classification of flour broken at 61st AOM conference in Buffalo. Amer. Mill. and Processor 85: (6) 26-39 (1957)

2. Buttrose, M.S. The ultrastructure of developing wheat endosperm. Aust J. Biol. Sci. 16: (2) 308-315 (1963)

3. Catlin, A. W. Formulas applicable to air separation. Rock Products 34: 46-48 (1931)

4. Cereal Laboratory Methods. Seventh edition. St. Paul, Minnesota: Amer. Assoc. of Cereal Chem., 1962.

5. Croteau, J. L. A practical method of measuring flour particle size. Milling Production 25: (5) 1, 10, 12, 18 (1960)

6. Duyckinck, Robert W. How a new classifying pulverizer improves efficiency. Amer. Mill. and Processor 92: (10) 18-19 (1964)

7. Feed Production Handbook. Kansas City: Feed Production School Inc., 1961

8. Fisher Sub Sieve Sizer Instruction Manual. Pittsburgh, Pa: Fisher Scientific Co.

9. Gracza, Rezsoe. The subsieve-size fractions of a hard red spring wheat flour produced by air classification. Cereal Chem. 37: 579-593 (1960)

10. Gracza, Rezsoe. The subsieve-size fractions of a soft wheat flour produced by air classification. Cereal Chem. 36: 465-487 (1959)

11. Gracza, Rezsoe. Studies of size classification indices. The Northwestern Miller Part 1, The efficiency of size classification 265: (1) 32-40 (1961) Part 2, The critical particle size 265: (3) 40-45 (1961)

12. Graham, J. C. The use of air classifiers in the flour milling industry. Milling 144: 215-219 (1965)

13. Hall, Arthur L. Introduction, air classification symposium. Mining Engineering 9: 1112-1113 (1957)

14. Herdan, G. Small Particle Statistics. Houston, Texas: Elsevier Publishing Co., 1958

15. Hess, Kurt. Die protein und lipoiddiferenzierung in Mehl und kleber. Getreide und Mehl 3: (11) 81-85 (1953)

16. Hibbs, Arthur N., Shellenberger, J. A., and Pence, R. D. The theory of impact grinding with centrifugal machines. Trans AACC 6: (1) 26-31 (1948)

17. Irani, Riyad. Particle size distribution data. Cereal Sci. Today 6: (2) 35-39 (1961)

18. Irani, R. R. and Callis, C. F. Particle Size: Measurement, Interpretation, and Application. New York: John Wiley & Sons, 1963

19. Jennings, A. C., Morton, R. K., and Palk, B. A. Cytological studies of protein bodies of developing wheat endosperm. Aust J. Biol. Sci. 16: (2) 366-373 (1963)

20. Kaizer, Fritz. Six years of impact milling and air separation for protein fractionation. Amer. Mill. and Processor 88: (8) 14-16, 36-37 (1960)

21. Kent, N. L. Subaleurone endosperm cells of high protein content. Cereal Chem. 43: 585-601 (1966)

22. Kent, N. L. and Jones, C. R. The cellular structure of wheat flour. Cereal Chem. 29: 383-398 (1952)

23. Lukens, Alan R. Fine particle classification. Mining Engineering 9: 1120-1127 (1957)

24. Lykken, William H. Grinding and classifying in the subsieve range. Mining Engineering 9: 1118-1120 (1957)

25. M-S-A Particle Size Analyzer, Operating Procedures and Applications. Pittsburgh, Pa: Mine Safety Appliance Company, Bulletin #993405, Rev. 1959

26. Nenninger, E. Impact disintegration and air sifting. The Northwestern Miller 263: 3a-4a (1960)

27. Newton, Harry W. and Newton, William H. A study of classification calculations. Rock Products 35: 26-30 (1932)

28. Payne, Robert E. The optimal vortex classifier. Mining Engineering 9: 1113-1117 (1957)

29. Ponte, J. G. Jr., Titcomb, S. T., and Cotton, R. H. The particle size distribution of commercial break flours. Bakers Digest 41: (4) 24-28, 79 (1967)

30. Random test results and operating data. Pulverizing Machinery. Summit, New Jersey

31. Rozsa, Tibor A., Gracza, Rezsoe, and Ward, Arlin B. Process of reducing and surface treating cereal endosperm particles and production of new products through attendant separations. U. S. Patent 3,077,308. Feb. 12, 1963

32. Rozsa, Tibor A., Harrel, Chastain G., and Manning, Truman W. Wheat flour fractionation processes. U. S. Patent 3,077,407. Feb. 12, 1963

33. Sandstedt, R. M. Photomicrographic studies of wheat starch. Cereal Chem. I Development of the starch granules 23: 337-359 (1946)

34. Sloggett, Gordon R., Mattern, Paul J., and Walsh, Richard G. Air classification of wheat flour: a case study of the economic effects of technological progress. The Northwestern Miller Part 1 270: (4) 12-18 (1964) Part 2 270: (5) 11-18 (1964)

35. Sohns, V. E. and Majors, K. R. Cost of fractionating selected hard and soft wheat flours. Amer. Mill. and Processor 92: (7) 6-9 (1964)

36. Sullivan, Betty, Engebietson, W. E., and Anderson, Merlin L. The relation of particle size to certain flour characteristics. Cereal Chem 37: 436-455 (1960)

37. Tanaka, Tatsuo. Comminution laws, several probabilities. I-&-EC Process Des. and Devel. 5: (4) 353-358 (1966)

38. Testing Sieves and Their Uses, Handbook 53. Cleveland, Ohio: W. S. Tyler Co., 1963, 26-29

39. Treasure, C. R. G. Fine particle-size classification. Trans. Instr. Chem. Engrs. 43: T199-T205 (1965)

40. Trotter, W. K. and Miller, D. L. Economics of air classifying typical wheat flours. Amer. Mill. and Processor 92: (6) 8-11 (1964)

41. Wall, Joseph S. Origin and behavior of flour proteins. The Bakers Digest 41: (5) 36-44 (1967)

42. Whitby, Kenneth T. Particle sizing in the milling industry. Cereal Sci. Today 6: (2) 49-56 (1961)

43. Wolf, M. J., Kwolek, W. F., and McCarthy, J. R. Quantitative microscopic evaluation of endosperm breakdown in conditioned hard red winter wheat. Cereal Chem. 43: 43-61 (1966)

APPENDIX

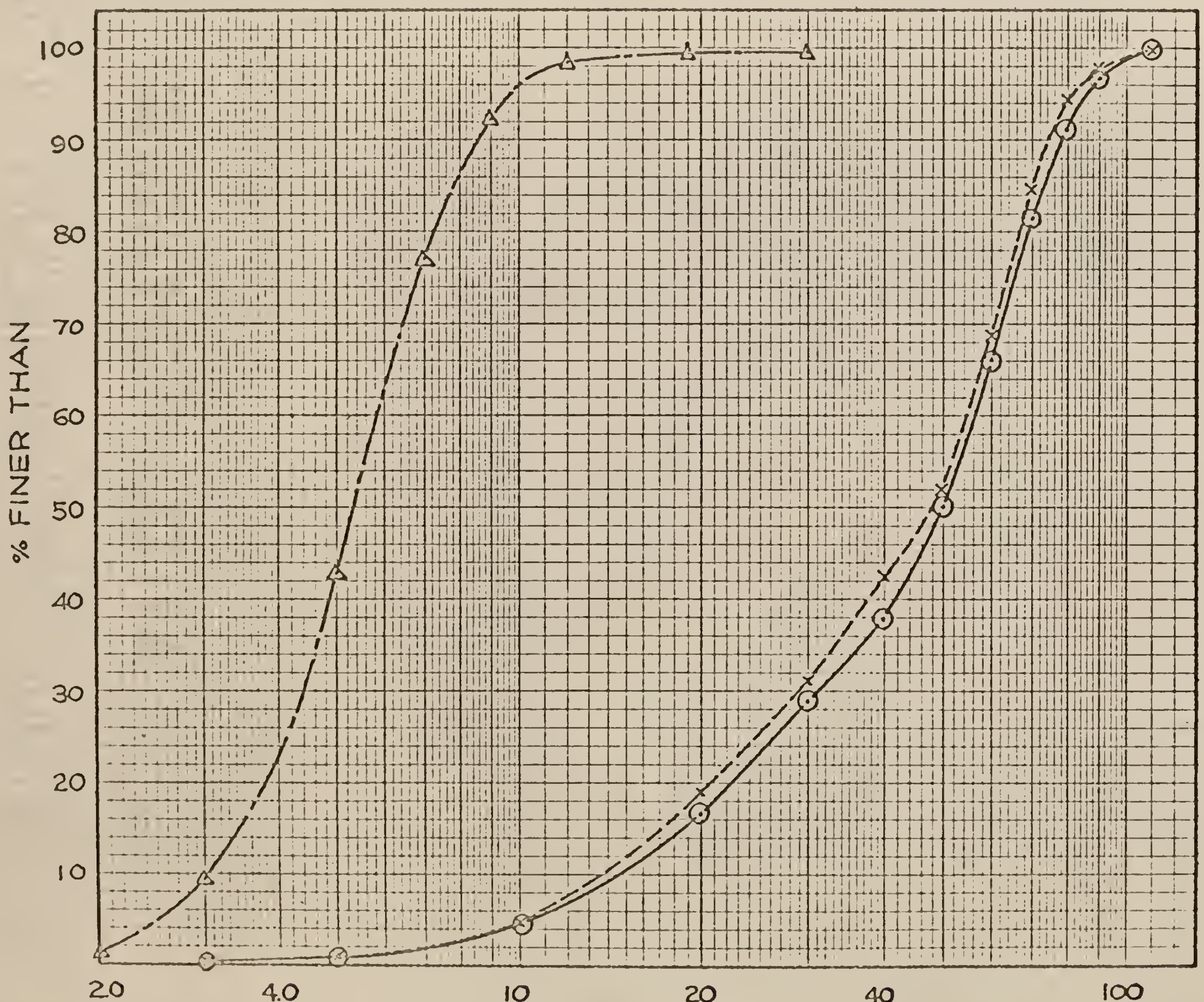

Turbo's B cut from unground flour

Graph Symbols	⊙	△	×
Sample Number	F023	F024	F025
Fraction	A	B	BB
S.E.D. (Micron) Size	% Finer		
160			
140			
120			
110	99.9		99.9
100			
90	96.7		97.8
80	91.2		94.5
70	81.5		84.6
60	66.0		68.7
50	50.0		52.0
40	37.8		42.4
30	28.8	99.8	31.1
20	16.6		18.9
19		99.6	
12		98.4	
10	4.3		4.5
9		92.2	
7		77.0	
5	0.6	42.8	0.7
3	0.1	9.2	0.1
2		1.3	
1		0.1	
Fisher	16.4	2.6	16.3
Prot.	11.3	24.7	11.2

S.E.D. (Micron) Size ⟶

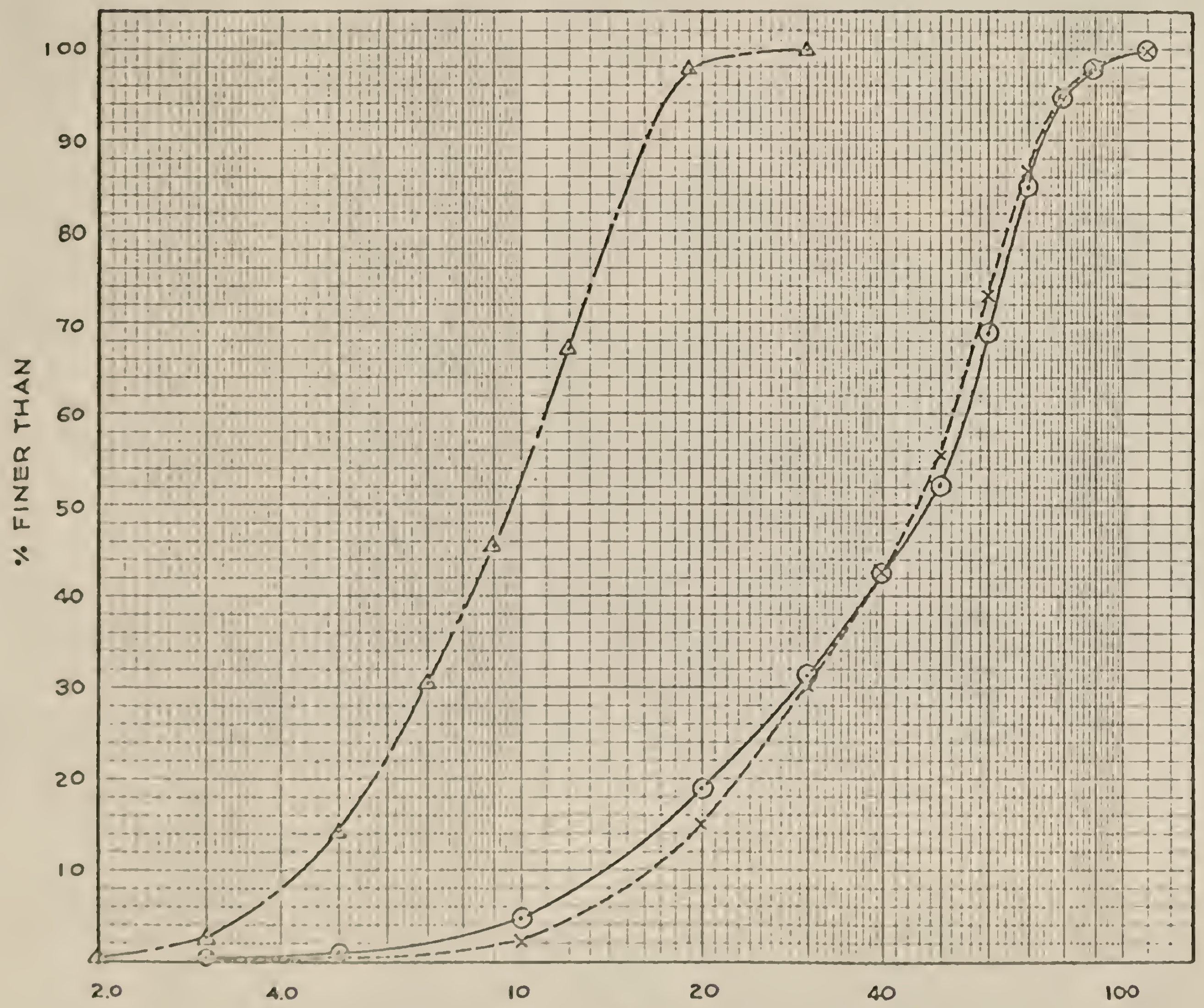

Turbo's C cut from unground flour

Graph Symbols	⊙	△	×
Sample Number	F025	F026	F027
Fraction	BB	C	CC
S.E.D. (Micron) Size	% Finer		
160			
140			
120			
110	99.9		99.9
100			
90	97.8		98.1
80	94.5		95.0
70	84.6		86.5
60	68.7		73.0
50	52.0		55.6
40	42.4		42.5
30	31.1	99.9	30.1
20	18.9		15.2
19		97.7	
12		67.1	
10	4.5		2.1
9		45.7	
7		30.2	
5	0.7	14.0	0.2
3	0.1	2.6	0.1
2		0.3	
1		0.1	
Fisher	16.3	4.4	18.6
Prot.	11.2	15.6	10.9

S.E.D. (Micron) Size ⟶

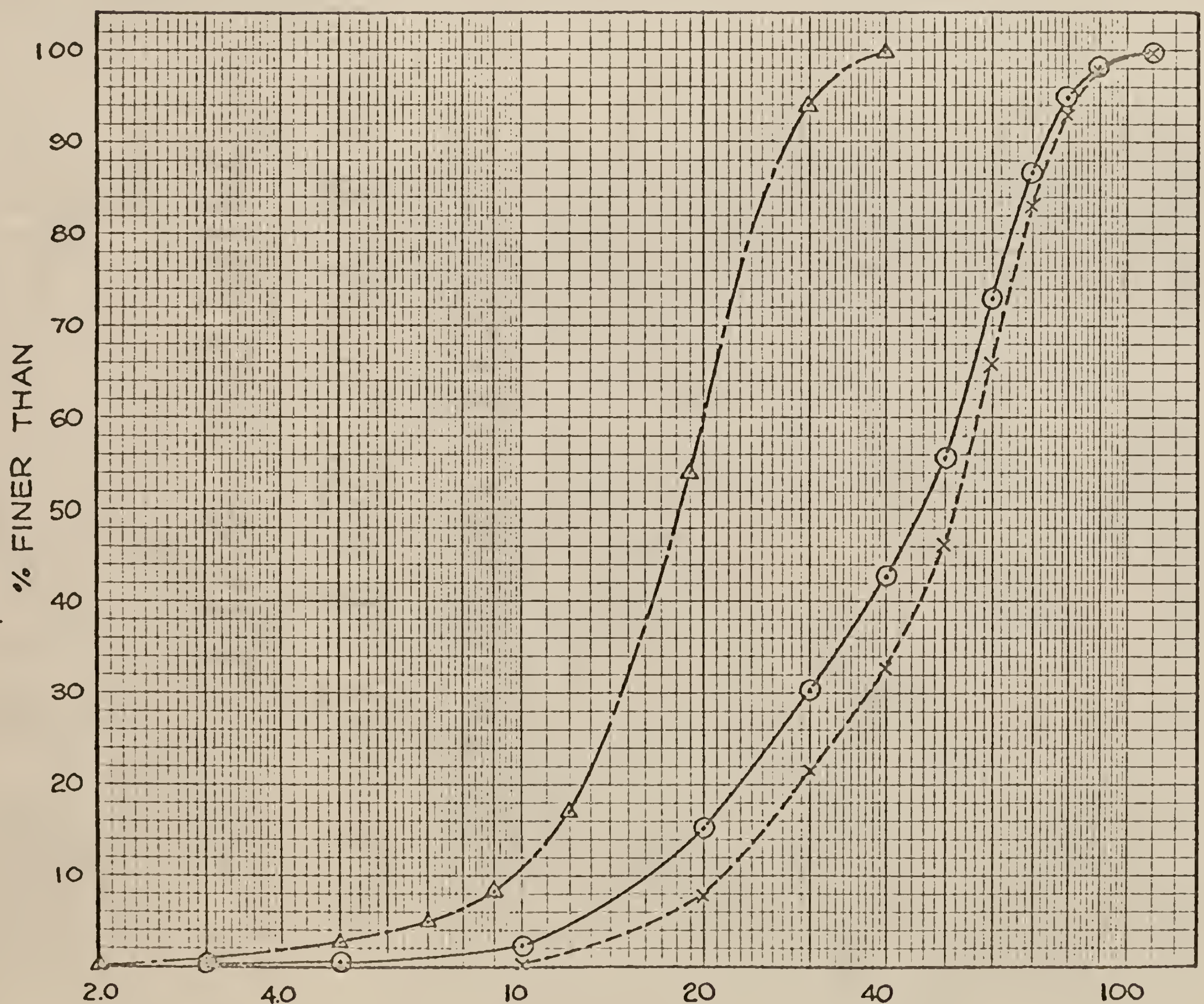

Turbo's D cut from unground flour

Graph Symbols	⊙	△	×
Sample Number	F027	F028	F029
Fraction	CC	D	DD
S.E.D. (Micron) Size	% Finer		
160			
140			
120			
110	99.9		99.9
100			
90	98.1		97.9
80	95.0		93.0
70	86.5		83.2
60	73.0		66.0
50	55.6		46.2
40	42.5	99.9	32.8
30	30.1	94.1	21.7
20	15.2		7.9
19		54.1	
12		17.0	
10	2.1		0.1
9		8.3	
7		4.9	
5	0.2	2.7	
3	0.1	0.5	
2		0.1	
1			
Fisher	18.6	9.2	22.7
Prot.	10.9	7.7	11.4

S.E.D. (Micron) Size →

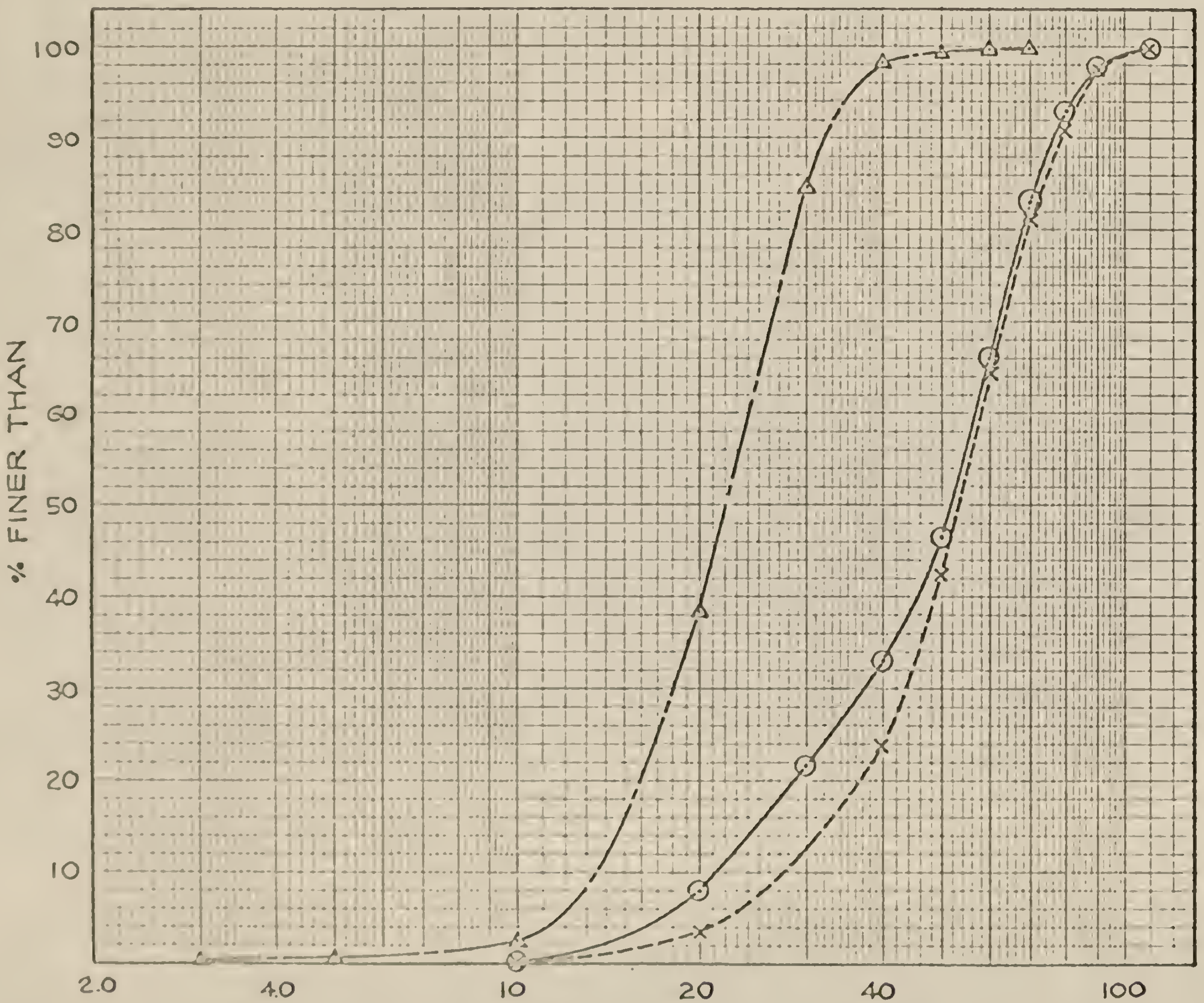

Turbo's E cut from unground flour

Graph Symbols	⊙	△	×
Sample Number	F029	F030	F031
Fraction	·DD	E	EE
S.E.D. (Micron) Size	% Finer		
160			
140			
120			
110	99.9		99.9
100			
90	97.9		97.8
80	93.0		90.8
70	83.2	99.9	81.2
60	66.0	99.8	64.4
50	46.4	99.3	42.5
40	32.8	98.2	23.8
30	21.7	84.7	12.5
20	7.9	38.2	3.6
19			
12			
10	0.1	2.4	0.1
9			
7			
5		0.7	
3		0.1	
2			
1			
Fisher	22.7	11.9	25.3
Prot.	11.4	8.7	12.0.

S.E.D. (Micron) Size ⟶

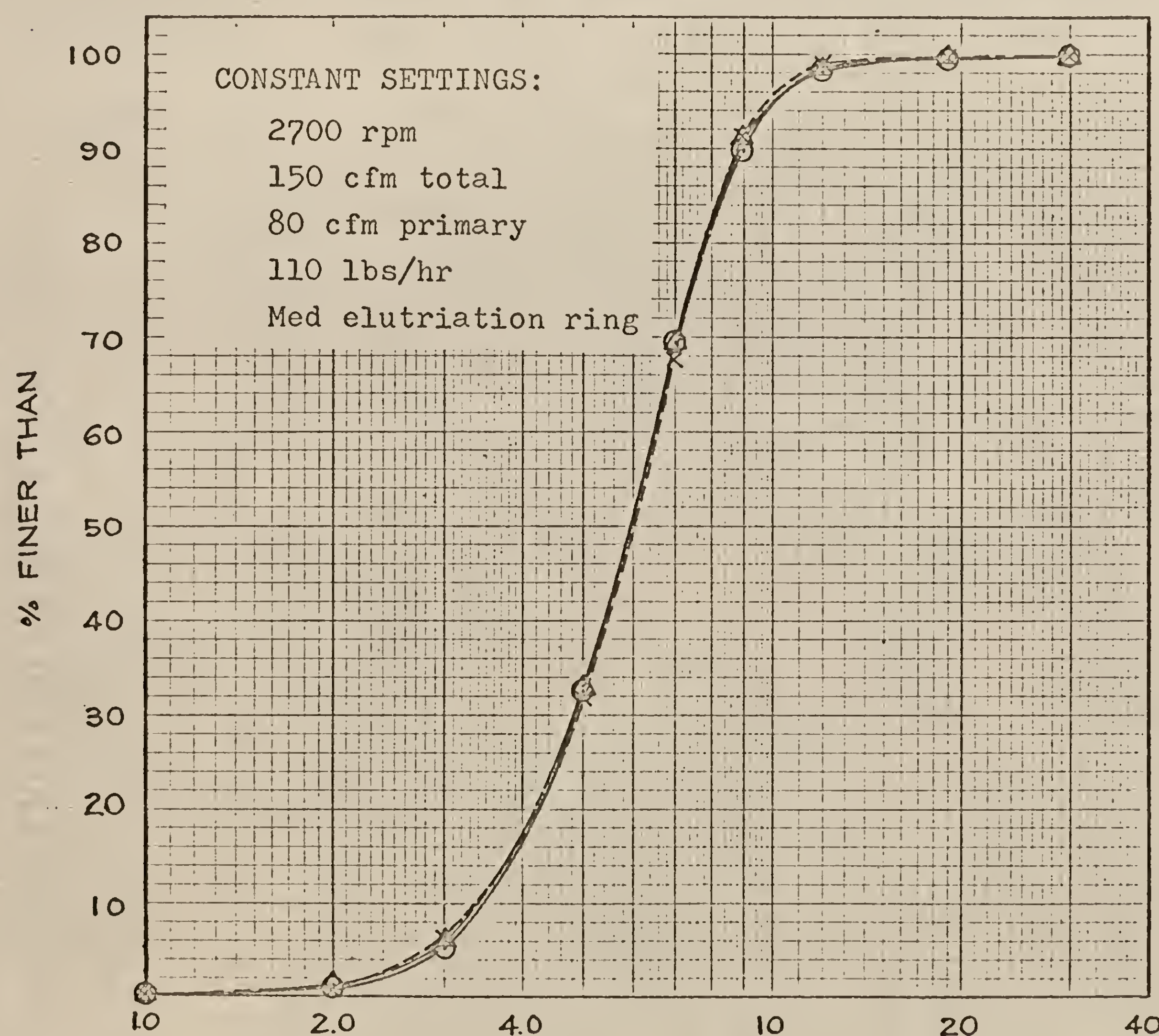

Effect of inner pipe height of Micron separator.

Pipe Height	Hi	Med	Lo
Graph Symbols	⊙	△	×
Sample Number	F057	F058	F060
Fraction	B	B	B
S.E.D. (Micron) Size	% Finer		
160			
140			
120			
110			
100			
90			
80			
70			
60			
50			
40			
30	99.9	99.9	99.9
20			
19	99.6	99.8	99.8
12	98.2	98.6	99.3
10			
9	90.8	89.8	91.1
7	69.3	69.2	67.8
5	32.4	32.7	32.0
3	5.2	5.9	6.4
2	0.8	1.0	0.8
1	0.1	0.1	0.1
Fisher	3.3	3.3	3.4
% of Parent	1.5	1.5	1.5

S.E.D. (Micron) Size ⟶

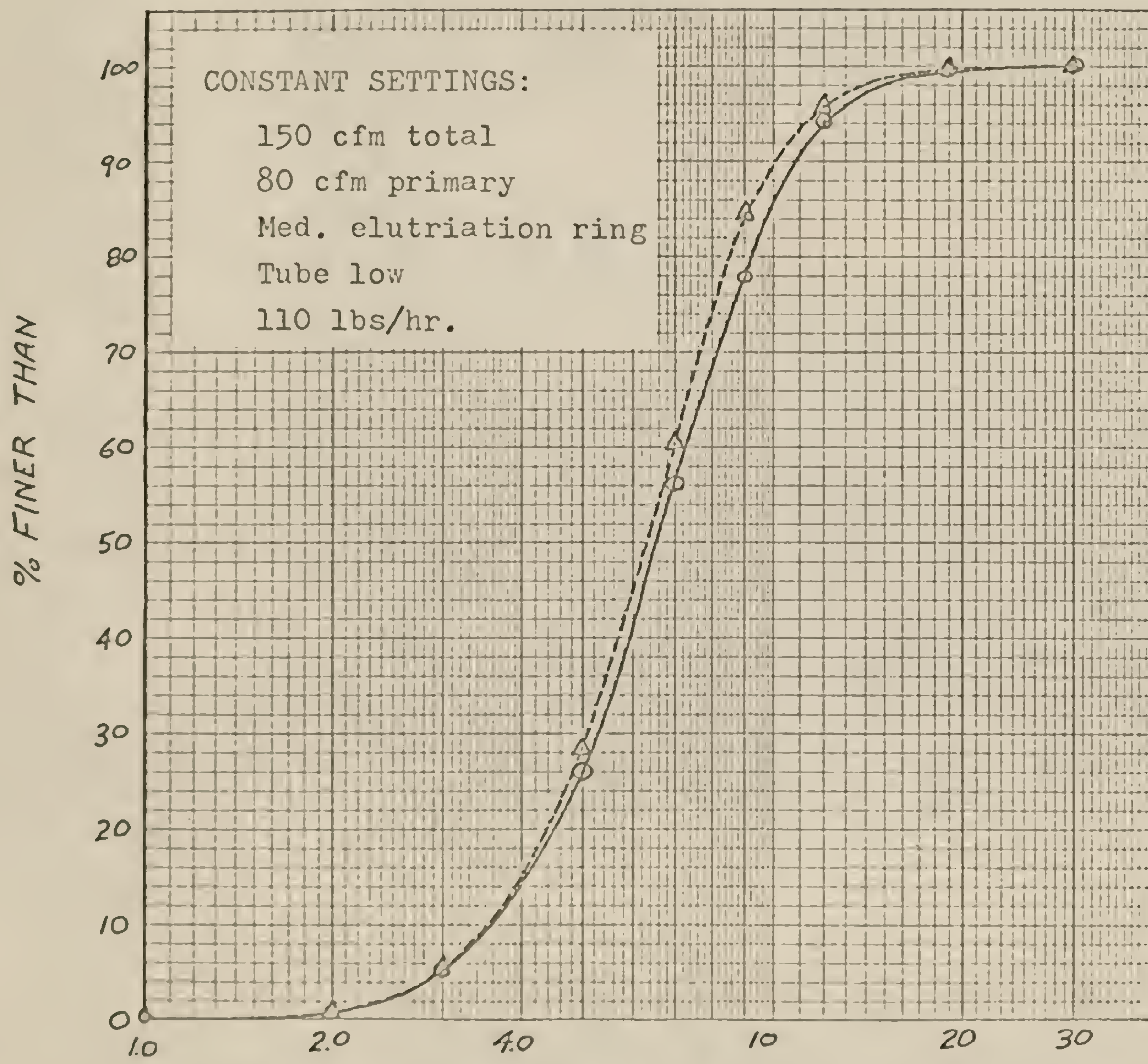

The effect of increasing the separator rpm from 2300 to 2700 on the Micrón separator.

RPM	2300	2700	
Graph Symbols	⊙	Δ	
Sample Number	F050	F051	
Fraction	B	B	
S.E.D. (Micron) Size	% Finer		
160			
140			
120			
110			
100			
90			
80			
70			
60			
50			
40			
30	99.7	99.9	
20			
19	99.3	99.7	
12	94.3	95.8	
10			
9	77.9	84.4	
7	56.0	60.1	
5	26.0	28.1	
3	5.3	5.5	
2	1.0	1.1	
1	0.1	0.1	
Fisher	3.7	3.6	
Prot.	—	—	
% of Parent	1.5	1.5	

S.E.D. (Micron) Size ⟶

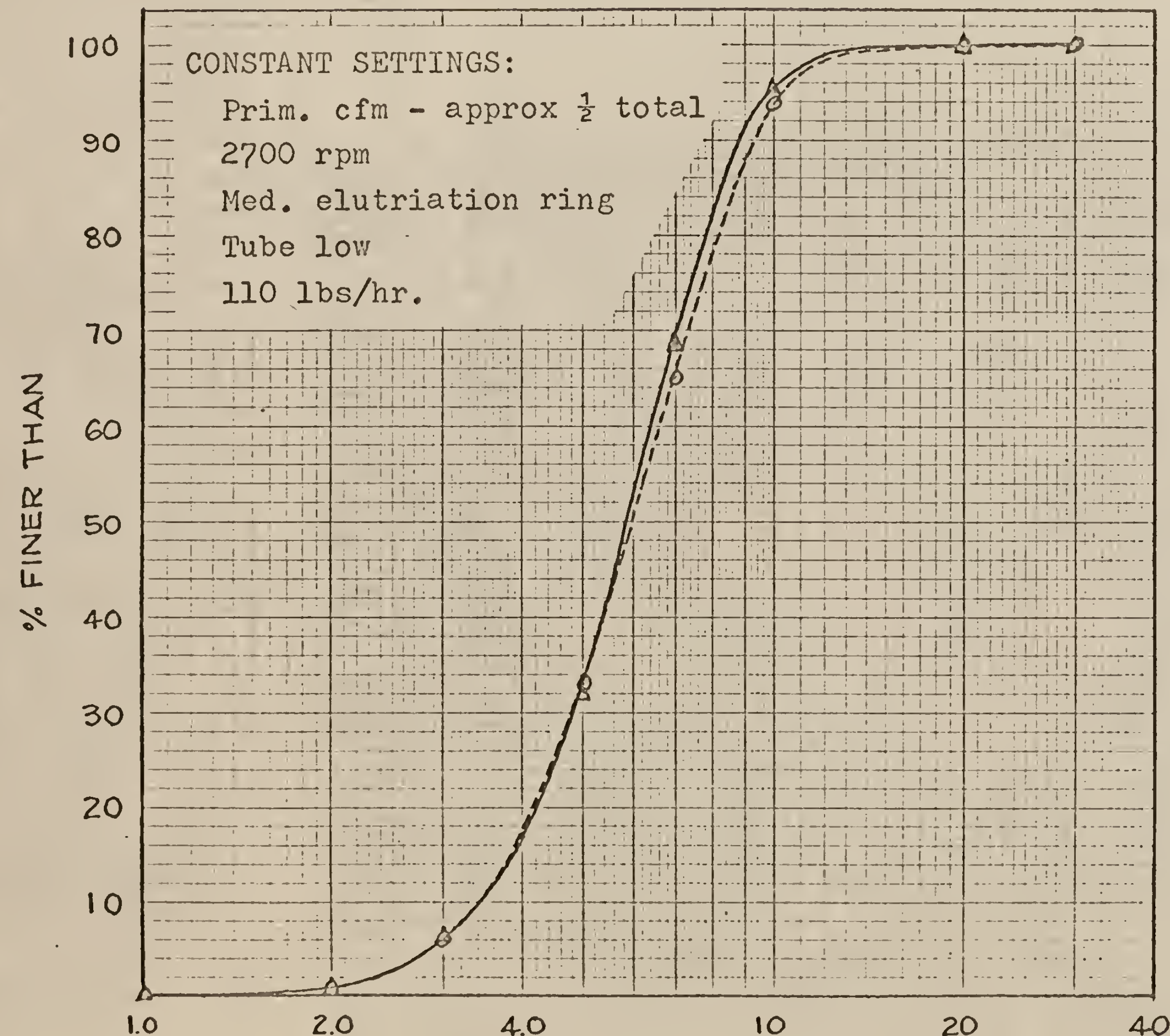

The effect of increasing total cfm air flow from 150 to 300 cfm on the Micron separator.

PRIMARY CFM	150	80	
TOTAL CFM	300	150	
Graph Symbols	⊙	△	
Sample Number	F059	F060	
Fraction	B	B	
S.E.D. (Micron) Size	% Finer		
160			
140			
120			
110			
100			
90			
80			
70			
60			
50			
40			
30	99.9	99.9	
20			
19	99.8	99.8	
12	98.4	99.3	
10			
9	88.0	91.1	
7	65.0	67.8	
5	32.9	32.0	
3	5.8	6.4	
2	0.7	0.8	
1	0.1	0.1	
Fisher	3.4	3.4	
% of Parent	2.5	1.5	

S.E.D. (Micron) Size ⟶

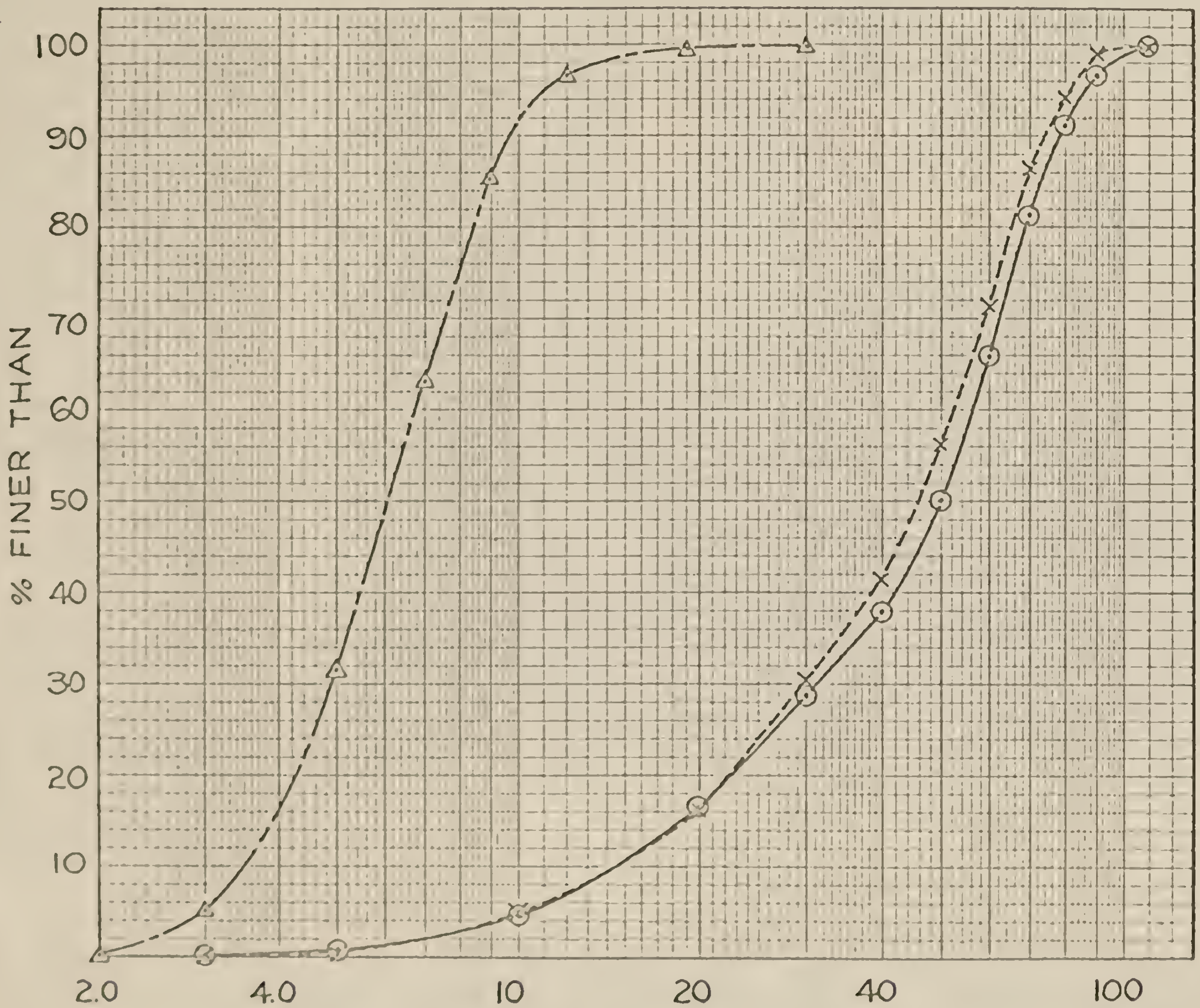

Micron's B cut from unground flour

Graph Symbols	⊙	△	X
Sample Number	F082	F083	F084
Fraction	A	B	BB
S.E.D. (Micron) Size	% Finer		
160			
140			
120			
110	99.9		99.9
100			
90	96.7		99.1
80	91.2		94.1
70	81.5		86.3
60	66.0		71.4
50	50.0		56.2
40	37.8		41.5
30	28.8	99.9	30.3
20	16.6		16.0
19		99.7	
12		96.7	
10	4.3		4.6
9		85.3	
7		63.0	
5	0.6	31.5	0.4
3	0.1	5.0	0.1
2		0.3	
1		0.1	
Fisher	16.2	2.9	16.2
Prot.	11.2	20.5	11.4

S.E.D. (Micron) Size ⟶

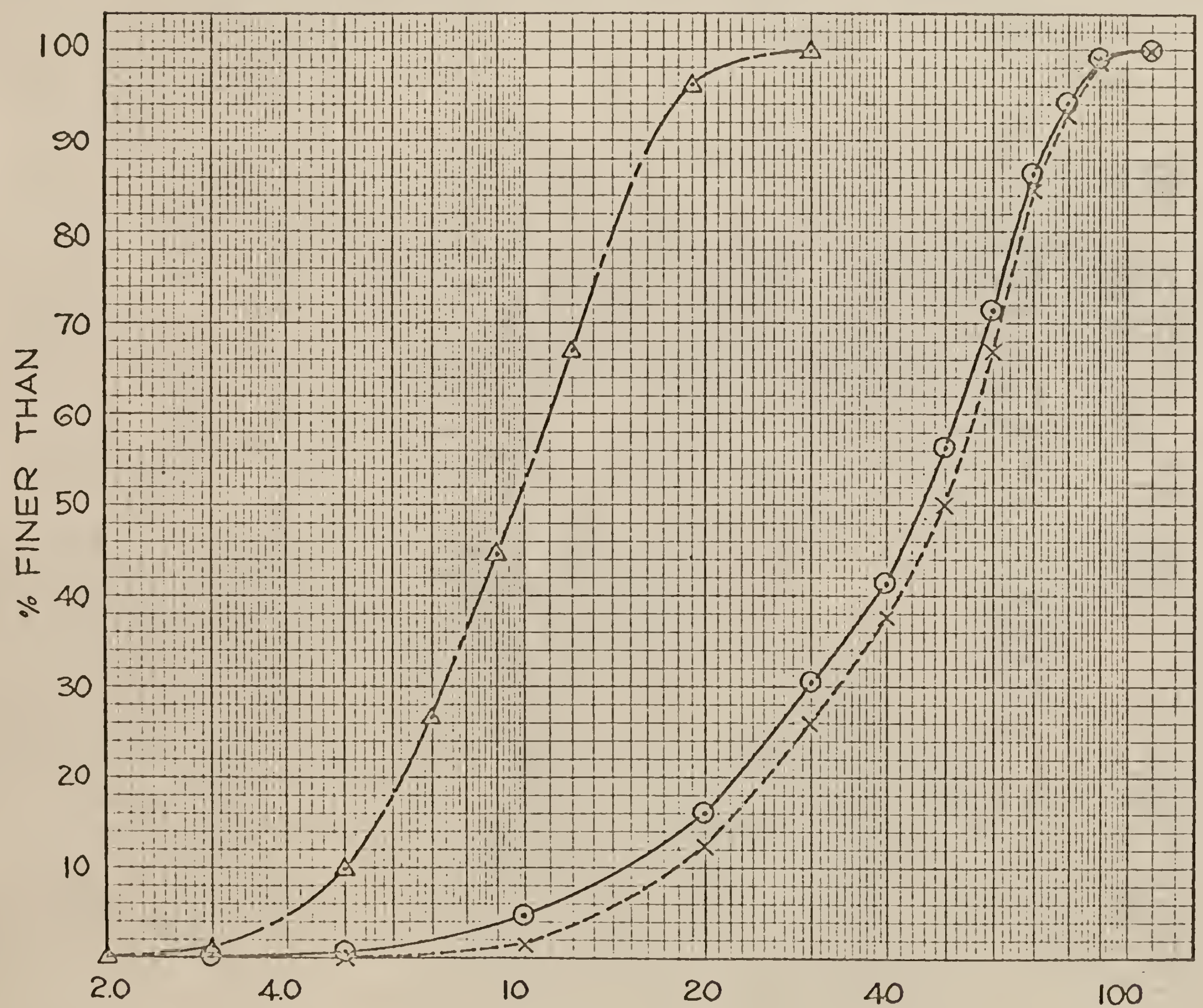

Micron's C cut from unground flour

Graph Symbols	⊙	△	×
Sample Number	F084	F085	F086
Fraction	BB	C	CC
S.E.D. (Micron) Size	% Finer		
160			
140			
120			
110	99.9		99.9
100			
90	99.1		98.8
80	94.1		92.8
70	86.3		84.4
60	71.4		67.0
50	56.2		50.0
40	41.5		38.7
30	30.0	99.9	26.0
20	16.0		12.3
19		96.2	
12		67.0	
10	4.6		1.6
9		44.6	
7		26.4	
5	0.4	9.9	0.1
3	0.1	1.0	
2		0.1	
1			
Fisher	16.2	4.5	19.0
Prot.	11.4	14.4	11.2

S.E.D. (Micron) Size ⟶

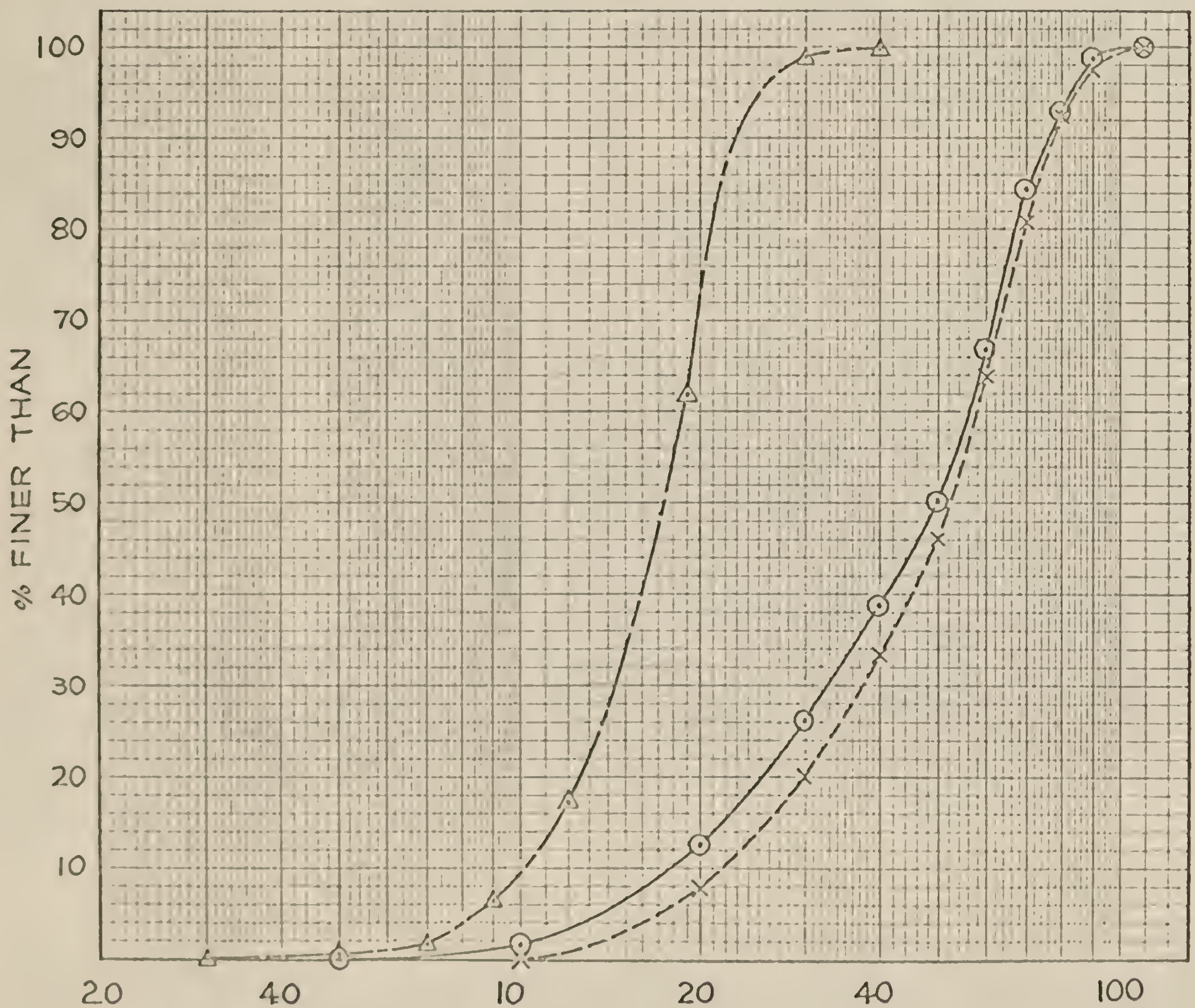

Micron's D cut from unground flour

Graph Symbols	⊙	△	×
Sample Number	F086	F087	F088
Fraction	CC	D	DD
S.E.D. (Micron) Size	% Finer		
160			
140			
120			
110	99.9		99.9
100			
90	98.8		97.8
80	92.8		92.4
70	84.4		80.7
60	67.0		64.0
50	50.0		48.0
40	38.7	99.9	33.4
30	26.0	99.1	20.0
20	12.3		7.8
19		62.0	
12		17.2	
10	1.6		0.1
9		6.3	
7		1.6	
5	0.1	0.6	
3		0.1	
2			
1			
Fisher	19.0	9.4	22.6
Prot.	11.2	7.3	11.6

S.E.D. (Micron) Size ⟶

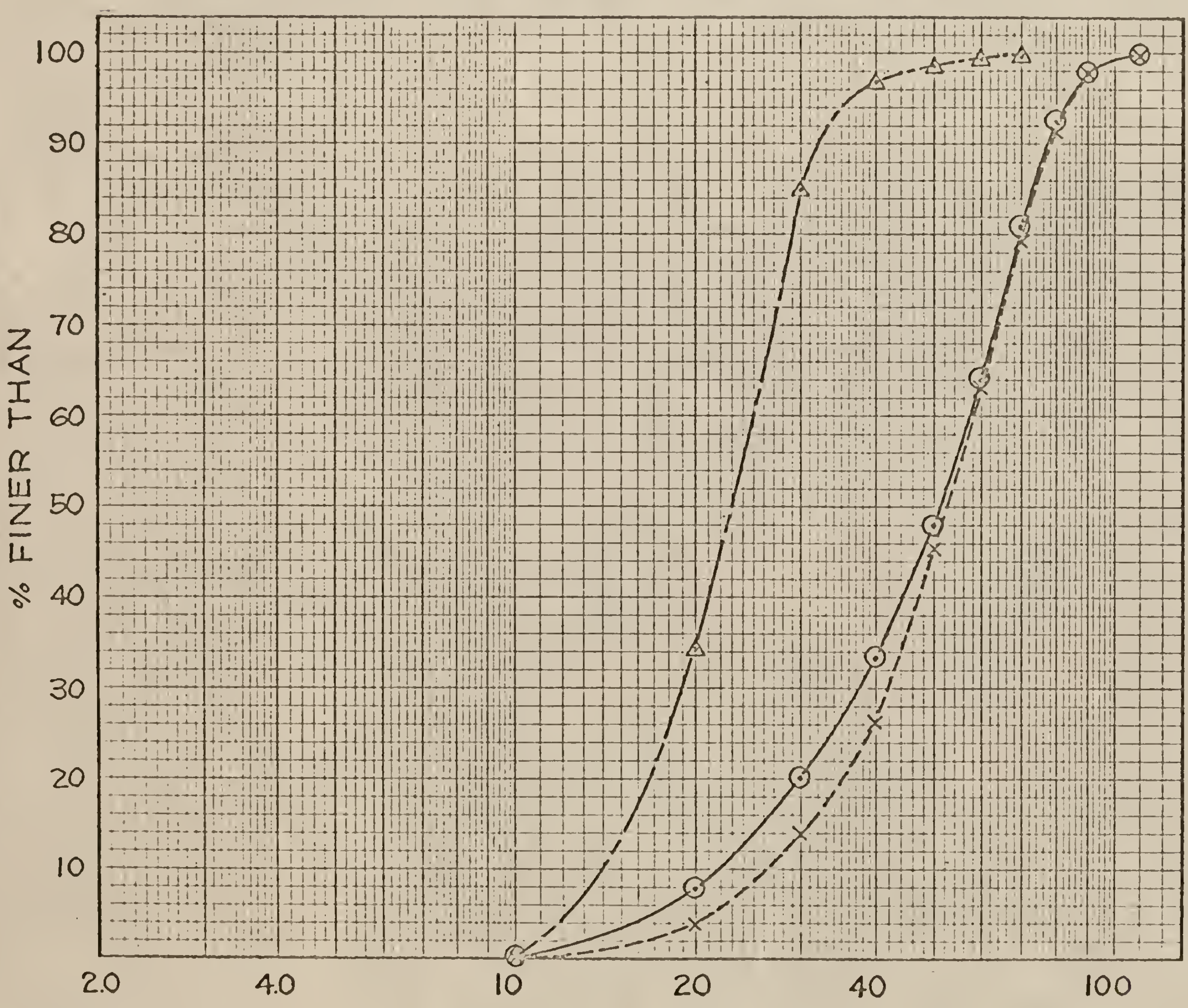

Micron's E cut from unground flour

Graph Symbols	⊙	△	×
Sample Number	F088	F089	F090
Fraction	DD	E	EE
S.E.D. (Micron) Size	% Finer		
160			
140			
120			
110	99.9		99.9
100			
90	97.8		97.8
80	92.4		91.6
70	80.7	99.9	79.5
60	64.0	99.6	63.3
50	48.0	98.7	45.6
40	33.4	97.1	26.2
30	20.0	85.0	14.0
20	7.8	34.3	4.0
19			
12			
10	0.1	0.1	0.1
9			
7			
5			
3			
2			
1			
Fisher	22.6	12.2	24.0
Prot.	11.6	7.3	12.1

S.E.D. (Micron) Size →

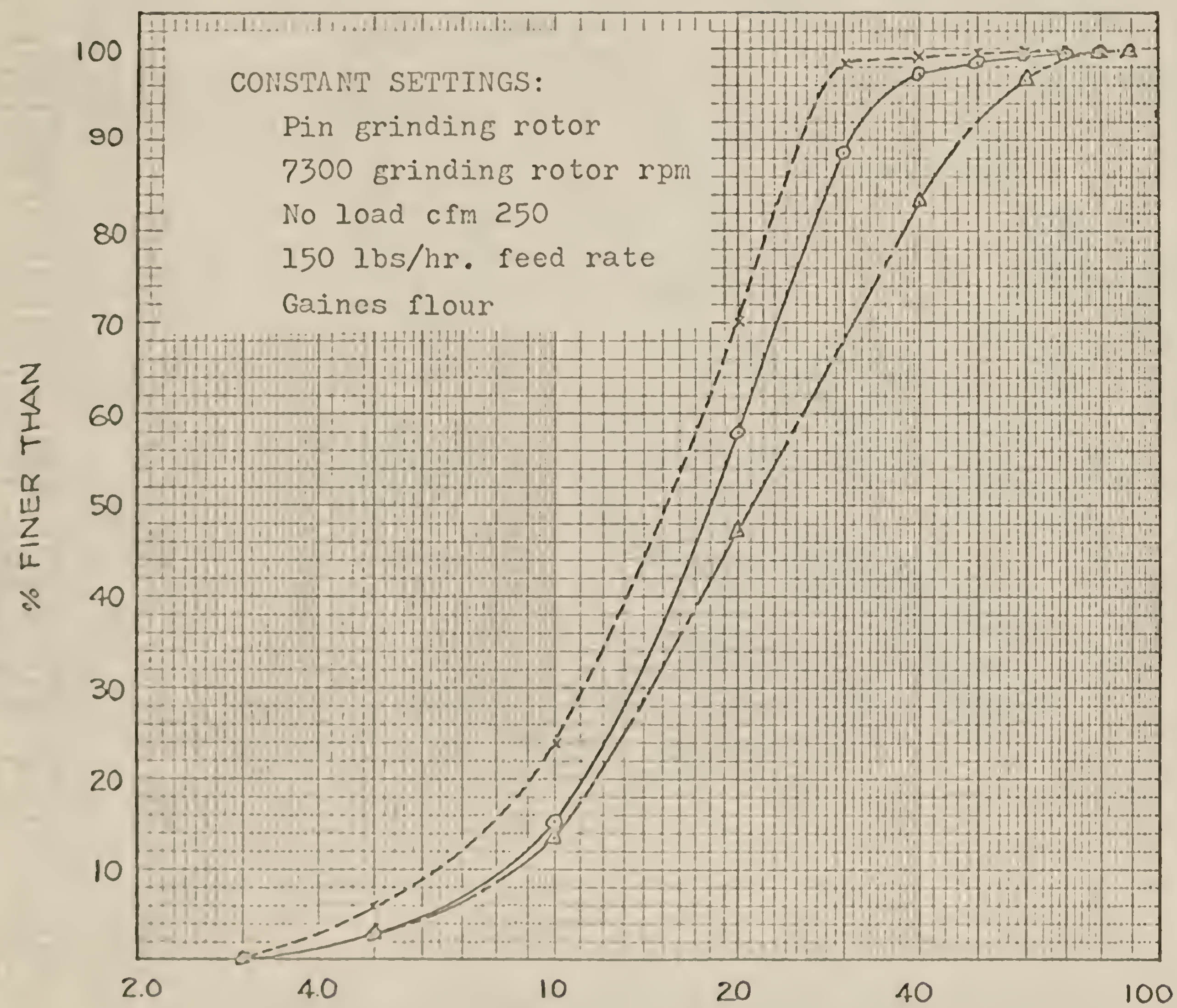

Mikro grinder; effect of separator rpm

RPM	2000	1000	3000
Graph Symbols	⊙	△	×
Sample Number	F037	F038	F039
Fraction	G_{2M}	G_{2M}	G_{2M}
S.E.D. (Micron) Size	% Finer		
160			
140			
120			
110			
100			
90		99.9	
80	99.9	99.8	
70	99.5	99.2	99.9
60	99.1	96.7	99.7
50	98.5	91.5	99.5
40	97.3	83.2	99.2
30	88.5	67.7	98.3
20	58.0	47.0	70.0
19			
12			
10	15.2	13.3	24.0
9			
7			
5	2.8	2.8	5.4
3	0.1	0.1	0.1
2			
1			
Fisher	8.6	9.2	7.2
Prot.	—	—	—

S.E.D. (Micron) Size ⟶

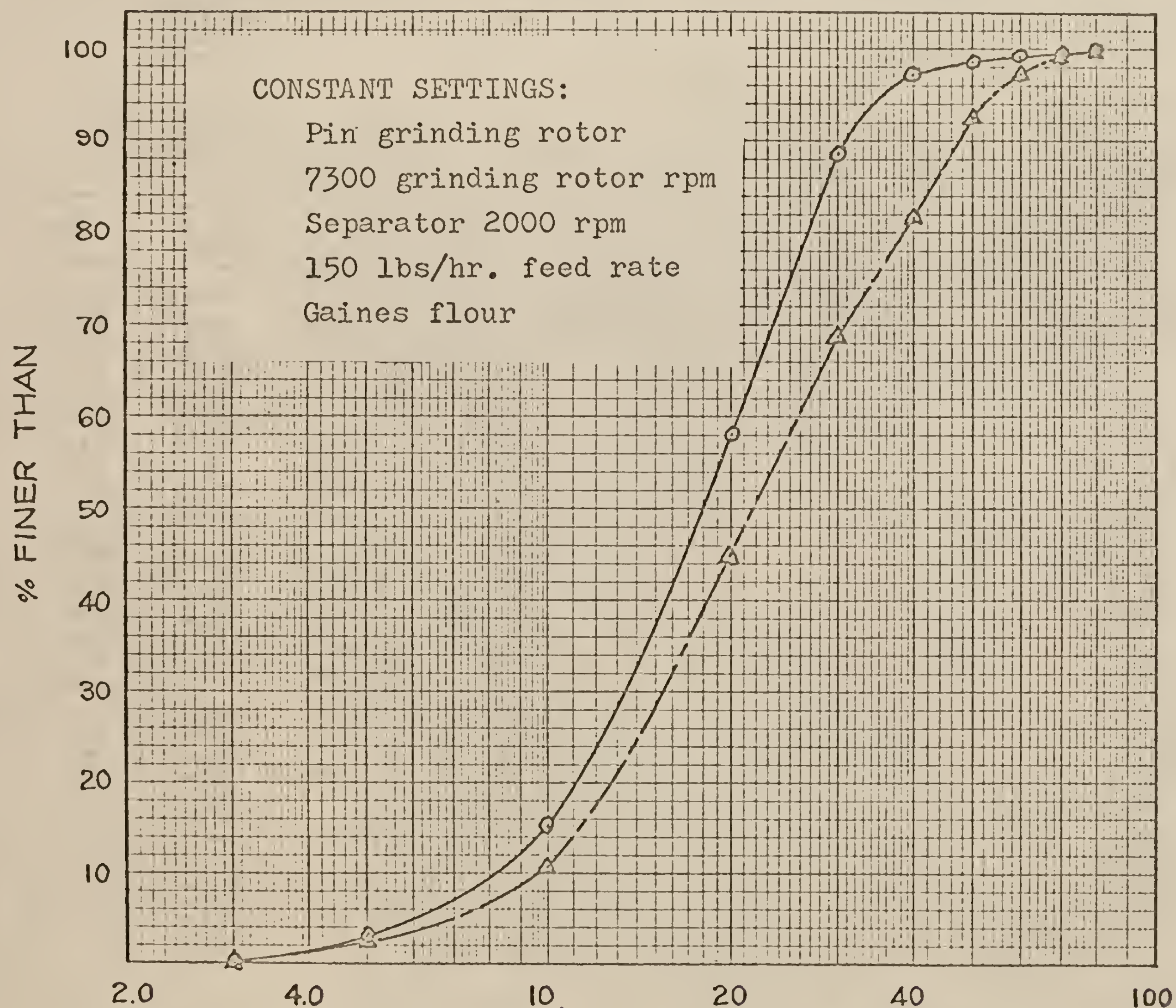

Effect of different air flows through Mikro grinder.

CFM	250	400	
Graph Symbols	⊙	△	
Sample Number	F037	F041	
Fraction	G_{2M}	G_{2M}	
S.E.D. (Micron) Size	% Finer		
160			
140			
120			
110			
100			
90			
80	99.9	99.8	
70	99.5	99.3	
60	99.1	97.3	
50	98.5	92.4	
40	97.3	81.7	
30	88.5	68.8	
20	58.0	45.0	
19			
12			
10	15.2	10.7	
9			
7			
5	2.8	2.5	
3	0.1	0.1	
2			
1			
Fisher	8.6	9.5	
Prot.	—	—	

S.E.D. (Micron) Size →

SETTINGS & DATA

	LO	MED	HI
Rotor rpm	7300	8300	10500
Separator rpm	2500	2500	2500
No load cfm	400	400	400
Grinder KW	7.8	8.7	10.0
Separator KW	0.56	0.58	0.53
Temp change	20-34°C	20-36°C	20-38°C
Lbs/hour	400	400	400
No load grinder KW	2.6	3.6	5.5

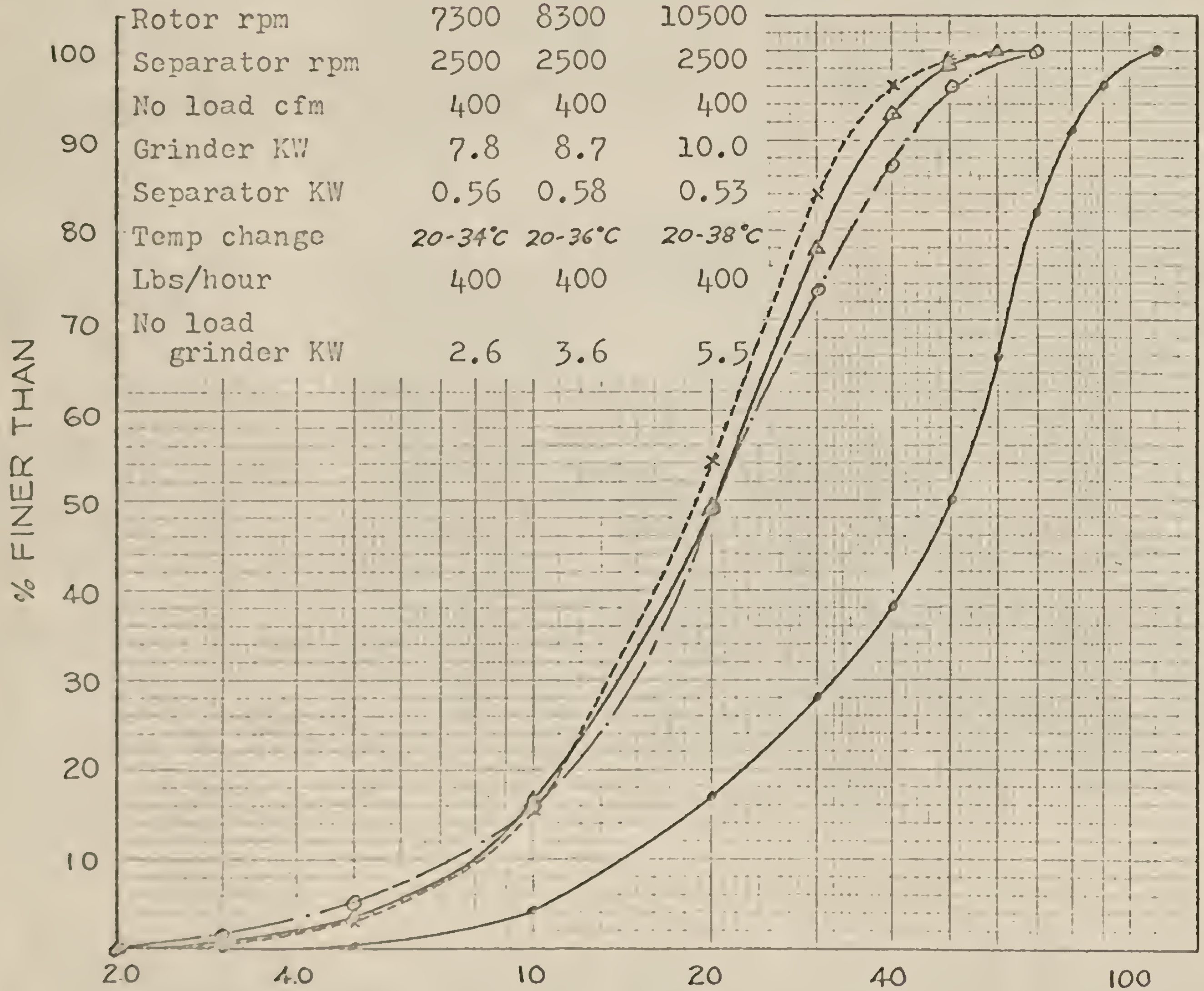

The effect of different grinding rotor speeds using pin rotor and special flour with Mikro grinder.

ROTOR SPEED	LO	MED	HIGH	UNGROUND
Graph Symbols	⊙	△	×	●
Sample Number	F073	F107	F108	F023
Fraction	A	A	A	A
S.E.D. (Micron) Size	% Finer			
160				
140				
120				
110				99.9
100				
90				96.7
80				91.2
70	99.9			81.5
60	99.6	99.9	99.7	66.0
50	96.6	98.6	98.8	50.0
40	87.0	93.3	96.0	38.0
30	73.0	77.8	84.0	29.0
20	49.0	49.0	54.5	16.6
19				
12				
10	16.0	16.2	14.8	4.3
9				
7				
5	5.0	3.6	3.2	0.6
3	1.5	0.8	0.4	0.1
2	0.1	0.1	0.1	
1				
Fisher	9.7	10.0	9.7	16.4
Prot.	—	—	—	—

S.E.D. (Micron) Size ⟶

CONSTANT SETTINGS: 7300 grinding rotor rpm, 2500 separator rpm, no load cfm 400, 400 lbs/hr feed rate, special flour.

DATA:

	PIN	BAR
Grinder no load KW	2.6	2.5
Grinder loaded KW	7.8	11.0
Separator loaded KW	.56	.62
Temp change	20-34°C	21-36°C
Gauge static pressure at grinder discharge:		
Loaded	13.4	14.5
Unloaded	11.2	11.4

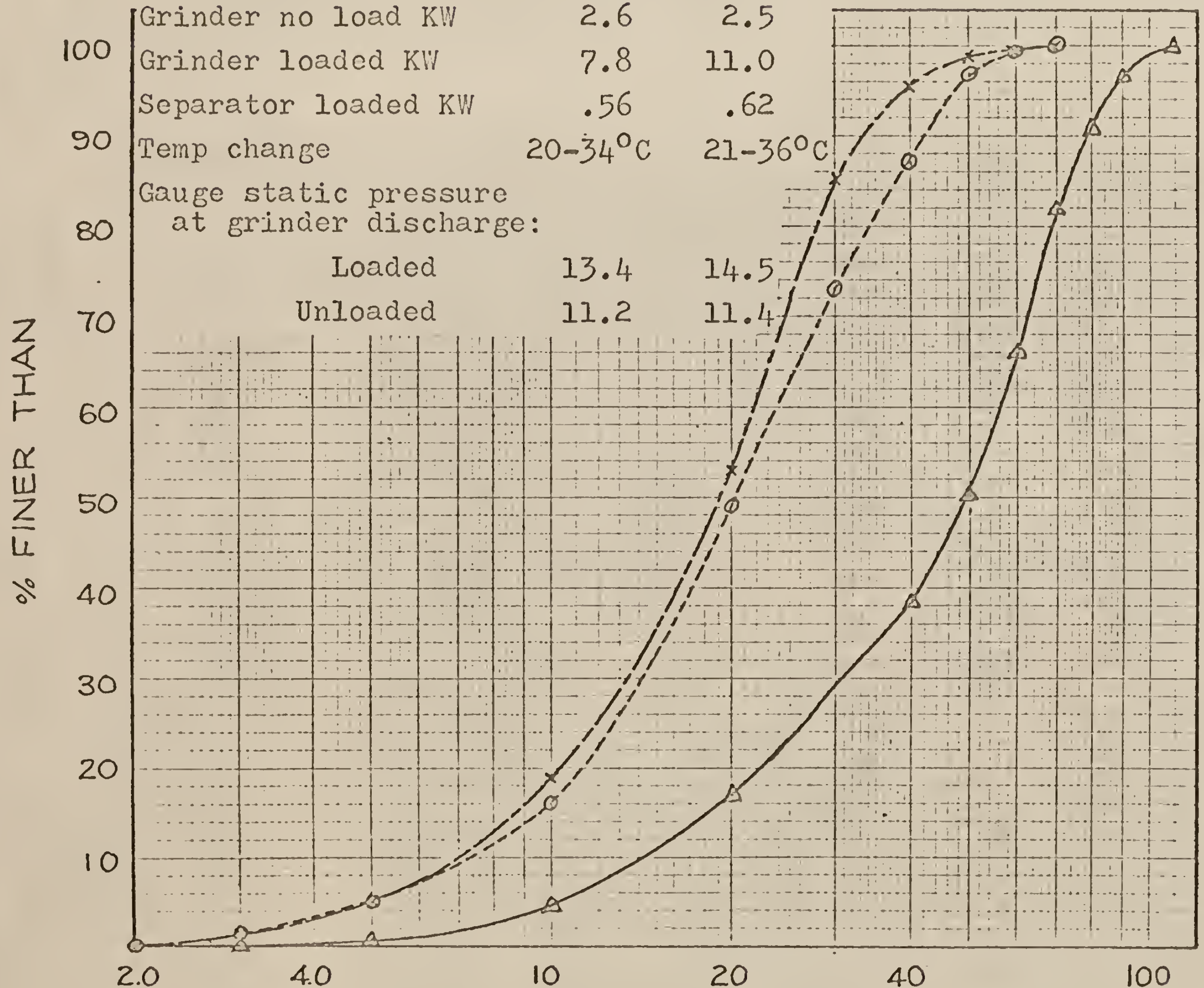

Mikro grinder; pin grinding rotor vs. bar grinding rotor

ROTOR	PIN	BAR	UNGROUND
Graph Symbols	O	×	△
Sample Number	F073	F111	F023
Fraction	A	A	A
S.E.D. (Micron) Size	% Finer		
160			
140			
120			
110			99.9
100			
90			96.7
80			91.2
70	99.9	99.9	81.5
60	99.6	99.7	66.0
50	96.6	98.8	50.0
40	87.0	95.8	38.0
30	73.0	85.3	29.0
20	49.0	53.0	16.6
19			
12			
10	16.0	19.0	4.3
9			
7			
5	5.0	5.0	0.6
3	1.5	0.9	0.1
2	0.1	0.1	
1			
Fisher	9.7	9.5	16.4
Prot.	—	—	—

S.E.D. (Micron) Size →

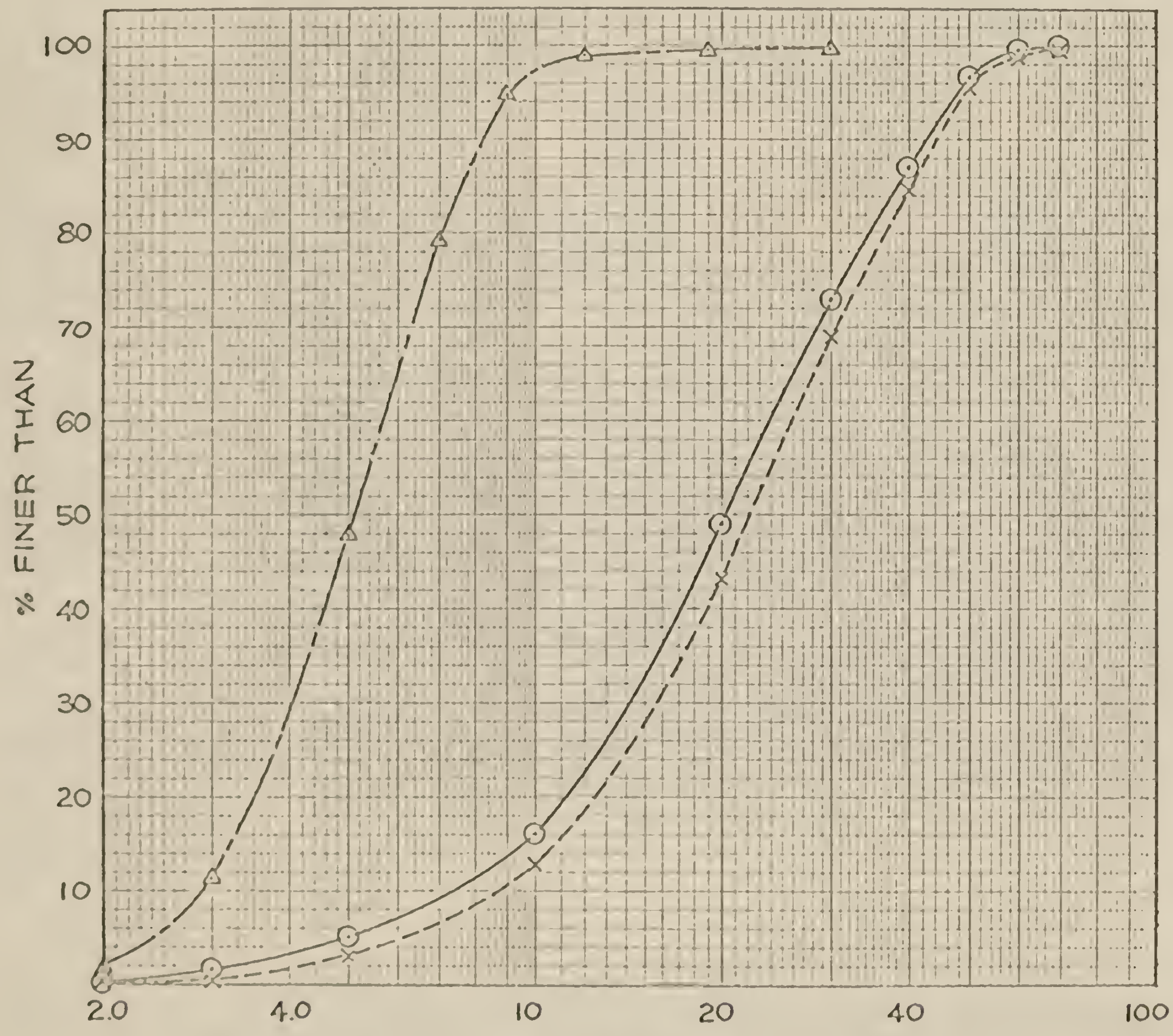

Turbo's B cut from Mikro ground flour

Graph Symbols	⊙	△	X
Sample Number	F073	F074	F075
Fraction	A	B	BB
S.E.D. (Micron) Size	% Finer		
160			
140			
120			
110			
100			
90			
80			
70	99.9		99.8
60	99.6		99.0
50	96.6		96.4
40	87.0		84.6
30	73.0	99.9	69.2
20	49.0		43.3
19		99.7	
12		98.8	
10	16.0		12.8
9		94.5	
7		79.2	
5	5.0	47.8	3.2
3	1.5	11.3	0.6
2	0.1	2.1	0.1
1		0.1	
Fisher	9.7	2.5	10.8
Prot.	11.0	24.5	9.8

S.E.D. (Micron) Size ⟶

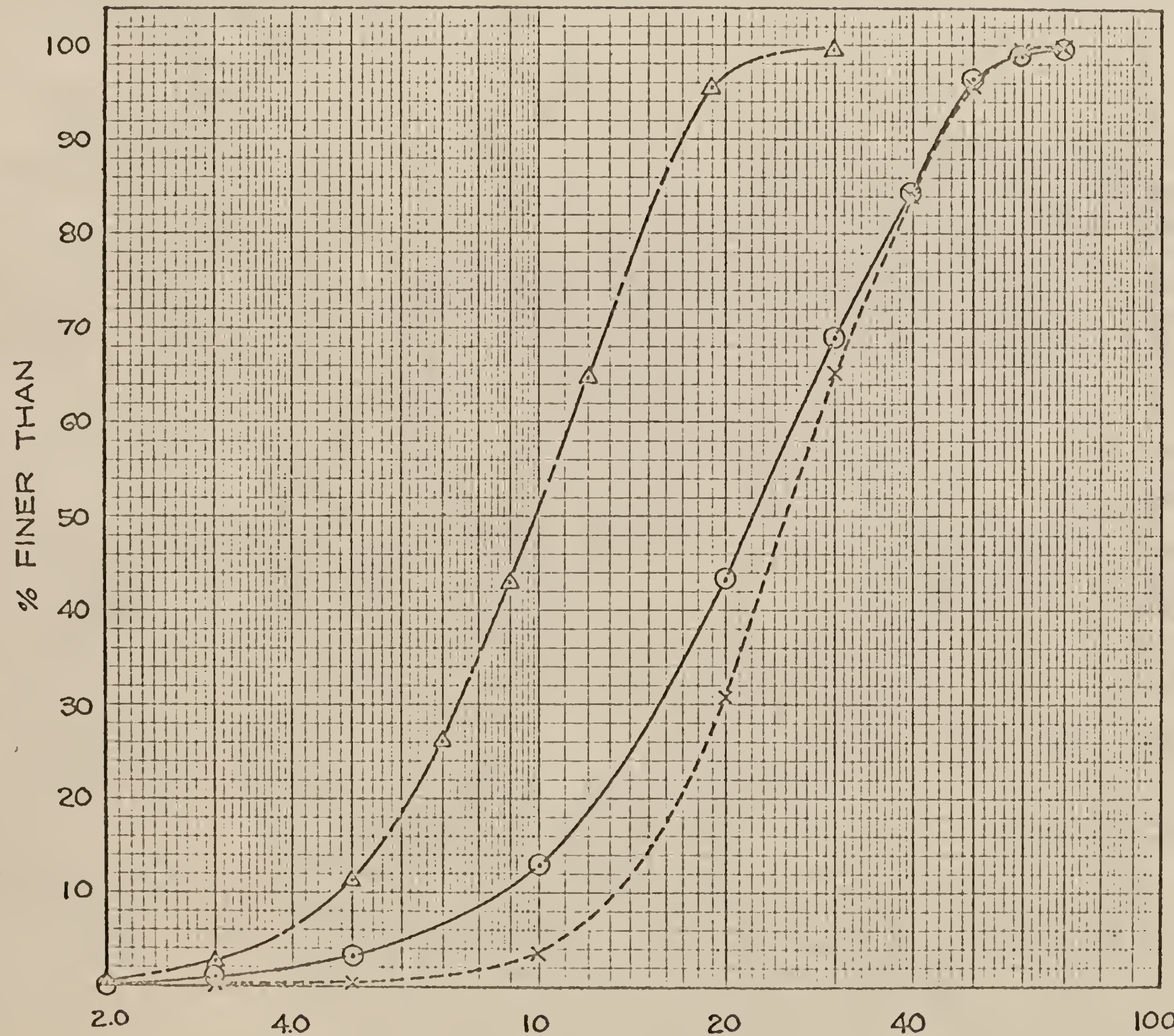

Turbo's C cut from Mikro ground flour

Graph Symbols	⊙	△	×
Sample Number	F075	F076	F077
Fraction	BB	C	CC
S.E.D. (Micron) Size	% Finer		
160			
140			
120			
110			
100			
90			
80			
70	99.8		99.9
60	99.0		99.7
50	96.4		95.8
40	84.6		84.2
30	69.2	99.8	65.4
20	43.3		30.7
19		95.7	
12		64.5	
10	12.8		3.5
9		43.0	
7		26.0	
5	3.2	11.3	0.2
3	0.6	2.6	0.1
2	0.1	0.3	
1		0.1	
Fisher	10.8	4.9	14.5
Prot.	9.8	14.5	8.1

S.E.D. (Micron) Size ⟶

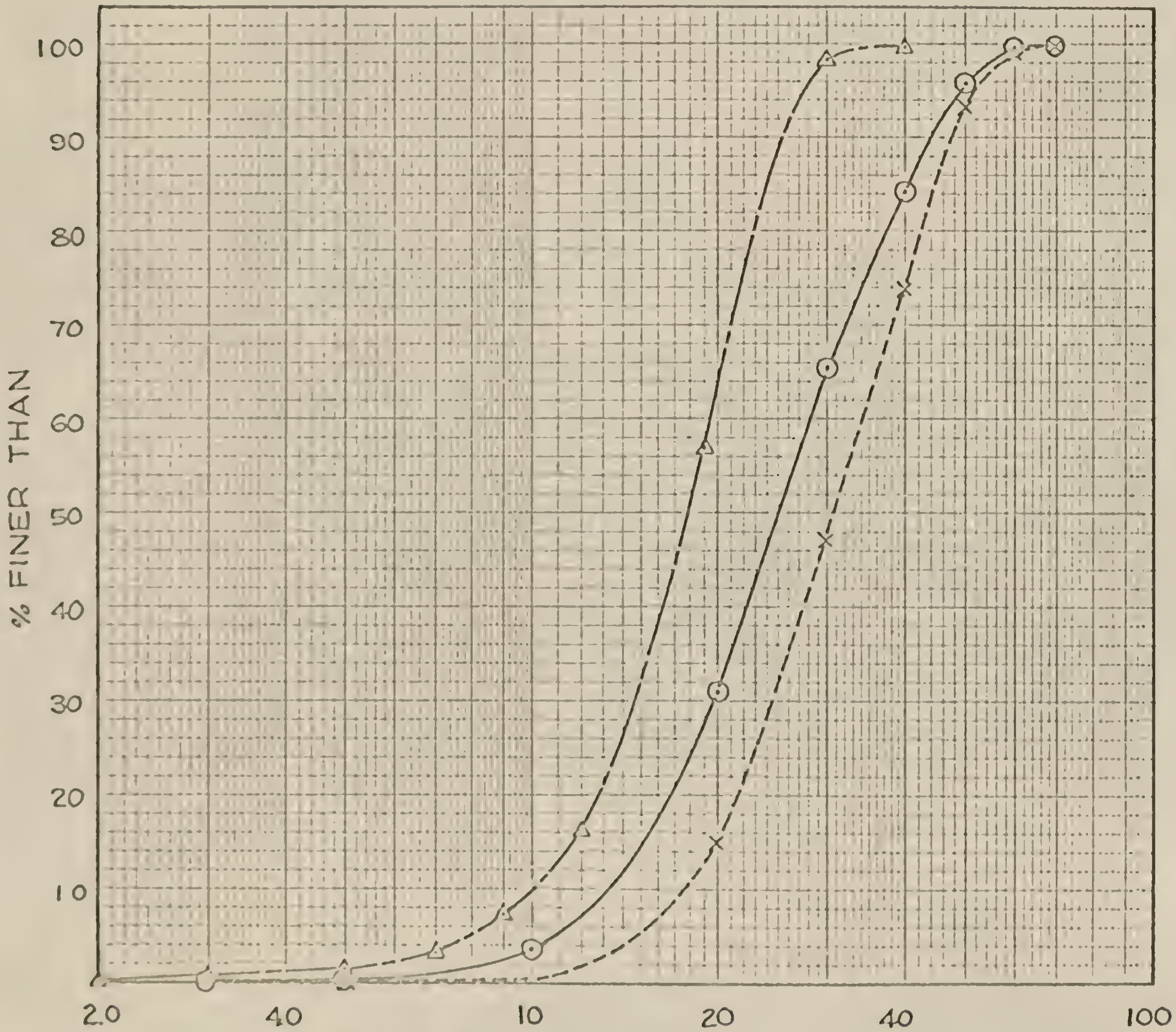

Turbo's D cut from Mikro ground flour

Graph Symbols	⊙	△	X
Sample Number	F077	F078	F079
Fraction	CC	D	DD
S.E.D. (Micron) Size	% Finer		
160			
140			
120			
110			
100			
90			
80			
70	99.9		99.9
60	99.7		99.1
50	95.8		93.4
40	84.2	99.9	73.9
30	65.4	98.3	47.2
20	30.7		14.8
19		57.0	
12		16.0	
10	3.5		0.2
9		7.4	
7		3.2	
5	0.2	1.2	0.1
3	0.1	0.7	
2		0.1	
1			
Fisher	14.5	10.4	18.0
Prot.	8.1	7.5	9.8

S.E.D. (Micron) Size ⟶

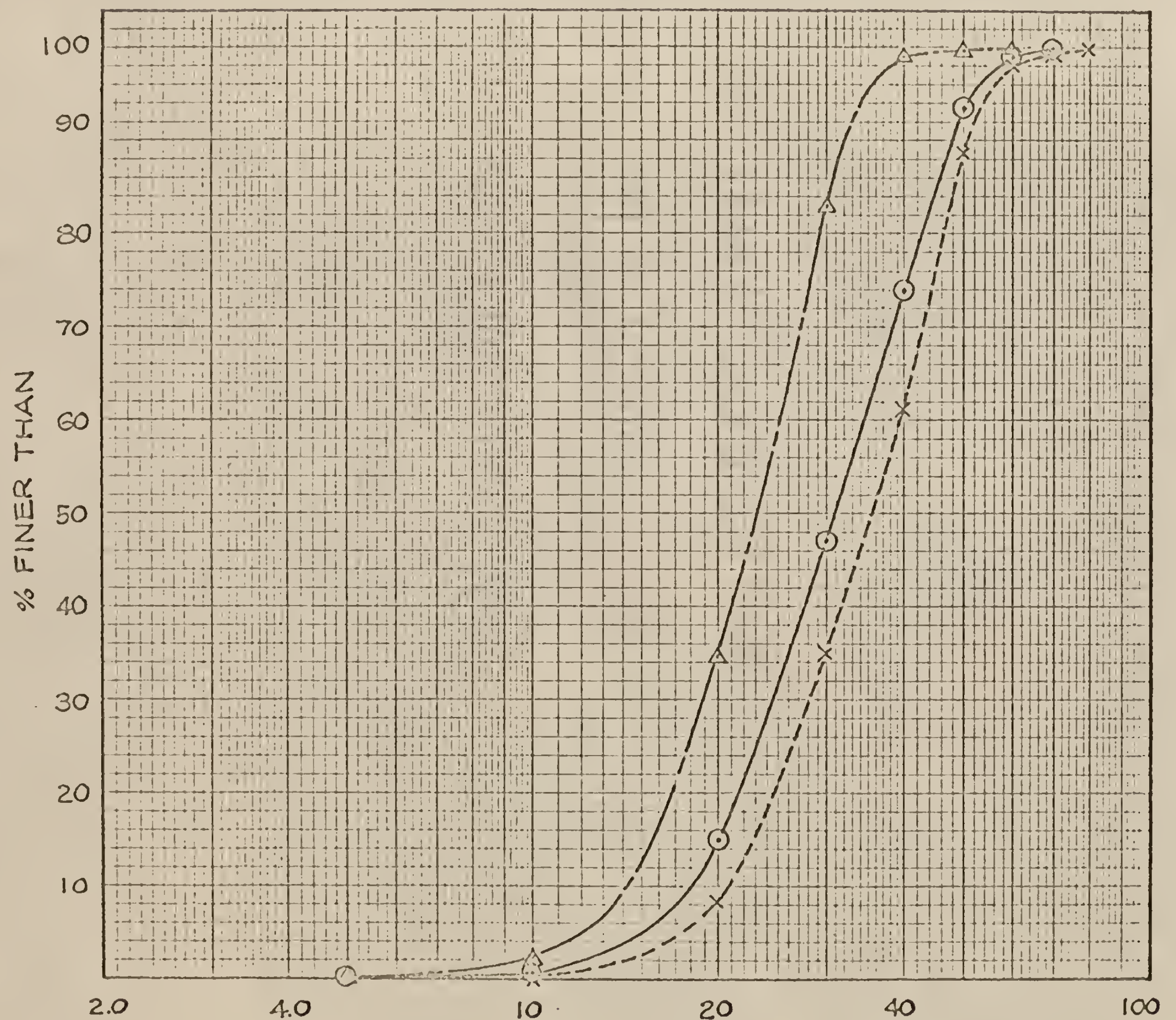

Turbo's E cut from Mikro ground flour

Graph Symbols	⊙	△	×
Sample Number	F079	F080	F081
Fraction	DD	E	EE
S.E.D. (Micron) Size	% Finer		
160			
140			
120			
110			
100			
90			
80			99.9
70	99.9		99.6
60	99.1	99.9	98.0
50	93.4	99.8	88.5
40	73.9	99.1	61.2
30	47.2	83.0	34.9
20	14.8	34.4	8.3
19			
12			
10	0.2	1.2	0.1
9			
7			
5	0.1	0.1	
3			
2			
1			
Fisher	18.0	13.9	21.0
Prot.	9.8	7.0	11.0

S.E.D. (Micron) Size ⟶

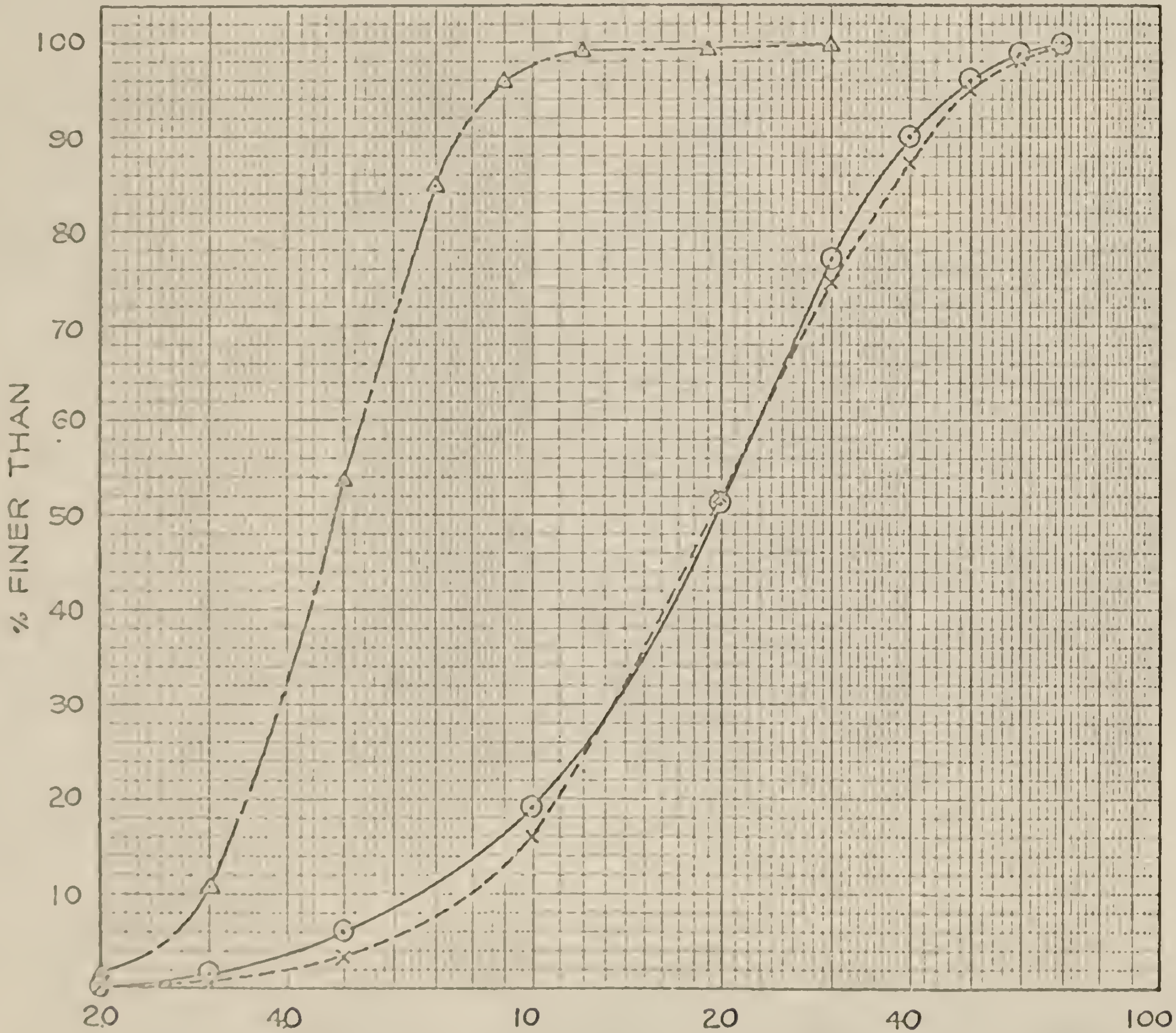

Turbo's B cut from Alpine ground flour

Graph Symbols	⊙	△	X
Sample Number	F072	F064	F065
Fraction	A	B	BB
S.E.D. (Micron) Size	% Finer		
160			
140			
120			
110			
100			
90			
80			
70	99.9		99.7
60	98.8		98.2
50	96.1		95.1
40	90.0		87.3
30	77.0	99.8	74.7
20	51.0		52.0
19		99.5	
12		99.3	
10	19.0		16.0
9		96.0	
7		85.0	
5	6.0	53.7	3.4
3	1.5	10.7	0.7
2	0.1	1.8	0.1
1		0.1	
Fisher	9.3	2.5	9.9
Prot.	11.0	25.6	10.3

S.E.D. (Micron) Size →

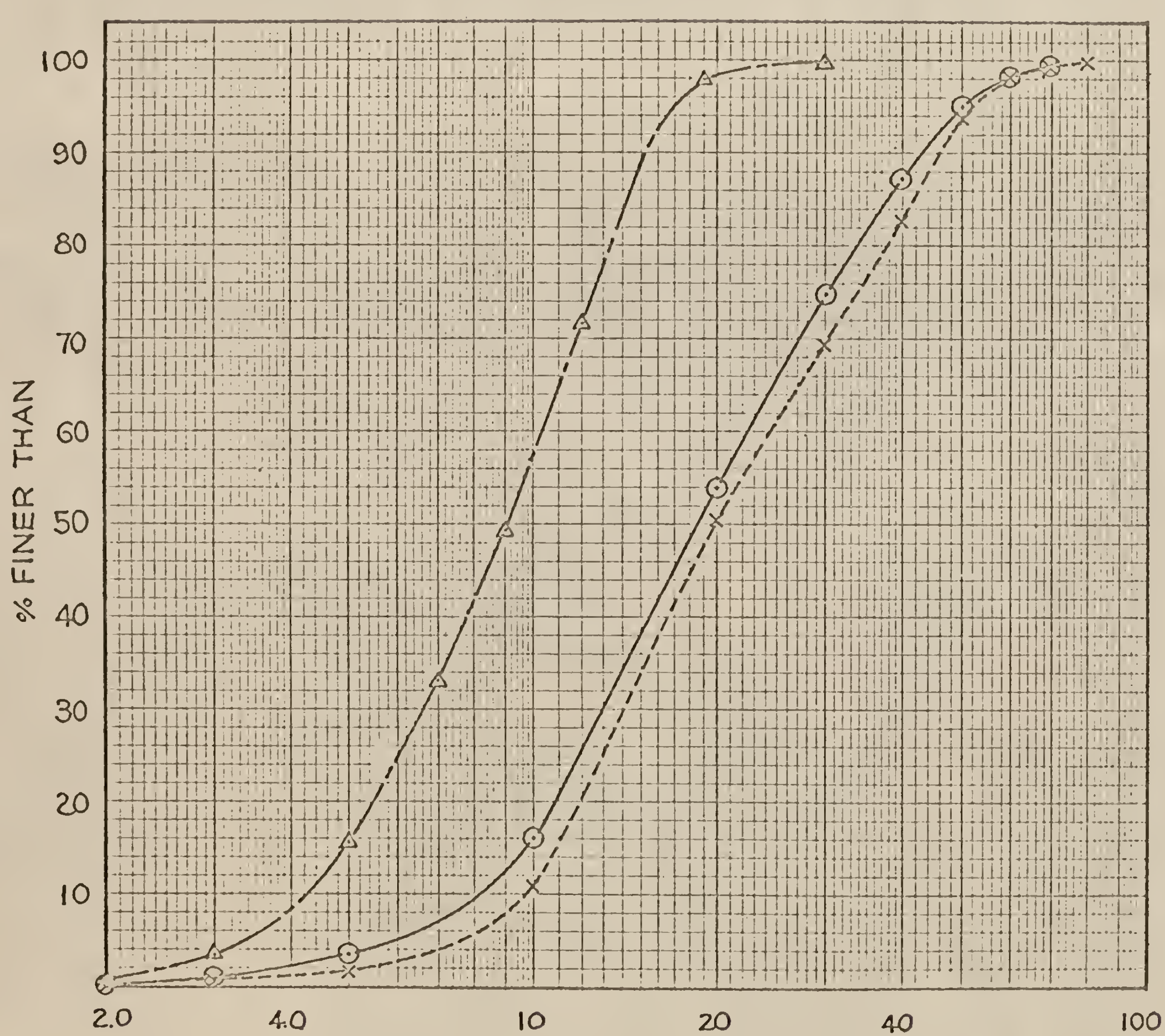

Turbo's C cut from Alpine ground flour

Graph Symbols	⊙	△	×
Sample Number	F065	F066	F067
Fraction	BB	C	CC
S.E.D. (Micron) Size	% Finer		
160			
140			
120			
110			
100			
90			
80			99.9
70	99.7		99.6
60	98.2		98.2
50	95.1		93.9
40	87.3		82.6
30	74.7	99.9	69.6
20	54.0		50.5
19		98.0	
12		71.8	
10	16.0		10.8
9		49.4	
7		33.2	
5	3.4	15.5	1.7
3	0.7	3.3	0.6
2	0.1	0.7	0.1
1		0.1	
Fisher	9.9	4.7	14.1
Prot.	10.3	15.6	9.5

S.E.D. (Micron) Sixe ⟶

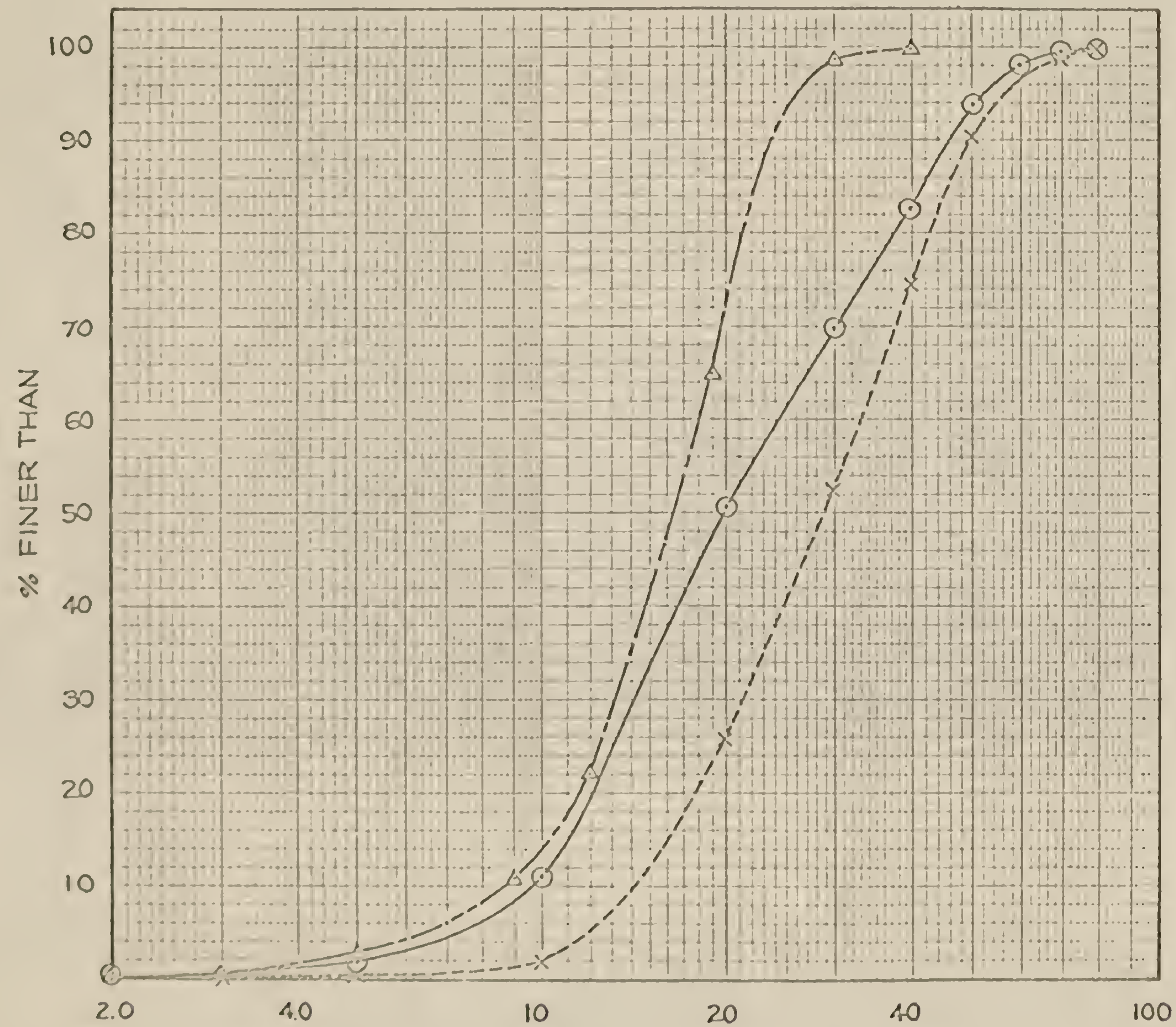

Turbo's D cut from Alpine ground flour

Graph Symbols	⊙	△	×
Sample Number	F067	F068	F069
Fraction	CC	D	DD
S.E.D. (Micron) Size	% Finer		
160			
140			
120			
110			
100			
90			
80	99.9		99.8
70	99.6		99.0
60	98.2		96.5
50	93.9		90.2
40	82.6	99.9	74.6
30	69.6	98.5	52.6
20	50.5		25.8
19		65.0	
12		22.0	
10	10.8		1.9
9		10.7	
7		6.0	
5	1.7	2.7	0.3
3	0.6	0.5	0.1
2	0.1	0.1	
1			
Fisher	14.1	9.8	17.3
Prot.	9.5	8.1	9.7

S.E.D. (Micron) Size ⟶

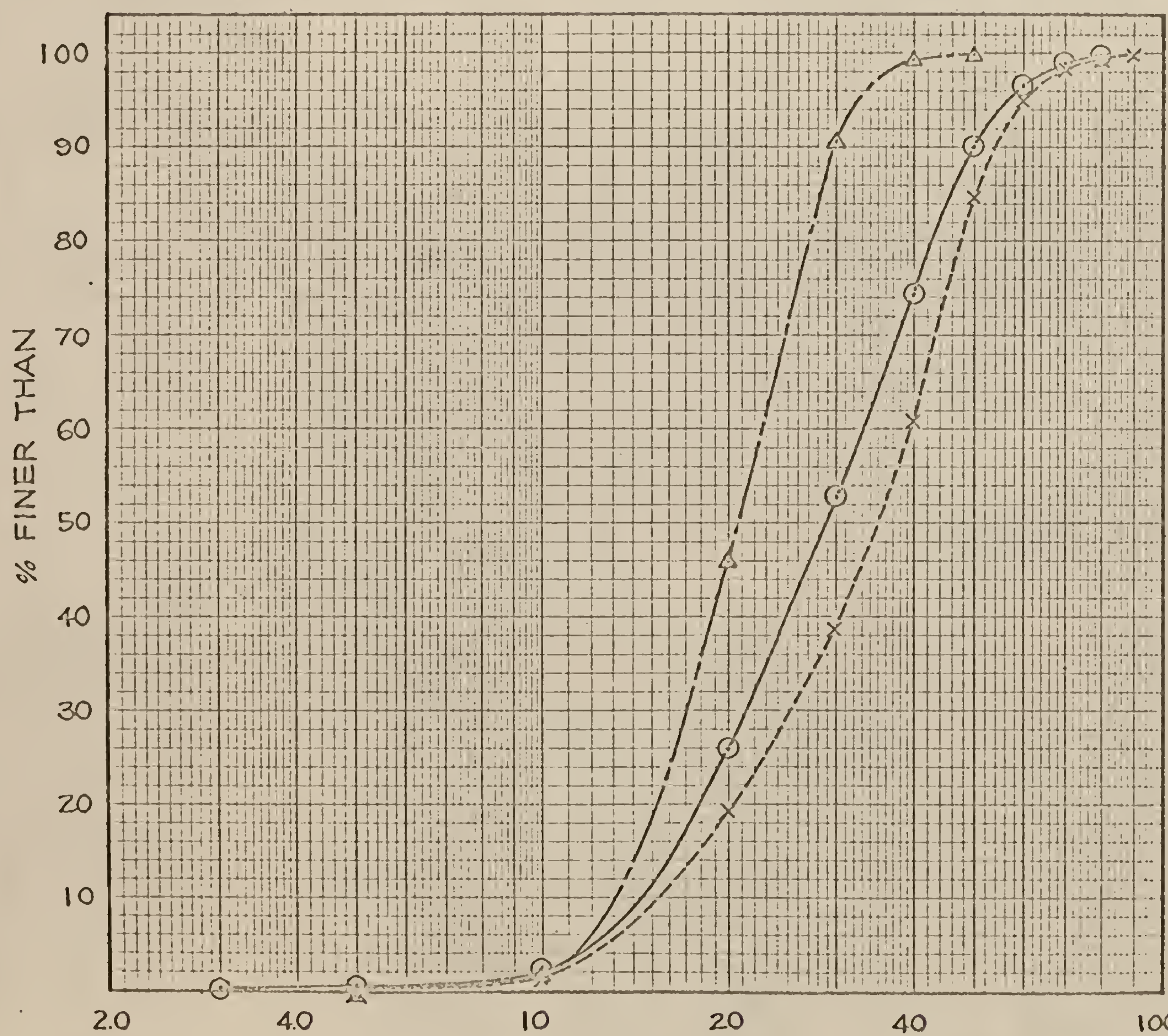

Turbo's E cut from Alpine ground flour

Graph Symbols	⊙	△	X
Sample Number	FO69	FO70	FO71
Fraction	DD	E	EE
S.E.D. (Micron) Size	% Finer		
160			
140			
120			
110			
100			
90			99.9
80	99.8		99.5
70	99.0		98.4
60	96.5		95.1
50	90.2	99.9	84.7
40	74.6	99.5	60.9
30	52.6	90.6	38.7
20	25.8	45.9	19.3
19			
12			
10	1.9	1.3	1.2
9			
7			
5	0.3	0.1	0.1
3	0.1		
2			
1			
Fisher	17.3	13.5	20.2
Prot.	9.7	6.8	10.8

S.E.D. (Micron) Size ⟶

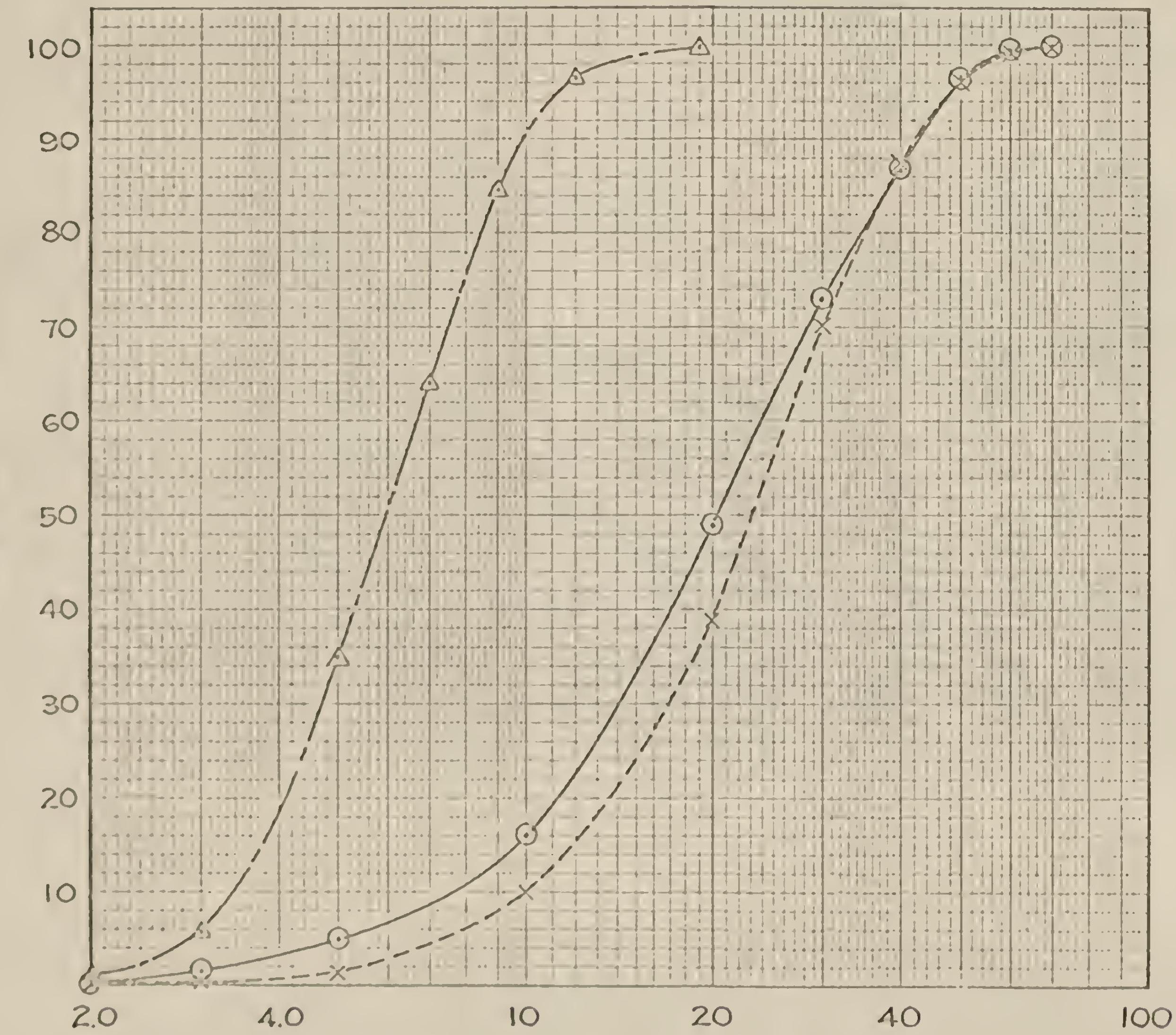

Micron's B cut from Mikro ground flour

Graph Symbols	⊙	△	X
Sample Number	F073	F091	F092
Fraction	A	B	BB
S.E.D. (Micron) Size	% Finer		
160			
140			
120			
110			
100			
90			
80			
70	99.9		99.9
60	99.6		99.4
50	96.6		96.2
40	87.0		87.5
30	73.0		70.1
20	49.0		38.8
19		99.9	
12		96.7	
10	16.0		10.0
9		84.4	
7		64.0	
5	5.0	35.2	1.3
3	1.5	5.8	0.3
2	0.1	1.0	0.1
1		0.1	
Fisher	9.7	2.9	10.8
Prot.	11.0	20.8	10.5

S.E.D. (Micron) Size ⟶

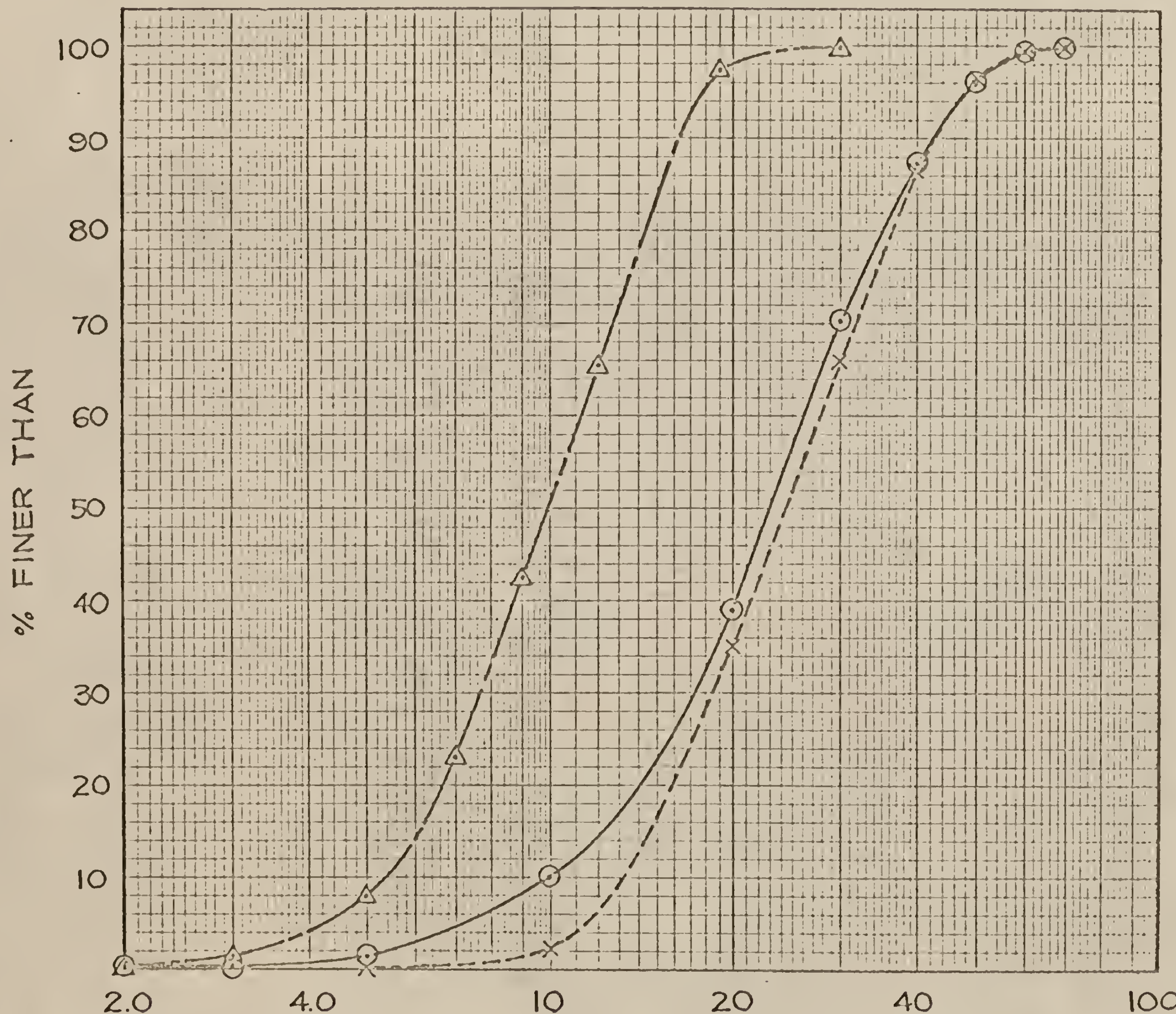

Micron's C cut from Mikro ground flour

Graph Symbols	⊙	△	×
Sample Number	F092	F093	F094
Fraction	BB	C	CC
S.E.D. (Micron) Size	% Finer		
160			
140			
120			
110			
100			
90			
80			
70	99.9		99.9
60	99.4		99.5
50	96.2		96.4
40	87.5		86.3
30	70.1	99.9	66.0
20	38.8		35.0
19		97.4	
12		65.5	
10	10.0		2.2
9		42.4	
7		23.3	
5	1.3	8.0	0.1
3	0.3	1.5	
2	0.1	0.1	
1			
Fisher	10.8	4.5	13.6
Prot.	10.5	14.6	9.6

S.E.D. (Micron) Size ⟶

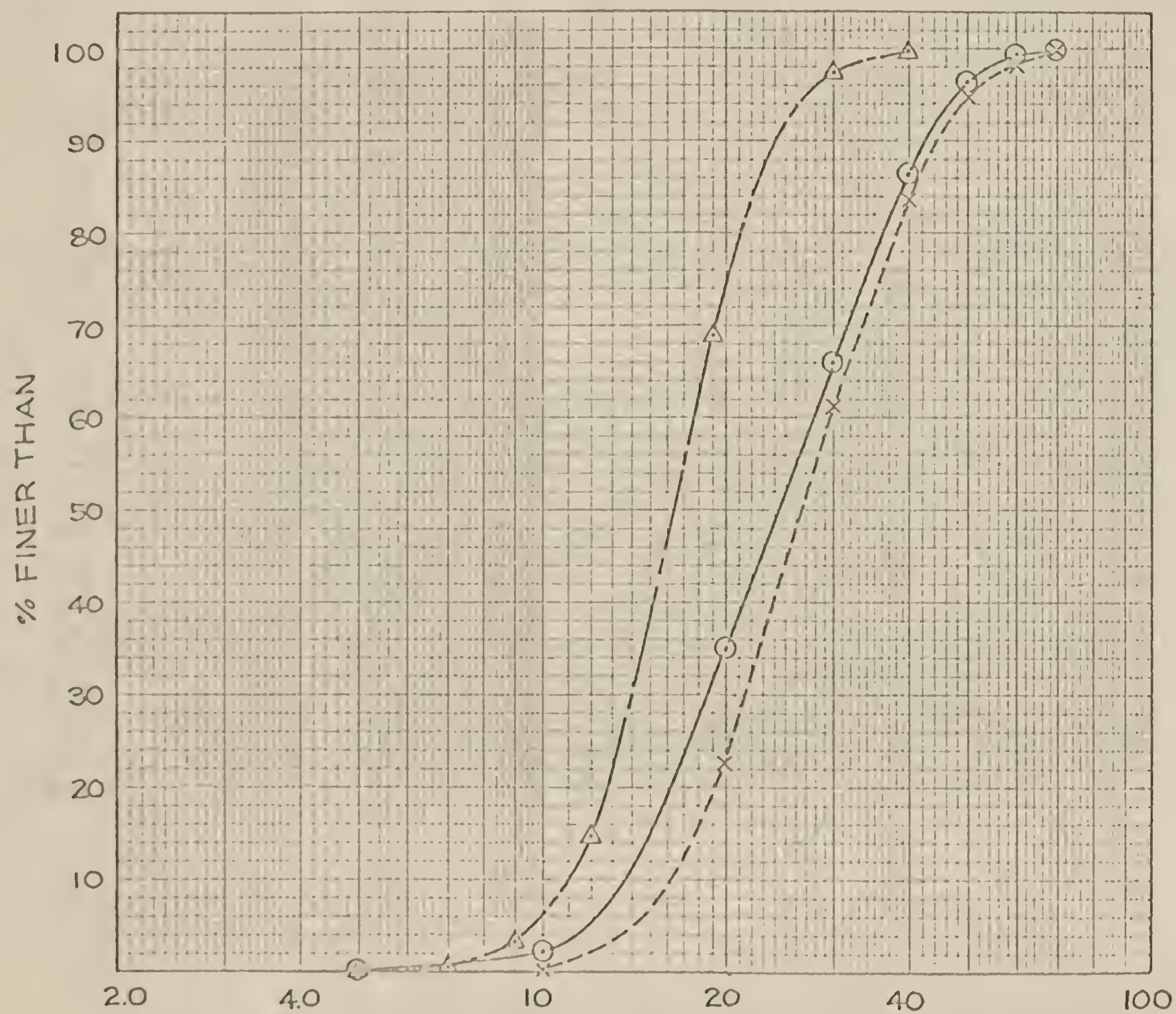

Micron's D cut from Mikro ground flour

Graph Symbols	⊙	△	×
Sample Number	F094	F095	F096
Fraction	CC	D	DD
S.E.D. (Micron) Size	% Finer		
160			
140			
120			
110			
100			
90			
80			
70	99.9		99.8
60	99.5		98.3
50	96.4		95.0
40	86.3	99.9	83.7
30	66.0	99.5	61.3
20	35.0		22.5
19		69.0	
12		14.4	
10	2.2		0.1
9		3.3	
7		0.4	
5	0.1	0.1	
3			
2			
1			
Fisher	13.6	9.6	15.6
Prot.	9.5	7.7	9.2

S.E.D. (Micron) Size ⟶

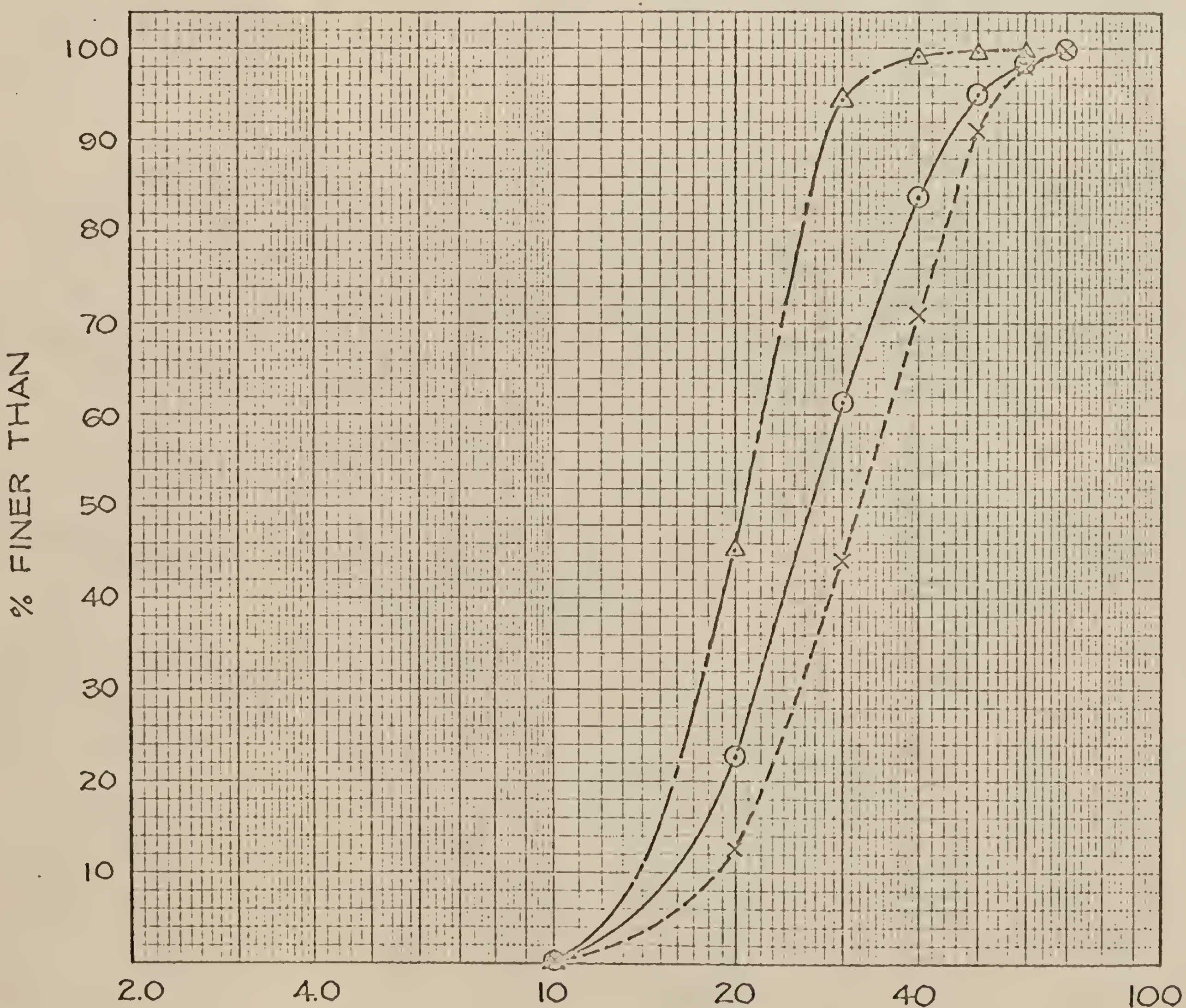

Micron's E cut from Mikro ground flour

Graph Symbols	⊙	△	×
Sample Number	F096	F097	F098
Fraction	DD	E	EE
S.E.D. (Micron) Size	% Finer		
160			
140			
120			
110			
100			
90			
80			
70	99.8		99.8
60	98.3	99.9	98.0
50	95.0	99.7	91.0
40	83.7	99.2	71.0
30	61.3	94.3	44.1
20	22.5	45.0	12.6
19			
12			
10	0.1	0.1	0.1
9			
7			
5			
3			
2			
1			
Fisher	15.6	12.4	18.5
Prot.	9.2	6.8	10.6

S.E.D. (Micron) Size ⟶

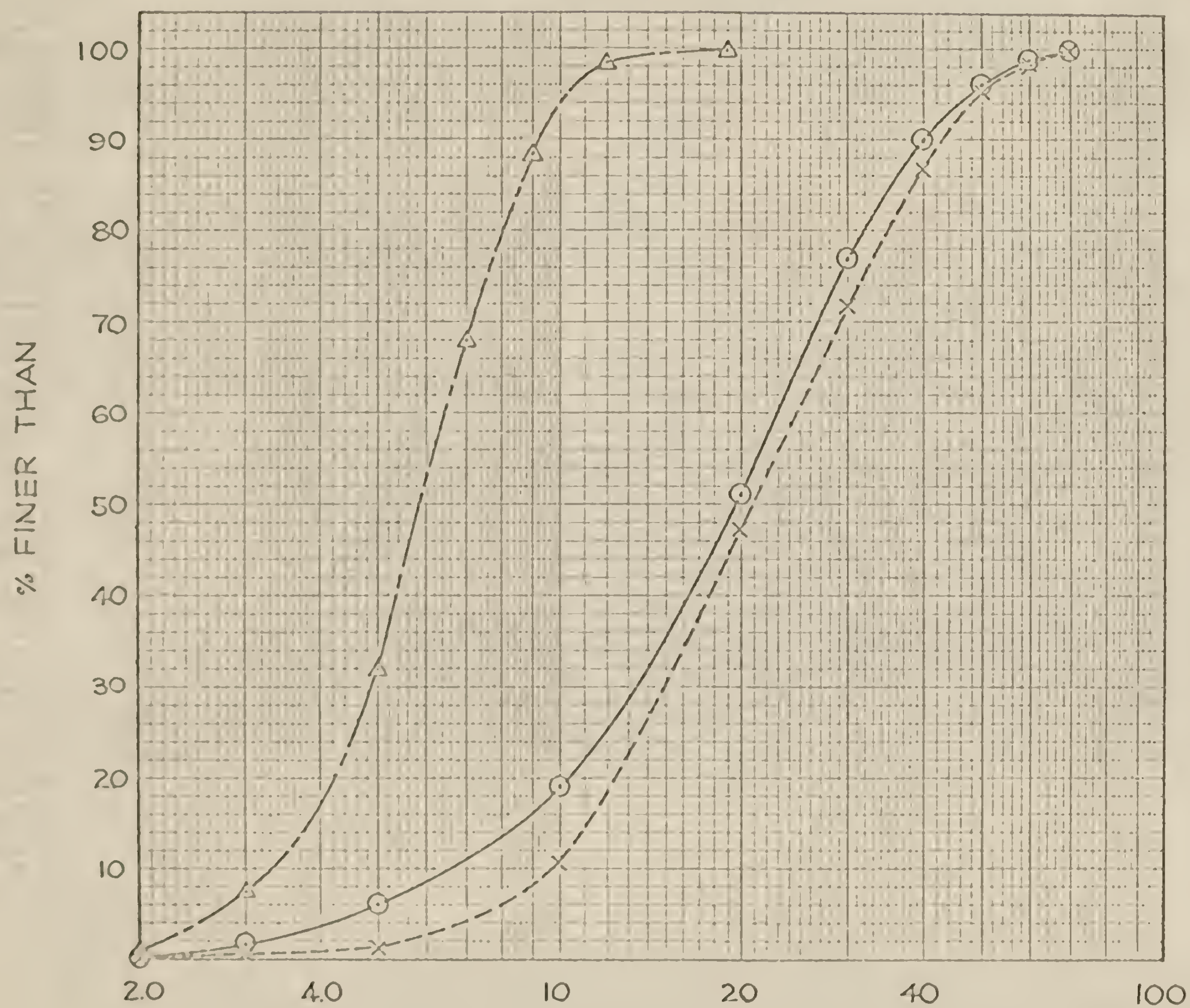

Micron's B cut from Alpine ground flour

Graph Symbols	⊙	△	×
Sample Number	F072	F099	F100
Fraction	A	B	BB
S.E.D. (Micron) Size	% Finer		
160			
140			
120			
110			
100			
90			
80			
70	99.9		99.8
60	98.8		98.5
50	96.1		95.6
40	90.0		86.7
30	77.0		71.7
20	51.0		47.3
19		99.9	
12		98.4	
10	19.0		10.6
9		88.4	
7		68.0	
5	6.0	32.0	1.3
3	1.5	7.5	0.5
2	0.1	1.0	0.1
1		0.1	
Fisher	9.3	2.7	10.2
Prol.	11.0	22.8	10.1

S.E.D. (Micron) Size ⟶

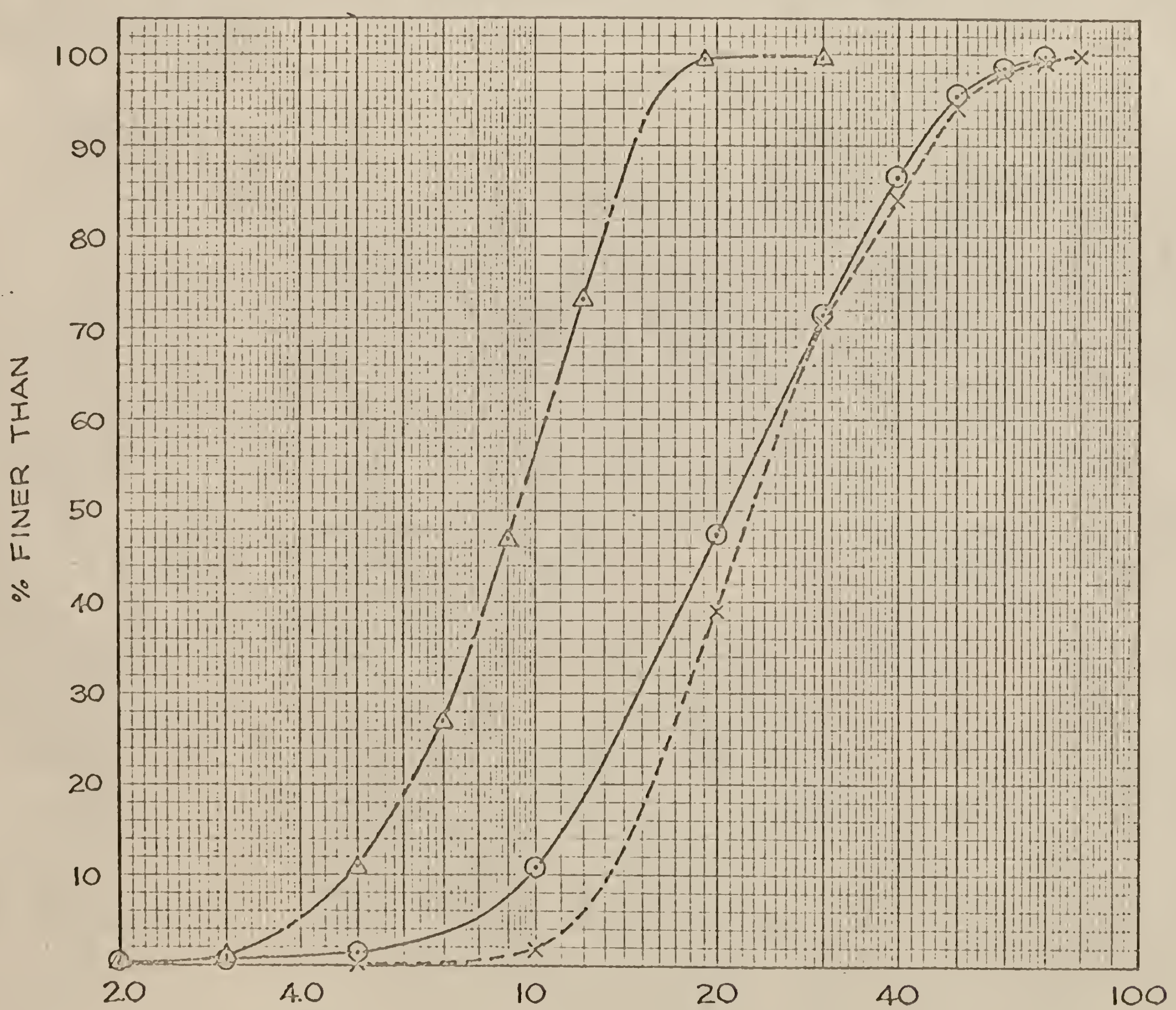

Micron's C cut from Alpine ground flour

Graph Symbols	⊙	△	×
Sample Number	F100	F101	F102
Fraction	BB	C	CC
S.E.D. (Micron) Size	% Finer		
160			
140			
120			
110			
100			
90			
80			99.9
70	99.8		99.5
60	98.5		97.9
50	95.6		94.2
40	86.7		84.0
30	71.6	99.9	71.1
20	47.3		39.0
19		99.5	
12		73.2	
10	10.6		1.8
9		47.1	
7		27.0	
5	1.3	11.2	0.1
3	0.5	0.8	
2	0.1	0.1	
1			
Fisher	10.2	4.4	13.2
Prot.	10.1	13.1	8.7

S.E.D. (Micron) Size ⟶

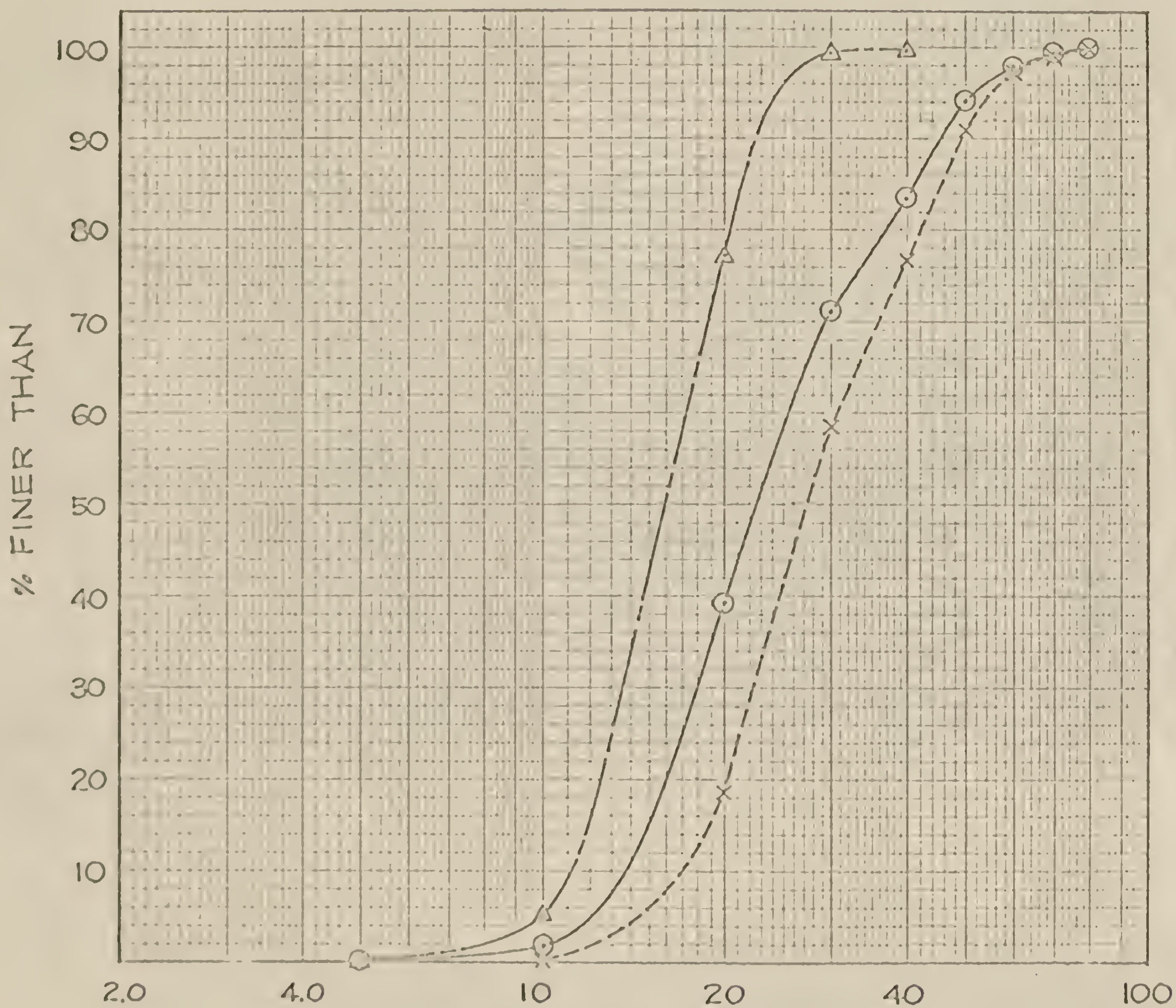

Micron's D cut from Alpine ground flour

Graph Symbols	⊙	△	X
Sample Number	F102	F103	F104
Fraction	CC	D	DD
S.E.D. (Micron) Size	% Finer		
160			
140			
120			
110			
100			
90			
80	99.9		99.9
70	99.5		99.4
60	97.9		97.6
50	94.2		91.0
40	83.4	99.9	76.6
30	71.1	99.6	58.4
20	39.0	77.3	18.5
19			
12			
10	1.8	5.1	0.1
9			
7			
5	0.1	0.2	
3			
2			
1			
Fisher	13.2	10.0	15.5
Prot.	8.7	7.8	9.3

S.E.D. (Micron) Size ⟶

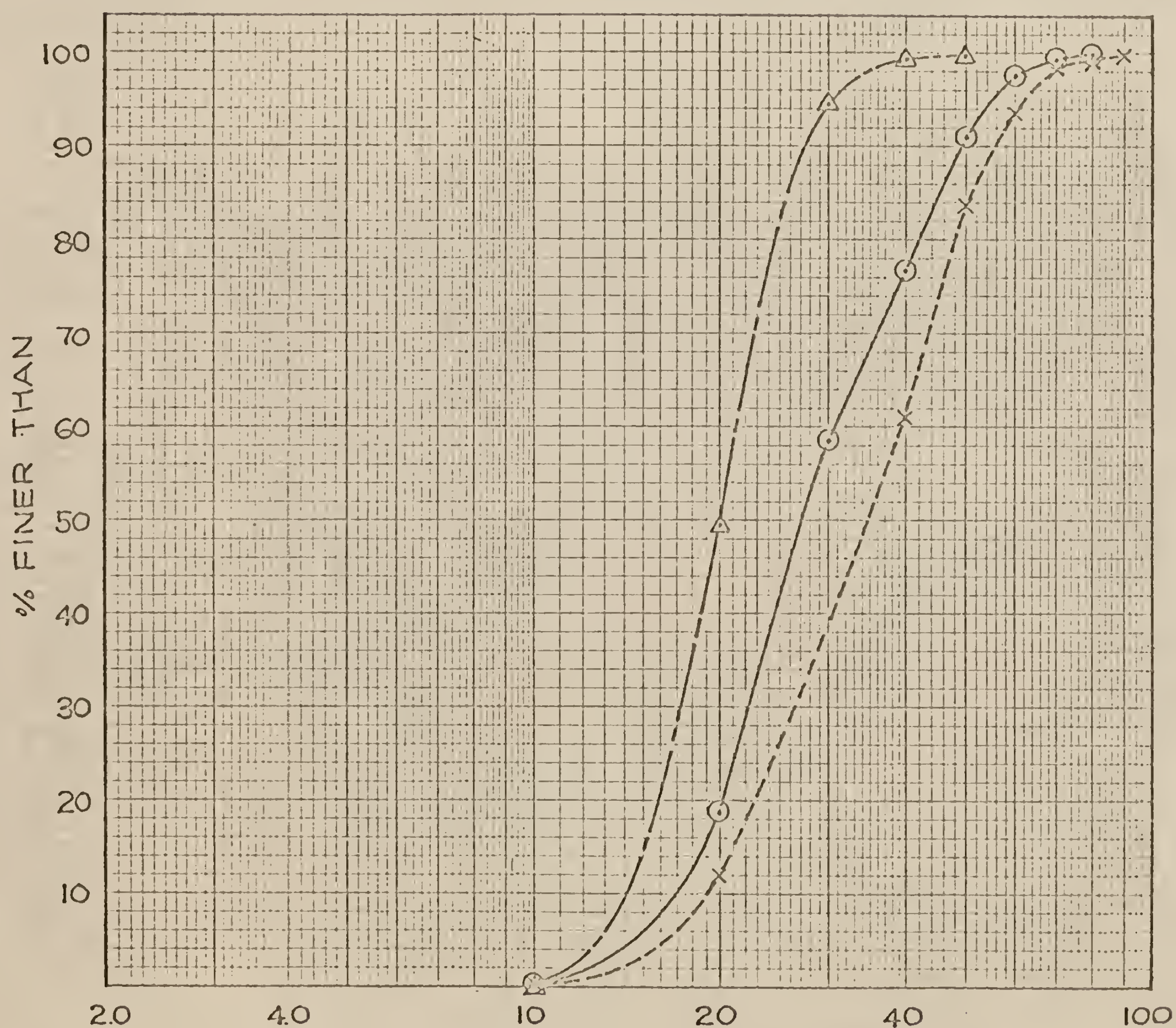

Micron's E cut from Alpine ground flour

Graph Symbols	⊙	△	X
Sample Number	F104	F105	F106
Fraction	DD	E	EE
S.E.D. (Micron) Size	% Finer		
160			
140			
120			
110			
100			
90			99.9
80	99.9		99.5
70	99.4		98.3
60	97.6		93.6
50	91.0	99.9	83.7
40	76.6	99.4	61.0
30	58.4	94.5	38.6
20	18.5	49.5	11.8
19			
12			
10	0.1	0.1	0.1
9			
7			
5			
3			
2			
1			
Fisher	15.5	12.5	18.2
Prot.	9.3	7.0	10.5

S.E.D. (Micron) Size ⟶

THE EVALUATION OF A FINE GRINDER AND AIR CLASSIFIER IN THE PERFORMANCE OF PROTEIN SHIFTING OF WHEAT FLOUR

by

FRED ALBERT FRANZ

B. S., Kansas State University, 1962

AN ABSTRACT OF A MASTER'S THESIS

submitted in partial fulfillment of the

requirements for the degree

MASTER OF SCIENCE

Department of Grain Science and Industry

KANSAS STATE UNIVERSITY
Manhattan, Kansas

1968

The purpose of this study was to evaluate a fine grinder and air classifier in the performance of protein shifting of wheat flour.

A Pillsbury Laboratory Turbo separator and an Alpine 160L Kolloplex grinder were used to set the standards by which to judge respectively the performance of a MS-1 Hosokawa Micron separator and a Mikro 'ACM-10' grinder. The Turbo and Alpine were known to be capable of reasonable performance in protein shift work and are being used successfully in commercial mills.

A commercially-milled 11.2 percent protein (14% M.B.) flour was broken down into three lots: unground, Mikro ground, and Alpine ground. Both separators were used to fractionate samples of these three lots of flour. Four sub-sieve-size separations were made during each of the six fractionations. The Fisher Sub-Sieve-Sizer was used to determine the Fisher number, and the Mine Safety Appliance (MSA) Particle Size Analyzer was used to determine the particle size distribution of all the fractions. Moisture, ash, and protein determinations plus physical dough tests using the farinograph and amylograph were accomplished on all the fractions.

Previously determined settings, known to provide reasonable results, were used on the Turbo and Alpine. The Fisher number and particle size distribution curves of the fractions produced by the Turbo were used as guides in obtaining the final settings used in the comparative tests. The Fisher number and particle size distribution curves of the Alpine ground flour were similarly used in testing the Mikro grinder.

The Fisher number and particle size distribution curves were also used in determining the effects of the various adjustments on the Micron separator and Mikro grinder. Separator rotor rpm was found to be the main adjustment of the Micron separator. The Mikro grinder was found to perform best at 7300 rpm using a pin grinding rotor. Higher rpm's required considerably more power and did not substantially increase the percentage of ground flour finer than 10 S.E.D. microns.

This study found that the Mikro grinder was capable of producing a ground product of narrow particle size distribution by controlling the top size and minimizing the grinding of the fines. However, the results of the grinding tests and six fractionations indicated the Mikro grinder was substantially capable of meeting the standards set by using the Alpine grinder.

The results of the six fractionations were summarized by using histograms and a protein shift index described by Gracza. From these it was determined that the Micron separator did not meet the standards of performance set by the Turbo separator. There were two main reasons for this: (1) the Micron separator did not produce the two ultra-fine fractions with protein contents as high as those produced by the Turbo, and (2) the Micron produced smaller percentages of all four sub-sieve-size fractions.